VOL. 5 NO. 3 MARCH 1963

Journal of

ELECTROANALYTICAL CHEMISTRY

International Journal Dealing with all Aspects of Electroanalytical Chemistry, Including Fundamental Electrochemistry

ELSEVIER

GENERAL INFORMATION

Types of contributions

(a) Original research work not previously published in other periodicals.
(b) Reviews on recent developments in various fields.
(c) Short communications.
(d) Bibliographical notes and book reviews.

Languages

Papers will be published in English, French or German.

Submission of papers

Papers should be sent to one of the following Editors:

Professor J. O'M. BOCKRIS, John Harrison Laboratory of Chemistry, University of Pennsylvania, Philadelphia 4, Pa., U.S.A.
Dr. R. PARSONS, Department of Chemistry, The University, Bristol 8, England.
Professor C. N. REILLEY, Department of Chemistry, University of North Carolina, Chapel Hill, N.C., U.S.A.

Authors should preferably submit two copies in double-spaced typing on pages of uniform size. Legends for figures should be typed on a separate page. The figures should be in a form suitable for reproduction, drawn in Indian ink on drawing paper or tracing paper, with lettering etc. in thin pencil. The sheets of drawing or tracing paper should preferably be of the same dimensions as those on which the article is typed. Photographs should be submitted as clear black and white prints on glossy paper.
All references should be given at the end of the paper. They should be numbered and the numbers should appear in the text at the appropriate places.
A summary of 50 to 200 words should be included.

Reprints

Twenty-five reprints will be supplied free of charge. Additional reprints can be ordered at quoted prices. They must be ordered on order forms which are sent together with the proofs.

Publication

The *Journal of Electroanalytical Chemistry* appears monthly and has six issues per volume and two volumes per year, each of approx. 500 pages.

Subscription price (post free): £ 10.15.0 or $ 30.00 or Dfl. 108.00 per year; £ 5.7.6 or $ 15.00 or Dfl. 54.00 per volume.
Additional cost for copies by air mail available on request.
For advertising rates apply to the publishers.

Subscriptions

Subscriptions should be sent to:

ELSEVIER PUBLISHING COMPANY, P.O. Box 211, Spuistraat 110-112, Amsterdam-C., The Netherlands.

Two important new books from ELSEVIER

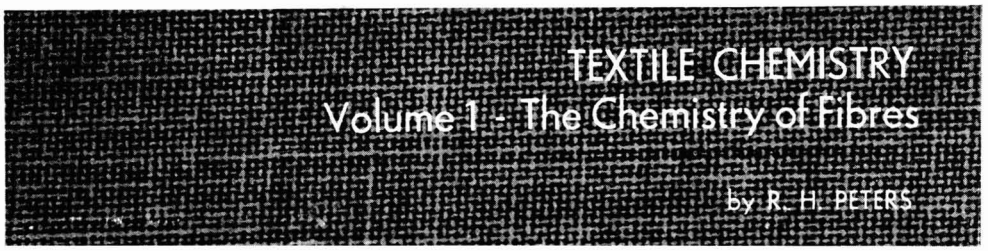

xiv + 475 pages 42 tables 164 figures 1083 references 1962 75s.

This first volume of a scheduled 3-volume account of the chemical principles of textile technology and processing is concerned with the origin, preparation and chemical constitution of the fibre-forming polymers and of the natural fibres.
Descriptions of the fine and molecular structure of polymers, the biosynthesis and histology of wool, silk and the principal vegetable staple fibres, and the mode of manufacture of synthetic fibres are all accorded detailed treatment.
Volumes II and III will deal respectively with the chemistry of scouring, bleaching and surface-active agents and the chemistry of dyeing and finishing agents.
The work is designed as an introduction to students and as a guide to advanced work in the field of textile chemistry.

contents

1. Introduction. 2. Condensation polymers. 3. Addition polymers. 4. Co-polymers. 5. Molecular weight determination. 6. Cotton and flax. 7. Chemistry of cellulose. 8. Amino acids and proteins. 9. Synthetic polypeptides. 10. Wool. 11. Silk. 12. Crystalline structures of polymers. 13. Melting and crystallization. 14. Fine structure. 15. Production of fibres. References. Index.

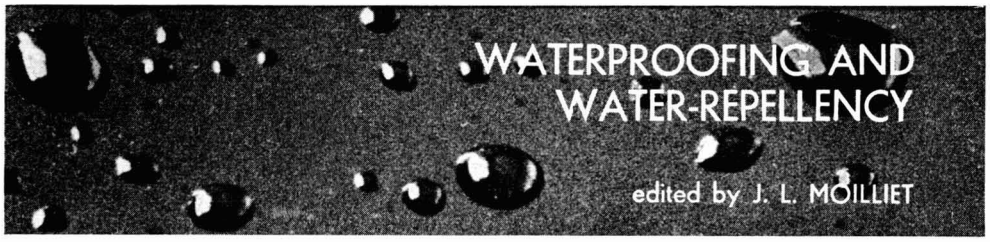

viii + 490 pages 36 tables 68 figures 820 references 1962 £5.—

This joint work by a number of experts considers the physical, organic and inorganic chemistry of waterproofing processes. Durable organic waterproofing agents, waterproofing emulsions and silicone compounds are described as well as special preparations. Their application to textiles and other substrates are considered, with due attention to the effect of the substrate structure — this in relation to the introductory chapters on the general physical chemistry of water-repellency.
Methods of evaluating waterproofed materials and the important techniques of coating textiles with impervious layers receive detailed treatment.
Finally, some of the more novel applications of waterproofing techniques to building materials and soils, the dropwise condensation of steam, and the very efficient waterproofing mechanisms found in plants and animals are discussed at length.

ELSEVIER PUBLISHING COMPANY
AMSTERDAM - LONDON - NEW YORK

499E

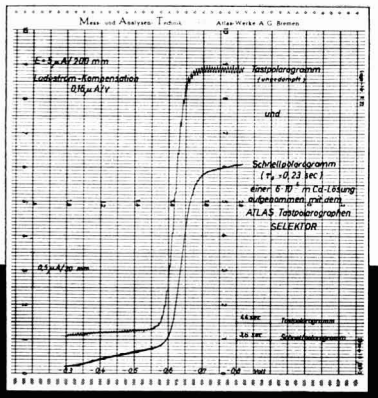

Selector

Tast-Polarograph

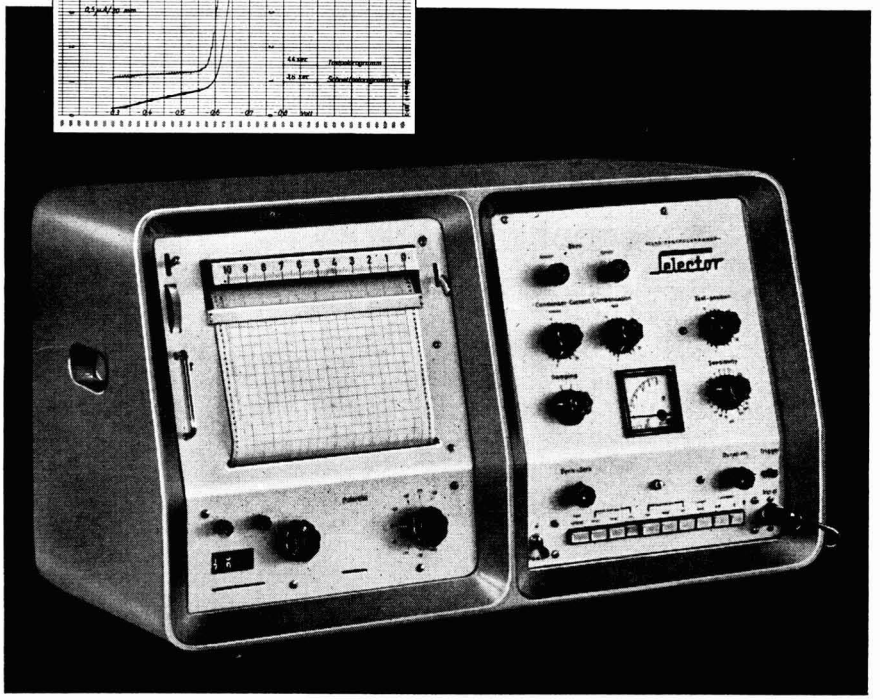

An instrument designed for high demands as to accuracy, sensitivity and safety in taking and recording

conventional polarograms
tast-polarograms
derivative tast polarograms
rapid polarograms

The construction of the SELECTOR combines the precision required for scientific tasks with easy operation necessary for routine analyses.

68 e

ATLAS MESS- UND ANALYSENTECHNIK GMBH
BREMEN

MAT

EFFECT OF TUNGSTEN(VI) ON MOLYBDENUM(VI)-CATALYZED REDUCTION WAVES OF CHLORATE, NITRATE AND PERCHLORATE

I. M. KOLTHOFF AND I. HODARA*

School of Chemistry, University of Minnesota, Minneapolis, Minn. (U.S.A.)

(Received June 8th, 1962)

In a previous paper[1], characteristics of catalytic reduction waves at the dropping mercury electrode, of chlorate, nitrate and perchlorate in the presence of molybdenum (VI) in the bulk of the solution, have been presented and discussed. In further work we have studied the catalytic effect of tungsten(VI) on the polarographic reduction of the above anions in the absence and presence of molybdenum(VI). The results were quite unexpected and interesting, both from an analytical and inorganic view point. Further research on the subject has been discontinued in this laboratory. This paper gives a brief account of the catalytic properties of tungsten(VI) in the reduction of the above anions. Our preliminary study may encourage other workers to investigate more systematically the analytical and structural implications of the combined molybdenum(VI)–tungsten(VI) effect on the chlorate reduction.

EXPERIMENTAL

For experimental details and chemicals used, reference is made to a previous paper[1]. Sodium tungstate was a C.P. Merck product. A 0.01 M stock solution was prepared.

RESULTS

Solutions $2 \cdot 10^{-4}$ M in tungsten(VI) remained clear for at least 24 h in 1 M sulfuric, or 0.5–1 N perchloric or nitric acid, or in the same acids which were 0.5 M in chlorate. Similar solutions 10^{-3} M in tungsten(VI) yielded immediately a white precipitate. The presence of 0.5 M chlorate, of molybdenum(VI) and a combination of both, had a retarding effect on the formation of precipitate and decreased the amount of precipitate formed.

Effect of W(VI) on Mo(VI)-catalyzed nitric and perchloric acid reduction waves

Polarograms in solutions which were $1–2 \cdot 10^{-4}$ M in tungsten(VI) and 0.5–1 M in nitric or perchloric acid differed little from those obtained in the absence of tungsten. A small wave was observed with a limiting current of 0.3 μA in 10^{-4} M tungsten solution in 0.5–1 M nitric acid. This wave did not increase with increasing tungsten concentration, and it was not found in perchloric acid solutions. In all acid solutions including sulfuric acid the hydrogen wave appeared at less negative potentials in the

* On leave from the Israel Atomic Energy Commission Laboratories.

presence of tungsten(VI). The shape of the catalytic waves observed in 0.5 M nitric or perchloric acid solutions which were $5 \cdot 10^{-5}$ M in molybdenum(VI), was not affected when the tungsten(VI) concentration was equal to or less than $2 \cdot 10^{-4}$ M. At higher concentrations of tungsten, the waves became distorted and a precipitate of tungsten oxide separated. The limiting kinetic current decreased in the presence of tungsten, even when no precipitate was formed. From Fig. 1 it is seen that the kinetic current continues to decrease with increasing tungsten(VI) concentration.

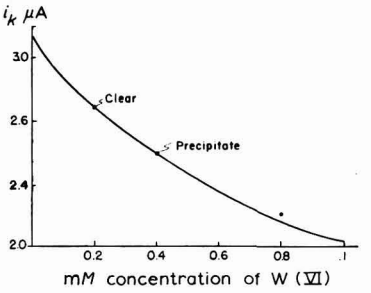

Fig. 1. Kinetic perchlorate current in $5 \cdot 10^{-5}$ M molybdenum(VI)–0.5 M perchloric acid in presence of tungsten(VI).

Effect of W(VI) on Mo(VI)-catalyzed chloric acid reduction waves

The effect of tungsten on molybdenum(VI)-catalyzed chloric acid current–potential curves is quite different from that on perchloric or nitric acid waves. In various acid media the molybdenum(VI)-catalyzed chlorate reduction wave is greatly enhanced by tungsten(VI).

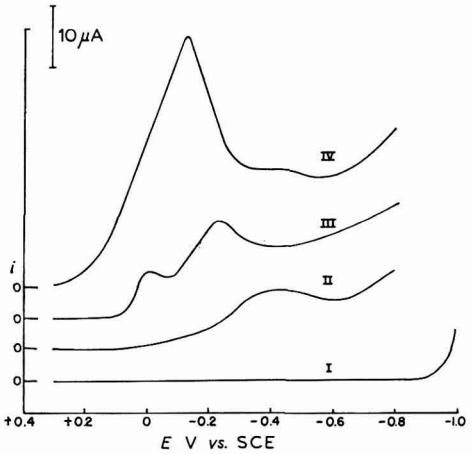

Fig. 2. Chlorate reduction currents in the presence of molybdenum(VI), tungsten(VI) and their mixtures in 1 M sulfuric acid–0.5 M $NaClO_3$. I, $2 \cdot 10^{-4}$ M W(VI), no chlorate; II, $2 \cdot 10^{-4}$ M W(VI); III, $5 \cdot 10^{-5}$ M Mo(VI); IV, $5 \cdot 10^{-5}$ M Mo(VI)–$2 \cdot 10^{-4}$ M W(VI).

Effect of W(VI) in 1 M sulfuric acid (plus chlorate)

Tungsten(VI) in 0.1–1 *M* sulfuric acid does not exhibit a reduction wave at the dropping electrode. As is seen from curve II in Fig. 2, tungsten(VI) gives rise to a small catalytic chlorate reduction wave in a mixture 1 *M* in sulfuric acid and 0.5 *M* in sodium chlorate. The polarogram exhibits a rounded maximum at −0.43 V and has characteristics which are quite different from those of the molybdenum(VI)-catalyzed reduction pattern (curve III, Fig. 2). The polarogram observed in the mixture (curve IV containing both molybdenum(VI), ($5 \cdot 10^{-5}$ *M*) and tungsten, ($2 \cdot 10^{-4}$ *M*)), has an appearence quite different from those observed with molybdenum and tungsten separately. Instead of two peaks with molybdenum alone, only one peak is observed at −0.13 V and the peak height is much greater than the sum of the currents observed at the same potential with molybdenum and tungsten separately. At potentials more negative than −0.3 V, the current observed in the presence of both molybdenum and tungsten becomes approximately equal to the sum of the currents found with molybdenum and tungsten separately. The effect of increasing concentrations of tungsten(VI) on the molybdenum(VI)-catalyzed chlorate reduction waves is illustrated in Fig. 3. The two peaks observed in $5 \cdot 10^{-5}$ *M* molybdate, without tung-

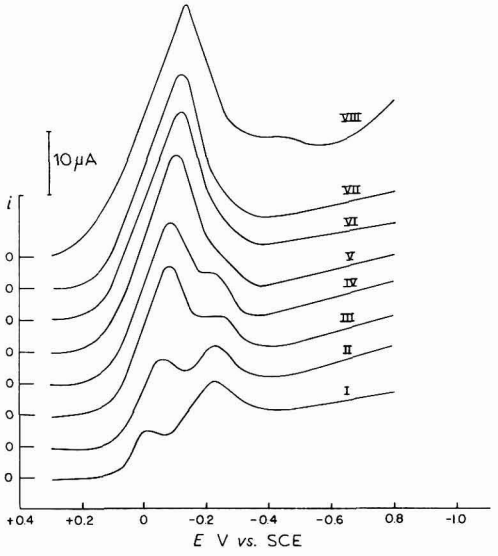

Fig. 3. Effect of tungsten(VI) on catalytic waves in $5 \cdot 10^{-5}$ *M* molybdate–0.5 *M* $NaClO_3$–1 *M* H_2SO_4. Not corrected for *iR* drop. Molar concentration of W(VI) $\cdot 10^5$: I, 0; II, 1.0; III, 3; IV, 5; V, 7; VI, 9; VII, 10; VIII, 20.

sten, disappear when the tungsten concentration becomes greater than 10^{-5} *M* and a single sharply defined peak is observed. When corrected for the *iR* drop, this peak occurs at -0.12 ± 0.01 V (*vs.* S.C.E.). The increase of the peak current with increasing tungsten concentration is illustrated in Fig. 4. Precipitation occurs when the tungsten concentration increases considerably above $2 \cdot 10^{-4}$ *M*. The peak current at −0.12 V was found proportional to the molybdenum(VI) concentration in the presence of $2 \cdot 10^{-4}$ *M*

tungsten(VI). No details are given, because the exaltation of the molybdenum wave was found to be considerably greater in a medium 0.5 *M* in sodium chlorate and 1 *M* in perchloric acid than in a similar mixture with 1 *M* sulfuric instead of perchloric acid. The perchloric acid-containing mixture is recommended for analytical purposes. Polarograms in mixtures containing 1 *M* nitric instead of 1 *M* perchloric acid were similar to those in sulfuric (Fig. 3) and perchloric acids, but the exaltation is greater in the latter acid.

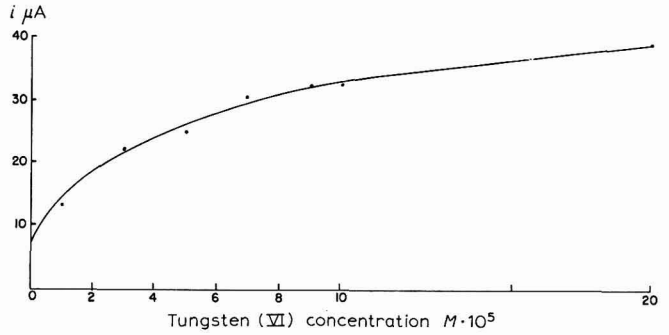

Fig. 4. Catalytic chlorate peak current (corrected for i_r) in $5 \cdot 10^{-5}$ *M* molybdate–0.5 *M* $NaClO_3$–1 *M* H_2SO_4 as a function of tungsten(VI) concentration.

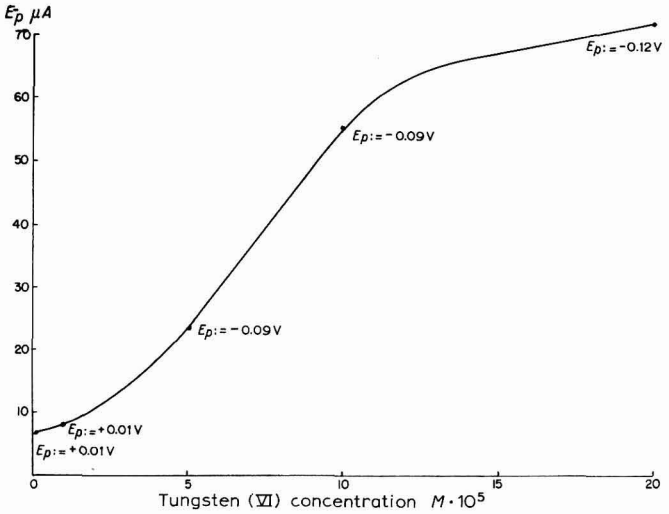

Fig. 5. Catalytic molybdenum current at different tungsten concentrations in a mixture $5 \cdot 10^{-5}$ *M* in Mo(VI), 0.5 *M* in $NaClO_3$ and 1 *M* in $HClO_4$.

Exaltation of Mo wave in a mixture 1 M in $HClO_4$, 0.5 M in $NaClO_3$ and $2 \cdot 10^{-4}$ M in W(VI)

Reproducible results were obtained when solutions were mixed in the following order: 10 ml 5 *M* perchloric acid, 10 ml 2.5 *M* sodium chlorate, molybdate solution, 10 ml 10^{-3} *M* sodium tungstate and water to 50 ml. When the mixture was prepared

by using 1 ml 10^{-2} M tungstate a white precipitate was formed (local excess) which did not dissolve on shaking. Apparently, the precipitation of tungstic acid polymer is a relatively slow process. As is shown in Table 1, the peak current (i_p) occurs at -0.12 ± 0.02 V (corrected for iR). When corrected at the peak potential for the residual current in the molybdenum-free solution, the catalytic molybdenum current $i_c = i_p - i_r$

TABLE I

VARIATION OF CATALYTIC CURRENT i_c AT PEAK WITH MOLYBDATE CONCENTRATION IN MIXTURE 0.5 M IN $NaClO_3$, 1 M IN $HClO_4$ AND $2 \cdot 10^{-4}$ M IN TUNGSTATE

$C_{Mo(VI)}$ $M \cdot 10^5$	E_{peak} (corr. f. iR)	i_p (μA)	i_r[a] (μA)	$i_c = i_p - i_r$ (μA)	$i_c/C_{Mo(VI)}$ ($\mu A/mM$)
0.1	−0.15	4.5	3.0	1.5	1500
0.5	−0.14	9.4	2.8	6.6	1320
1	−0.13	18.3	2.6	15.7	1570
2	−0.12	33.7	3.0	30.7	1540
3	−0.12	52.5	3.0	49.5	1650
4	−0.11	67.5	2.5	65.0	1630
5	−0.09	80.5	2.5	78.0	1560
					Average 1540 ± 6%

[a] from blank solution containing $2 \cdot 10^{-4}$ M W(VI), 0.5 M $NaClO_3$, 1 M $HClO_4$ at the corresponding peak potential.

(i_r includes the current given by $2 \cdot 10^{-4}$ M tungsten(VI)) is close to proportional to the molybdenum concentration. By the presence of $2 \cdot 10^{-4}$ M tungsten(VI) the sensitivity of the method for molybdenum determination is increased by one order of magnitude. In a solution 10^{-6} M in molybdenum, i_c was equal to 1.5 μA.

Catalytic Mo(VI) wave as function of W concentration

From Fig. 5 it is seen that the exaltation of the catalytic molybdenum current in a solution $5 \cdot 10^{-5}$ M in molybdenum(VI) is virtually proportional to tungsten concentration in the concentration range between $5–10 \cdot 10^{-5}$ M tungsten. In the absence of tungsten the catalytic current was 7 μA, with $5 \cdot 10^{-5}$ M tungsten 24 μA and with 10^{-4} M tungsten 55 μA. This suggests that analytical use of the exaltation can be made for the determination of traces of tungsten. Such a method would require careful calibration.

DISCUSSION

From the effect of tungsten(VI) on the molybdenum-catalyzed reduction waves of nitric or perchloric acids (Fig. 1), it is concluded that molybdenum(VI) and tungsten(VI) form mixed heteropolyacids in these media. At potentials where molybdenum(VI) alone is reduced to molybdenum(III), the molybdenum which is not bound in the mixed heteropolyacid can exert its normal effect on the catalytic nitric or perchloric acid reduction.

It would appear that the mixed heteropolyacid does not contribute to the catalytic reduction waves. It is of interest to mention that the decrease of the catalytic molybdenum current occurs already at tungsten concentrations where no precipitate of tungstic acid is formed (Fig. 1). Thus, the decrease of the catalytic current by tung-

sten(VI) cannot be attributed solely to a coprecipitation of molybdenum(VI) with tungstic acid. In 0.5 M chlorate solutions which are 1 M in sulfuric, perchloric or nitric acid, the large exaltation of the first molybdenum(V)-catalyzed reduction wave of chlorate[1] is accounted for by a large contribution from the tungsten(V) formed upon reduction of the mixed heteropoly acid at potentials where the first catalytic wave occurs. The second molybdenum-catalyzed chlorate wave, observed in the absence of tungstate, is not enhanced in the presence of tungsten(VI). As a matter of fact, the current observed at more negative potentials than -0.3 V in the presence of both molybdenum(VI) and tungsten(VI), in the bulk of the solution, is about equal to the sum of the currents observed with the same concentrations molybdenum and tungsten separately.

From the analytical point of view, it is important to realize that the determination of small concentrations of molybdenum(VI) by measuring the height of the catalytic chlorate peaks[1], is interfered with by the presence of tungsten. As a matter of fact, in the presence of $2 \cdot 10^{-4}$ M tungsten(VI), the sensitivity is increased some 10 times and concentrations less than 10^{-6} M molybdenum(VI) can be determined. When it is unknown whether the solution contains tungsten in addition to molybdenum, a simple determination of the catalytic reduction current of perchlorate or nitrate will yield the approximate molybdenum content. It is obvious from Fig. 1 that a relatively large excess of tungsten decreases the limiting catalytic perchloric acid current only to a relatively small extent. Thus the combined determinations of the perchloric acid catalytic current and that of chlorate will yield an indication of the approximate tungsten content of the solution.

The possibility of determining small concentrations of tungsten(VI) by measuring its effect on the molybdenum-catalyzed chlorate wave is evident from Fig. 5.

ACKNOWLEDGEMENT

Partial financial support of this work was received from the United States Air Force Office of Scientific Research of the Air Research and Development Command under Contract No. AF 49(638)519. Reproduction in whole or in part is permitted for any purpose of the United States Government.

SUMMARY

Tungsten(VI) does not catalyze the polarographic reduction of nitric or perchloric acid. It decreases the molybdenum-catalyzed reduction currents of these acids. This is attributed to the formation of a mixed heteropolyacid of molybdenum(VI) and tungsten(VI) which does not cause a catalytic reduction at potentials where molybdenum yields a limiting catalytic current. The molybdenum(V)-catalyzed reduction current of chloric acid is greatly enhanced by the presence of tungsten(VI) in the bulk of the solution, and the sensitivity of the polarographic molybdenum determination is increased by one order of magnitude in the presence of $2 \cdot 10^{-4}$ M tungstate in a mixture 1 M in perchloric acid and 0.5 M in sodium chlorate. It is suggested that the exaltation can be used for the determination of small concentrations of tungsten(VI).

REFERENCES

1 I. M. KOLTHOFF AND I. HODARA, *J. Electroanal. Chem.*, 5(1963) 2.

THE DETERMINATION OF RHODIUM AND PALLADIUM USING OSCILLOGRAPHIC POLAROGRAPHY

W. H. DOUGLAS AND R. J. MAGEE

Department of Chemistry, The Queen's University, Belfast (N. Ireland)

(Received July 30th, 1962)

Most of the platinum metals catalyse the reduction of the hydrogen ion at the dropping electrode and the oxidation potentials of the various couples involving these metals are high. This results in reduction to the metallic state on contact with mercury. As a result, the number of polarographic methods available for the determination of the platinum metals is small. It is only within the past few years that these difficulties associated with the platinum metals have been solved[1], mainly by complexing with a reagent which is not spontaneously reduced. WILLIS[2] studied the reduction of a number of complex compounds of rhodium(III) at the dropping electrode and recommended $RhPy_6Cl_3$ as the best for determination of the element. For palladium the same author[3] suggested that several complexes of the metal could be used analytically within a limited range of concentration. WILSON AND DANIELS[4] studied the determination of palladium in an ammoniacal medium (where the complex is $Pd(NH_3)_4^{2+}$), but found interference from rhodium and iridium.

However, it seems that the choice of complexing agent has always been empirical in nature. In the present work an approach is made to the problem of formulating principles of choice of complexing agent using the Ligand Field theory.

THE LIGAND FIELD THEORY

The Ligand Field theory[5,6] deals with the relation of the behaviour of non-bonding electrons in the valency shell of an atom to the symmetry and strength of the electric field arising from the attached ligands. This theory has interested chemists in connection with absorption spectra of complexes, stereochemistry, and magnetic behaviour. The basic physical idea of the Ligand Field theory is that the electrons of the central metal ion tend to avoid those regions where the field due to the attached negative ions is largest. This tendency results in the removal of the degeneracy of the ground state of transition metal ions. Thus, in the case where $6CN^-$ ligands are brought up to the Fe^{3+} ion the following occurs:

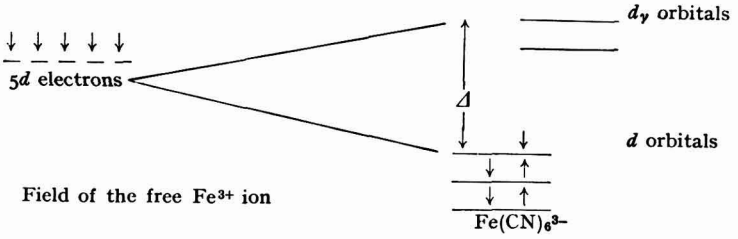

i.e., a set of d orbitals of lower energy and a set of d_γ orbitals of higher energy are produced.

The energy of separation, Δ, between these two levels, where the central metal ion is the same, depends on the strength of the applied field, *i.e.* on the incoming ligand, so that changing the field by changing the ligand has a significant effect.

In 1938, Tuschida discovered that certain spectral peaks of given complexes changed their position as the ligands were replaced by new ones. Much later this shift of peak was rationalised in terms of Ligand Field theory given above.

The relevant peak (d–d transition peak) was engendered by the promotion of an electron from d_ε to d_γ levels, with a concomitant absorption of energy. As the separation, Δ, of the two levels increased, the spectral peaks moved to shorter wavelengths because more energy was required.

From observations of the absorption spectra of metal ions the size of Δ for almost any metal and set of ligand can be deduced. With metal ions in their normal valencies the following series for increasing Δ is found: I^-, Br^-, Cl^-, F^-, SCN^-, H_2O, oxalate, pyridine, NH_3, ethylenediamine, NO_2^-, CN^-.

However it will also be realised that any physical phenomenon which involves the addition of one or more electrons is going to become more difficult (require more energy) as the separation Δ increases. Polarography presents such a case. Therefore, it can be seen that there is a relation between optical and polarographic properties.

This is borne out in practice by the well-known observation that the half-wave potential moves to more negative values on complex formation. For a series of ligands given above the $E_{\frac{1}{2}}$ becomes more negative as we move to the right, *i.e.* the complex becomes more stable towards mercury. It has already been noted that the platinum metals are spontaneously reduced by mercury. However, one now has a principle to follow in choosing a complexing agent for analytical purposes (according to its position in the spectrochemical series). For instance, if the thiocyanate complex of a platinum metal is spontaneously reduced, there is no point in trying a chloro-complex as this will also be spontaneously reduced; a suitable complexing agent might be found between SCN^- and CN^- in the spectrochemical series.

However, it is also necessary that the electrode reaction should be fast in order that the process should be diffusion-controlled. The authors have found that this phenomenon acts conversely to the stability of the complex towards mercury. In other words, in the normal spectrochemical series, chloro-complexes tend to be reversibly reduced, and the reduction of cyano-complexes tends to be kinetically controlled. Therefore, a suitable complexing agent represents a balance between stability on the one hand and reactivity on the other. Its choice is indicated by the spectrochemical series, interpreted in the light of the Ligand Field theory.

EXPERIMENTAL

In the following work a K 1000 Cathode Ray Polarograph supplied by Southern Instruments was used. The ligands with which investigations were carried out were Cl^-, SCN^-, pyridine, NH_3, and CN^-. In general, investigations were begun with the chloro-complex and the ligand changed through the series. No special conditions were necessary to effect the ligand change. In Table I the polarographic behaviour of five of the platinum metals in complexes with these ligands is shown. The cross ($\times$)

indicates the presence of a reduction wave, while a stroke (—) indicates that no polarographic wave was formed.

TABLE I

Metal/Ligand	*Cl–*	*SCN–*	*Pyridine*	NH_3	*CN–*
Ru	×	×	×	×	×
Rh	×	×	×	×	×
Pd	—	—	×	×	×
Os	—	—	—	—	—
Ir	—	—	—	—	—

Rhodium

A number of complexes of rhodium were investigated by WILLIS[2] at the dropping mercury electrode. He found that $[Rh(CN)_6]^{3-}$, $[Rh(NH_3)_5Cl]^{2+}$ $[Rh(CNS)_6]^{3-}$ and $[Rh(Py)_6]^{3+}$ gave clearly defined polarographic waves and recommended the pyridine complex for the determination of rhodium. REPIN[7] also used the pyridine complex of rhodium(III) for the determination of the element. (Py represents pyridine.)

It will be seen from Table I that, in agreement with WILLIS, rhodium gives clearly defined polarographic waves for all the complexes shown. Of these the best was $[Rh(CNS)_6]^{3-}$, which gave a very clear reduction wave at $E = -0.60$ V. The height of this peak was examined for use in quantitative determinations. The complex was prepared by dissolving the chloro-compound of rhodium in a 1 *M* thiocyanate solution. To obtain a good wave and ensure quantitative complex formation it is necessary to boil the mixture for a few minutes and then cool before registering the polarogram. Amounts of rhodium of 10^{-3} g and less were polarographed. It is possible to determine amounts of rhodium as low as $5 \cdot 10^{-5}$ *M* with ease. Smaller amounts may be determined, but minor features of the polarogram are enlarged and accuracy is forfeited.

Palladium

WILLIS[3] obtained polarographic waves for the cyanide, ammonia and pyridine complexes of palladium, but claimed that they could not be used analytically at concentrations of approximately $5 \cdot 10^{-5}$ *M*. RUIS AND MOLERA[8], on the other hand contradict WILLIS and claim that palladium is not reduced from a cyanide solution. WILSON AND DANIELS[4] studied the conditions for the determination of palladium in ammoniacal solution and found that rhodium and iridium interfere in the determination.

In the present work it can be seen from Table I that good polarographic reduction waves were obtained for the pyridine, ammonia and cyanide complexes. It was found that the polarographic reduction waves for these three complexes are reversible and increase linearly with the concentration of palladium. The wave of the pyridine complex is particularly good for the determination of the metal.

The analysis of rhodium–palladium alloys

Since the palladium thiocyanate complex is spontaneously reduced by the mercury drop (*cf.* Table I), it does not interfere with the rhodium thiocyanate reduction peak used for the determination of rhodium. This point was confirmed by preparing a calibration curve for rhodium, in which varying arbitrary amounts of palladium were included (Fig. 1). It was clear, therefore, that the most suitable method for polarographic determination of rhodium was likely to be based on the thiocyanate complex,

for those cases where palladium was likely to be present and its prior separation undesirable.

Experiments carried out on the dissolution of alloys showed that, where the rhodium content was moderate, solution was easily effected by aqua regia. When,

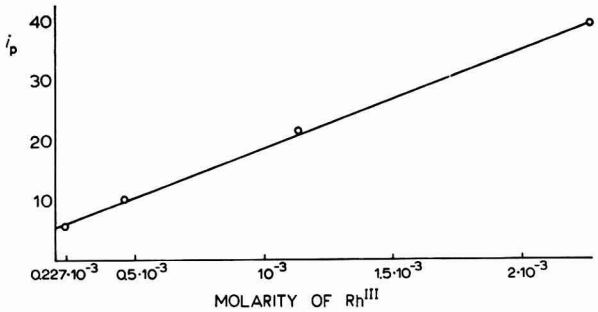

Fig. 1. Calibration curve for Rh–Rd alloys.

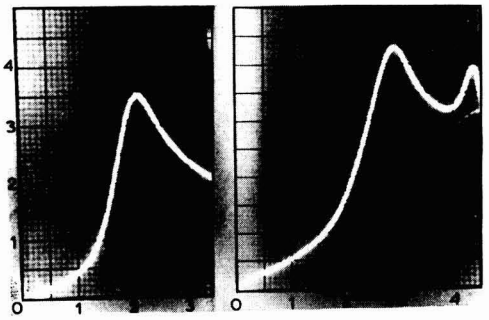

Fig. 2 Fig. 3

however, the rhodium content was large, all the rhodium did not go readily into solution but was left behind as a fine suspension which, after separation by filtration, could be brought into solution with sodium bisulphite fusion.

When the alloy was dissolved in aqua regia, experiments were carried out in an attempt to form the thiocyanate complex of rhodium in strong acid. This was not successful, since a polymer of thiocyanic acid was precipitated on heating to boiling. The acidity was therefore reduced before forming the complex. This was achieved by adding 5 *N* NaOH dropwise to the solution of the metals until a pH of 5 was obtained. Above pH 5 palladium hydroxide was precipitated. Potassium thiocyanate could now be added to the solution at pH 5 without the risk of precipitation on subsequent boiling. From Table I it can be seen that the first ligand to form a suitable complex with palladium is pyridine. Experiments were, therefore, carried out to see if palladium, as a constituent of an alloy, could be determined by means of the pyridine complex. An alloy was dissolved, and it was found that a palladium–pyridine complex was readily formed on addition of pyridine to the solution. The solution gave an excellent reduction wave suitable for the determination of palladium (Fig. 2).

A procedure was then developed for the determination of both elements in alloys, as follows: — Dissolve the alloy in aqua regia. Dilute the solution carefully and add 5 *N* NaOH, drop by drop, until a pH of 5 is obtained (Universal Indicator paper is satisfactory). Make the solution 1 *M* in potassium thiocyanate and bring to boiling point for twenty seconds. Cool to room temperature. Bring the total volume to 25 ml in a volumetric flask. Set the starting potential at −0.3 V and polarograph the solution, or an aliquot. Refer the peak height at −0.6 V to a prepared calibration graph and calculate the amount of rhodium in the alloy.

For the determination of palladium in the alloy, take the solution of aqua regia and dilute carefully. Add 5 ml. of pyridine. Polarograph the solution, setting the starting potential at −0.2 V and refer the peak height at −0.4 V to a prepared calibration graph. Calculate the amount of palladium in the alloy.

Results

The above procedure was tested on two alloys. These were supplied by the Mond Nickel Company and contained rhodium and palladium only. Each alloy was in the form of 32 gauge wire. Results are shown in Table II. It can be seen from these

TABLE II

Alloy	*Value supplied by Mond Nickel Co. for Rh content*	*Values obtained by the polarographic method*	
		Rh	*Pd*
1	~ 2%	1.88%	98.1%
2	~ 5%	4.8 %	95.2%

results that there is close agreement with the figures given by the Mond Nickel Company. The rhodium reduction wave corresponding to alloy no. 2 is shown in Fig. 3. The first peak is that due to the reduction of rhodium thiocyanate, while the second is an adsorption peak probably due to the species $Pd(SCN)_5OH$.

SUMMARY

Using oscillographic polarography, the half-wave potentials of rhodium and palladium were investigated in the presence of different ligands such as thiocyanate, pyridine, cyanide, etc. As a result of this investigation it was possible to form complexes of these metals which reduced readily at the dropping electrode, giving reduction waves which could be used quantitatively. For rhodium the thiocyanate complex was the most suitable, while for palladium the pyridine complex was best. By means of these complexes a method was developed which permits the determination of both elements in alloys, without prior separations.

REFERENCES

1 N. K. PSHENITSYN, N. A. EZERSKAYA AND M. B. BARDIN, *J. Anal. Chem. U.S.S.R.* English Transl., [4] 14 (1959) 499.
2 J. WILLIS, *J. Am. Chem. Soc.*, 66 (1944) 1067.
3 J. WILLIS, *J. Am. Chem. Soc.*, 67 (1945) 547.
4 R. WILSON AND R. DANIELS, *Anal. Chem.*, 27 (1955) 904.
5 R. J. GILLESPIE AND R. S. NYHOLM, *Quart. Rev. Chem. Soc.*, 11 (1957) 339.
6 J. S. GRIFFITH AND L. E. ORGEL, *ibid.*, 11 (1957) 381.
7 S. A. REPIN, *J. Appl. Chem.*, 20 (1947) 55.
8 A. RUIS AND M. MOLERA, *Anales Real. Soc. Espan. Fis. Quim. (Madrid)*, 45B (1949) 1151.

ÉTUDE DE COMPLEXES THIOCYANATE AU MOYEN DES VAGUES POLAROGRAPHIQUES CINÉTIQUES DU COMPLEXE MONOTHIOCYANATE DE TITANE(IV)

S. TRIBALAT ET J. M. CALDERO

Laboratoire de Chimie Physique de la Faculté des Sciences de Paris (France)

(Reçu le 31 juillet 1961)

INTRODUCTION

Dans un précédent mémoire de notre laboratoire, une nouvelle méthode d'étude des complexes a été décrite[2]; il s'agit d'une application de notre travail antérieur sur les vagues cinétiques que donnent certains composés électrochimiquement actifs en équilibre avec des ions simples moins actifs.

Parmi les complexes de titane actifs à électrode d'Gouttes de mercure, nous avions considéré, avec D. DELAFOSSE, les complexes thiocyanate — et montré que la réaction électrochimique est la suivante[1].

$$Ti(IV)SCN + e \rightleftarrows Ti(III)SCN$$

$E_0 \sim 0{,}V$ à pH 0, $I = 0.5$, $\theta \sim 20°$.

Pour une concentration donnée de Ti(IV), lorsque la concentration de l'ion complexant SCN^- est suffisamment faible, c'est la vitesse de la formation chimique du complexe

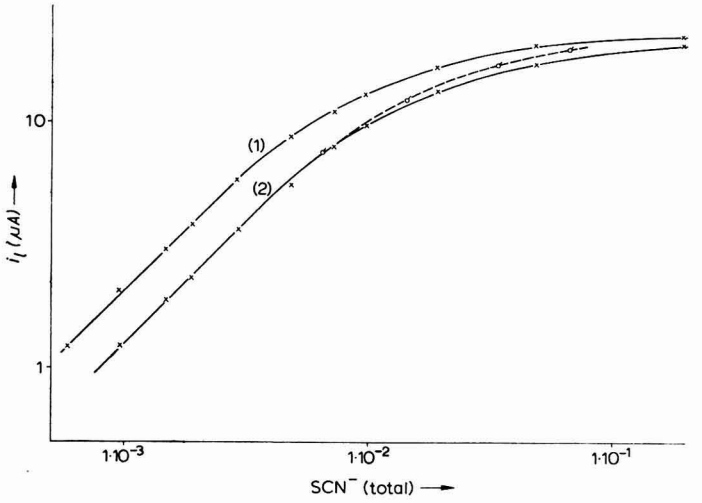

Fig. 1. (1), Ti(IV), $7.3 \cdot 10^{-3}$ M + $HClO_4$, 0.5 N + HCl, 0.3 N + SCN^-,variable; (2), Ti(IV), $7.3 \cdot 10^{-3}$ M + $HClO_4$, 0.5 N + HCl, 0.3 N + SCN^- variable + Ni(II), $4.33 \cdot 10^{-2}$ M, I_{NaClO_4} = 1.0; (3), ligne pointillée — courbe théorique calculée avec les valeurs de FRONAEUS.

Ti(IV)SCN qui limite la vitesse de réduction du Ti(IV) à l'électrode. On observe alors une vague cinétique dont la hauteur est proportionnelle à la concentration de l'ion SCN^- libre. Cette dernière se trouve confondue avec la concentration totale en ions thiocyanate, la quantité de thiocyanate liée au titane étant négligeable.

Lorsque, par contre, la concentration de SCN^- est assez élevée, la vitesse de la réaction chimique devient rapide et le courant limite ne dépend plus de cette concentration; il atteint une valeur maximum limitée par la vitesse de diffusion du Ti(IV) en solution.

Dans le travail préliminaire donnant le principe de la méthode[2], nous avons montré comment il est possible d'étudier des réactions qui font disparaître SCN^-, au moyen des vagues cinétiques, lorsque celles-ci ne sont pas perturbées par la présence de l'accepteur de SCN^- en prenant comme exemple la détermination des constantes des monothiocyanate de Co(II), Fe(III) et Cr(III).

Dans le présent travail, résumé par ailleurs[6], nous avons d'abord considéré la formation des complexes monothiocyanate de Ni(II), Cd(II), Mn(II) et de nouveau Co(II), en examinant la précision de cette méthode de détermination des constantes de réaction. Une fois connue la constante d'un certain complexe, il est possible de déterminer celle d'un autre complexe en équilibre avec le premier, dont la présence affecte la concentration des ions SCN^- dans la solution. Ainsi, nous avons obtenu des résultats satisfaisants dans le cas de complexes monochlorure[6]. Nous avons essayé ensuite de voir si la méthode permettait l'étude des complexes thiocyanate supérieurs des cations considérés.

CONDITIONS EXPÉRIMENTALES

Pour tracer les courbes $i = f(E)$, nous avons employé un polarographe Du Bellay A.O.I.P. La température de la cellule—facteur auquel les vagues cinétiques sont très sensibles—était maintenue constante à $25 \pm 0.05°$, au moyen d'un thermostat Prolabo. Tous les produits employés étaient de qualité *pur pour analyse*. Les dosages ont été effectués par les méthodes suivantes:

Ti(IV), par spectrophotométrie du complexe avec l'eau oxygénée,

SCN^-, par la méthode de Volhard,

Ni(II), Co(II), Cd(II), Mn(II); par volumétrie avec le sel disodique de l'acide éthylènediaminetétracétique en présence de l'indicateur noir ériochrome T.

Les solutions mères du Ti(IV) ont été préparées par précipitation de l'hydroxyde après hydrolyse de tétrachlorure de titane, suivie de la dissolution dans l'acide chlorhydrique ou dans l'acide perchlorique. Les solutions de Ni(II), Co(II) et Cd(II) ont été obtenues par dissolution des oxydes correspondants dans l'acide perchlorique et la solution de Mn(II), par action de l'acide perchlorique sur le carbonate de Mn(II).

COMPLEXE MONOTHIOCYANATE DE NICKEL

Après KISS[3] ET CSOKAN qui ont signalé l'existence de complexes thiocyanate de nickel, FRONAEUS[4] a étudié quantitativement ces complexes au moyen des échangeurs d'ions. Il a donné pour les constantes globales de formation à partir de Ni^{2+}, les valeurs:

$$\beta_1 = 15.0 \pm 0.5, \quad \beta_2 = 44 \pm 4, \quad \beta_3 = 65 \pm 10$$

à force ionique $I = 1$.

Sur la Fig. 2, la courbe de réduction du Ni(II) à l'électrode à gouttes de mercure en

présence d'ions SCN^- est représentée à côté de celle du complexe thiocyanate de titane dans le même milieu ; la hauteur de la vague de Ti(IV) est donc mesurable en présence de Ni(II). Nous avons remarqué que la réduction de Ni(II) est facilitée quand la concentration de SCN^- augmente comme cela a déjà été signalé[5]. Pour une solution donnée de Ti(IV), nous avons considéré le déplacement des courbes d'étalonnage $i_l = f(SCN^-)_t$ avec l'addition de Ni(II), toutes les autres concentrations demeurant égales par

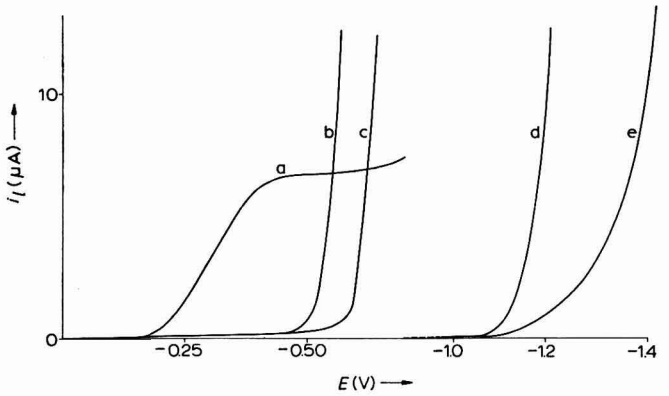

Fig. 2. (a), Ti(IV), $6.0 \cdot 10^{-3}$ M + SCN^-, $5 \cdot 10^{-3}$ M; (b), Cd(II), $5.07 \cdot 10^{-2}$ M + SCN^-, $5.62 \cdot 10^{-3}$ M; (c), Ni(II), $4.51 \cdot 10^{-2}$ M + SCN^-, $5.62 \cdot 10^{-3}$ M; (d), Co(II), $9.2 \cdot 10^{-2}$ M + SCN^-, $5.62 \cdot 10^{-3}$ M; (e), Mn(II), $6.85 \cdot 10^{-2}$ M + SCN^-, $5.62 \cdot 10^{-3}$ M. $I_{NaClO_4} = 1.5$, $H^+_{HClO_4} = 0.5$ N.

TABLEAU I

SCN⁻ total	*SCN⁻ libre*	*NiSCN⁺*	*Ni²⁺*	K_1
$9.65 \cdot 10^{-4}$	$5.85 \cdot 10^{-4}$	$3.80 \cdot 10^{-4}$	$4.29 \cdot 10^{-2}$	$6.6 \cdot 10^{-2}$
$1.38 \cdot 10^{-3}$	$8.30 \cdot 10^{-4}$	$5.50 \cdot 10^{-4}$	$4.27 \cdot 10^{-2}$	$6.4 \cdot 10^{-2}$
$2.05 \cdot 10^{-3}$	$1.24 \cdot 10^{-3}$	$8.10 \cdot 10^{-4}$	$4.25 \cdot 10^{-2}$	$6.6 \cdot 10^{-2}$
$2.90 \cdot 10^{-3}$	$1.75 \cdot 10^{-3}$	$1.15 \cdot 10^{-3}$	$4.21 \cdot 10^{-2}$	$6.4 \cdot 10^{-2}$
$3.75 \cdot 10^{-3}$	$2.26 \cdot 10^{-3}$	$1.49 \cdot 10^{-3}$	$4.18 \cdot 10^{-2}$	$6.3 \cdot 10^{-2}$
$4.60 \cdot 10^{-3}$	$2.77 \cdot 10^{-3}$	$1.83 \cdot 10^{-3}$	$4.14 \cdot 10^{-2}$	$6.3 \cdot 10^{-2}$

$K_d = (6.4 \pm 0.3) \cdot 10^{-2}$, $(I = 1)$.

TABLEAU II

Série	*Ti(IV)*	$HClO_4$	*HCl*	*Ni(II)*	I_{NaClO_4}	$K_d \cdot 10^{-2}$
1	$5.0 \cdot 10^{-3}$	0.5	$8 \cdot 10^{-3}$	$4.51 \cdot 10^{-2}$	0.7	6.1 ± 0.2
2	$5.0 \cdot 10^{-3}$	0.5	$8 \cdot 10^{-3}$	$4.51 \cdot 10^{-2}$	1.0	6.7 ± 0.2
3	$5.0 \cdot 10^{-3}$	0.5	$8 \cdot 10^{-3}$	$4.51 \cdot 10^{-2}$	1.5	7.6 ± 0.3
4	$5.0 \cdot 10^{-3}$	0.5	$8 \cdot 10^{-3}$	$4.51 \cdot 10^{-2}$	2.5	7.7 ± 0.2
5	$6.9 \cdot 10^{-3}$	0.5	0.3	$4.51 \cdot 10^{-2}$	5.0	5.4 ± 0.4
6	$7.3 \cdot 10^{-3}$	0.5	0.3	$4.33 \cdot 10^{-2}$	1.0	6.4 ± 0.3
7	$7.3 \cdot 10^{-3}$	0.5	0.3	$4.51 \cdot 10^{-2}$	1.0	6.5 ± 0.3
8	$7.3 \cdot 10^{-3}$	0.5	0.3	$4.51 \cdot 10^{-2}$	1.5	7.5 ± 0.3

ailleurs. Ainsi ont été tracées huit paires de courbes dont l'une est représentée Fig. 1. Deux solutions dont les points figuratifs ont mêmes ordonnées sur ces figures sont correspondantes, elles contiennent SCN^- libre à la même concentration. Cette dernière est directement connue, c'est l'abcisse du point figuratif de la courbe d'étalonnage[2].

Le Tableau I donne les valeurs de la constante de dissociation de $NiSCN^+$ calculée d'après les deux courbes de la Fig. 1.

Nous avons procédé de la même manière pour les huit séries: dans le Tableau II, sont groupées les valeurs obtenues pour la constante du premier complexe, dans différents milieux et pour différentes forces ioniques.

En considérant ce Tableau II, nous voyons d'abord que les déterminations de K_d sont très précises; les valeurs obtenues diffèrent de moins de 2% pour les deux séries 6 et 7 correspondant aux mêmes conditions expérimentales. La méthode utilise en effet une fonction expérimentale i_l sensible aux variations de notre variable puisqu'elle lui est proportionnelle. D'autre part cette variable est déterminée avec précision grâce à l'étalonnage obtenu dans les mêmes conditions. La connaissance des constantes électrochimiques est inutile et la manière de déterminer graphiquement i_l a relativement peu d'importance. Il faut seulement opérer toujours de la même manière.

D'après les séries 2–7 et 3–8, le Ni(II) ne serait pas sensiblement complexé par les ions Cl^- à la concentration $\leqslant 0.3\ M$; à force ionique constante, la présence de ces ions ne fait pas varier la concentration des ions SCN^- libres en solution.

TREMILLON a donné la valeur 4.6 pour la constante de dissociation de $NiCl^+$ ($I = 1.5$). D'après cette valeur, la proportion de $NiCl^+$ serait égale à 0.2% du Ni(II) dans nos solutions $8 \cdot 10^{-3}\ M$ en Cl^-, et 6% dans nos solutions $0.3\ M$. En considérant notre précision, nous avons pensé que la constante de dissociation de $NiCl^+$ devait être un peu plus élevée que ne l'indique TREMILLON. Une étude spectrophotométrique de l'absorption de $NiSCN^+$ dans l'ultra-violet, avec et sans ions Cl^-, nous a donné, $K_{NiCl^+} = 7.3 \pm 0.5$ ($I = 1.5$)[6]. La proportion de $NiCl^+$ pour Cl^- $0.3\ M$ est donc de l'ordre de grandeur de l'erreur expérimentale ce qui explique que les ions Cl^- ne modifient pas les résultats pour $Cl^- \leqslant 0.3\ M$.

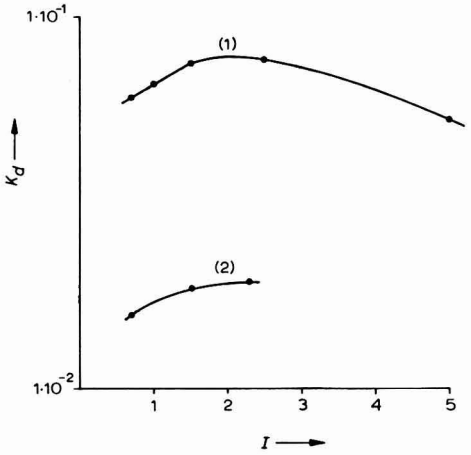

Fig. 3. Log $K_d = f(I)$: (1), pour Ni(II); (2), pour Mn(II).

A partir des valeurs de K_d du tableau II, nous avons tracé la courbe $\log K_d = f(I)$ (Fig. 3). Notre valeur de K_d pour $I = 1$, $(6.7 \pm 0.2)\,10^{-2}$, soit $\beta_1 = 14.9$, correspond exactement à celle donnée par FRONAEUS ($\beta_1 = 15$ pour $I = 1$).

COMPLEXE MONOTHIOCYANATE DE COBALT

Les complexes thiocyanate de cobalt ont déjà été étudiés, en particulier dans notre laboratoire[7], où les valeurs 9 ± 1.5, 40 ± 15 et 60 ± 20 ont été trouvées pour les constantes de formation β_1, β_2 et β_3. Dans le travail préliminaire sur l'utilisation des vagues cinétiques pour l'étude des complexes, nous avions déjà donné comme exemple le monothiocyanate de cobalt[2]. En effet, les positions relatives des courbes de réduction du Co(II) et du Ti(IV) en présence d'ions SCN^- sont très favorables à l'emploi de cette méthode. Nous avons repris l'étude du Co(II) pour tracer la courbe $i_l = f(SCN^-)$ dans un plus grand domaine de concentration et pour chercher la meilleure précision.

Les courbes de la Fig. 4 permettant de calculer $K_d = (1.04 \pm 0.03)10^{-1}$, Tableau III,

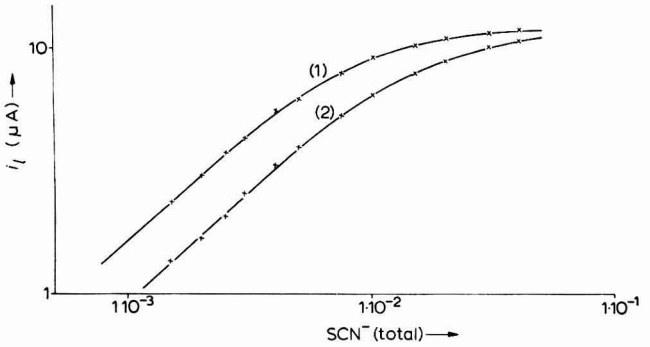

Fig. 4. (1), Ti(IV), $6.0 \cdot 10^{-3}$ M + $HClO_4$, 0.6 N + SCN^-, variable; (2), Ti(IV), $6.0 \cdot 10^{-3}$ M + $HClO_4$, 0.6 N + SCN^-, variable + Co(II), $9.28 \cdot 10^{-2}$ M. $I_{NaClO_4} = 1.5$.

TABLEAU III

SCN^- total	SCN^- libre	$CoSCN^+$	Co^{2+}	K_1
$2.36 \cdot 10^{-3}$	$1.25 \cdot 10^{-3}$	$1.11 \cdot 10^{-3}$	$9.17 \cdot 10^{-2}$	$1.03 \cdot 10^{-1}$
$3.03 \cdot 10^{-3}$	$1.62 \cdot 10^{-3}$	$1.41 \cdot 10^{-3}$	$9.14 \cdot 10^{-2}$	$1.05 \cdot 10^{-1}$
$3.71 \cdot 10^{-3}$	$2.00 \cdot 10^{-3}$	$1.71 \cdot 10^{-3}$	$9.11 \cdot 10^{-2}$	$1.06 \cdot 10^{-1}$
$4.42 \cdot 10^{-3}$	$2.37 \cdot 10^{-3}$	$2.05 \cdot 10^{-3}$	$9.07 \cdot 10^{-2}$	$1.05 \cdot 10^{-1}$
$5.18 \cdot 10^{-3}$	$2.76 \cdot 10^{-3}$	$2.42 \cdot 10^{-3}$	$9.04 \cdot 10^{-2}$	$1.03 \cdot 10^{-1}$

$K_d = (1.04 \pm 0.03)\ 10^{-1}$, $(I = 1.5)$.

pour $I NaClO_4 = 1.5$, valeur en très bon accord avec nos premiers résultats ($K_d = 8.8 \cdot 10^{-2}$, $I_r = 0{,}82$), si on tient compté de l'influence de la force ionique. Nous avons tracé une autre paire de courbes non représentée ici pour une concentration en cobalt et une force ionique un peu différentes, $Co(II) = 7.86 \cdot 10^{-2}$, $(I = 2)$. Le calcul donne la même valeur $K_d = (1.04 \pm 0.03)10^{-1}$; nous sommes en effet dans le domaine où la constante ne varie pratiquement pas avec la force ionique (Fig. 3).

COMPLEXE MONOTHIOCYANATE DE CADMIUM(II)

Des méthodes variées — polarographie, potentiométrie, spectrophotométrie—ont été utilisées pour étudier les complexes thiocyanate de cadmium[8,9,10]. Les valeurs $pK_1 = 1.39$, $pK_2 = 0.59$ et $pK_3 = 0.60$ ($I = 3$) ont été données par LEDEN et les valeurs $pK_1 = 1.04$, $pK_2 = 0.71$, $pK_3 = 0.97$ et $pK_4 = 1.00$ par HUME ($I = 2$). D'après la Fig. 2, la courbe de réduction du Cd(II) est proche de celle du Ti(IV). La détermination de la constante K_d à partir des courbes de la Fig. 5 est donc un peu moins bonne que dans les cas précédents. Nous trouvons $K_d = (4.9 \pm 0.4)10^{-2}$ pour $I = 1$, Tableau IV, valeur plus proche de celle de LEDEN que de celle de HUME.

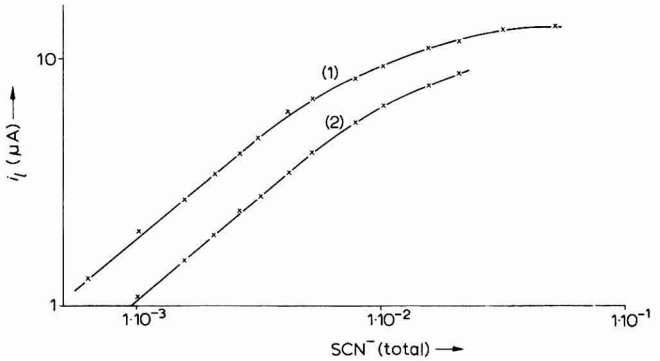

Fig. 5. (1), Ti(IV), $5.0 \cdot 10^{-3}$ M + $HClO_4$, 0.5 N + Cl^-, $8 \cdot 10^{-3}$ + SCN^-, variable; (2), Ti(IV), $5.0 \cdot 10^{-3}$ M + $HClO_4$, 0.5 N + Cl^-, $8 \cdot 10^{-3}$ + SCN^-, variable + Cd(II), $4.9 \cdot 10^{-2}$ M. $I_{NaClO_4} = 1$.

TABLEAU IV

SCN⁻ total	*SCN⁻ libre*	*CdSCN⁺*	*Cd²⁺*	K_1
$1.54 \cdot 10^{-3}$	$7.8 \cdot 10^{-4}$	$7.6 \cdot 10^{-4}$	$4.83 \cdot 10^{-2}$	$4.96 \cdot 10^{-2}$
$2.16 \cdot 10^{-3}$	$1.09 \cdot 10^{-3}$	$1.07 \cdot 10^{-3}$	$4.80 \cdot 10^{-2}$	$4.88 \cdot 10^{-2}$
$2.80 \cdot 10^{-3}$	$1.43 \cdot 10^{-3}$	$1.37 \cdot 10^{-3}$	$4.77 \cdot 10^{-2}$	$4.98 \cdot 10^{-2}$
$3.50 \cdot 10^{-3}$	$1.79 \cdot 10^{-3}$	$1.71 \cdot 10^{-3}$	$4.73 \cdot 10^{-2}$	$4.95 \cdot 10^{-2}$
$4.16 \cdot 10^{-3}$	$2.15 \cdot 10^{-3}$	$2.01 \cdot 10^{-3}$	$4.70 \cdot 10^{-2}$	$5.03 \cdot 10^{-2}$
$4.90 \cdot 10^{-3}$	$2.53 \cdot 10^{-3}$	$2.37 \cdot 10^{-3}$	$4.66 \cdot 10^{-2}$	$4.93 \cdot 10^{-2}$

$K_d = (4.9 \pm 0.4)\ 10^{-2}$, ($I = 1.0$).

COMPLEXE MONOTHIOCYANATE DE MANGANÈSE(II)

Les complexes thiocyanate de manganèse n'ont pas été beaucoup étudiés. Un mémoire assez récent donne $K_1 = 0.058 \pm 0.002$, valeur obtenue par une méthode colorimétrique[11].

La position relative des courbes de réduction du Ti(IV) et du Mn(II) en présence d'ions SCN^- est très favorable à l'étude du complexe monothiocyanate au moyen des vagues cinétiques.

Le tracé d'une première paire de courbes pour une concentration de Mn(II) $6.86 \cdot 10^{-2}$ M nous a montré que le complexe $MnSCN^+$ est moins stable que les monocomplexes précédemment étudiés. Nous avons donc augmenté la concentration du Mn(II), ce qui améliore la précision en écartant les deux courbes, Fig. 6. Le tableau V

TABLEAU V

SCN^- total	SCN^- libre	$MnSCN^+$	Mn^{2+}	K_1
$1.61 \cdot 10^{-3}$	$1.00 \cdot 10^{-3}$	$6.1 \cdot 10^{-4}$	$1.1 \cdot 10^{-1}$	$1.80 \cdot 10^{-1}$
$2.01 \cdot 10^{-3}$	$1.26 \cdot 10^{-3}$	$7.5 \cdot 10^{-4}$	$1.1 \cdot 10^{-1}$	$1.85 \cdot 10^{-1}$
$2.68 \cdot 10^{-3}$	$1.69 \cdot 10^{-3}$	$9.9 \cdot 10^{-4}$	$1.1 \cdot 10^{-1}$	$1.88 \cdot 10^{-1}$
$3.36 \cdot 10^{-3}$	$2.12 \cdot 10^{-3}$	$1.24 \cdot 10^{-3}$	$1.1 \cdot 10^{-1}$	$1.88 \cdot 10^{-1}$
$4.02 \cdot 10^{-3}$	$2.55 \cdot 10^{-3}$	$1.47 \cdot 10^{-3}$	$1.1 \cdot 10^{-1}$	$1.90 \cdot 10^{-1}$

$K_d = (1.86 \pm 0.05) 10^{-1}$, $(I = 1.5)$.

résume le calcul de K_1 d'après la Fig. 6. Les valeurs moyennes K_d trouvées pour trois séries différentes figurent dans le Tableau VI. La force ionique agit comme dans le cas du nickel; nous avons porté les résultats log $K_d K = f(I)$ dans la Fig. 3.

La concentration du cation M^{2+} n'a pas d'influence sur la valeur de la constante de dissociation du complexe $M\,SCN^+$; les monocomplexes ne sont donc pas condensés.

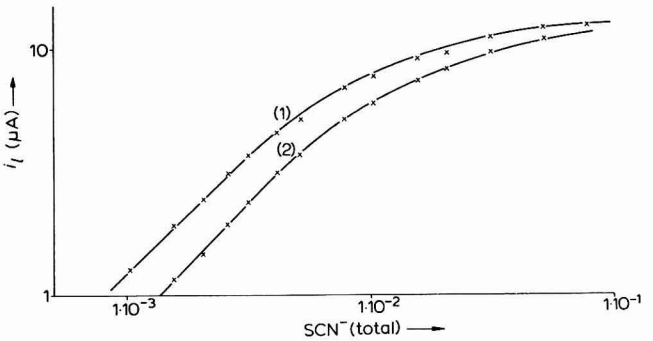

Fig. 6. (1), Ti(IV), $4.5 \cdot 10^{-3}$ M + $HClO_4$, 0.33 M + SCN^-, variable; (2), Ti(IV), $4.5 \cdot 10^{-3}$ M + $HClO_4$, 0.33 M + SCN^-, variable + Mn(II), $1.11 \cdot 10^{-1}$ M. $I_{NaClO_4} = 1.5$.

TABLEAU VI

Mn(II)	I	$K_{d\,MnSCN^+}$
$6.86 \cdot 10^{-2}$ M	0.7	$1.58 \cdot 10^{-1} \pm 0.07$
$1.11 \cdot 10^{-1}$ M	1.5	$1.86 \cdot 10^{-1} \pm 0.05$
$2.22 \cdot 10^{-1}$ M	2.3	$1.93 \cdot 10^{-1} \pm 0.03$

ÉTUDE DES COMPLEXES THIOCYANATE SUPÉRIEURS

Considérons les paires de courbes qui ont permis le calcul des constantes de dissociation K_1 en déformation β_1 dans le domaine cinétique; lorsqu'on effectue le même calcul pour les concentrations de SCN^- plus élevés, on constate que les valeurs trouvées pour β_1 augmentent régulièrement avec SCN^-. Ceci indique une consommation supplémentaire en ions complexants que l'on est tenté d'attribuer à la formation de complexes supérieurs. A partir de cette hypothèse, il est possible de déterminer

graphiquement les constantes de formation de ces complexes supérieurs au moyen d'une méthode inspirée de celle de LEDEN[12].

Dans le cas présent, la grandeur suivie expérimentalement est la concentration de l'ion complexant libre. En désignant par β_i les différentes constantes de formation globales à partir des ions M^{2+} on définit les fonctions

$$F = \frac{SCN^-_{complexe}}{(M^{2+})\,(SCN^-)} = \beta_1 + 2\beta_2\,(SCN^-) + 3\beta_3\,(SCN^-)^2 + \ldots$$

$$G = \frac{F-\beta_1}{2(SCN^-)} = \beta_2 + \tfrac{3}{2}\beta_3(SCN^-) + \ldots$$

$$H = \frac{G-\beta_2}{\frac{3}{2}(SCN^-)} = \beta_3 + \tfrac{4}{3}\beta_4(SCN^-)$$

lesquelles tendent respectivement vers β_1, β_2 et β_3 quand SCN^- tend vers zéro.

Il faut connaître la concentration M^{2+} pour tracer ces fonctions; on la calcule d'abord à partir de β_1 et d'une valeur approchée de β_2 obtenue en supposant un seul complexe supérieur $M\,(SCN)_2$ présent à côté de $M\,(SCN)^+$ connu, puis on reprend le calcul à partir des premières valeurs trouvées pour les constantes au moyen des fonctions. La correction est d'ailleurs faible tant que la concentration du cation métallique est grande devant celle du thiocyanate ce qui est souvent le cas. En effet, il n'est pas possible d'utiliser les portions de courbes qui sont trop proches du domaine de diffusion. Il serait cependant souhaitable d'augmenter la concentration du thiocyanate pour stabiliser les complexes supérieurs. Mais une telle augmentation entraîne rapidement une chute de précision dans la détermination de SCN^- libre,

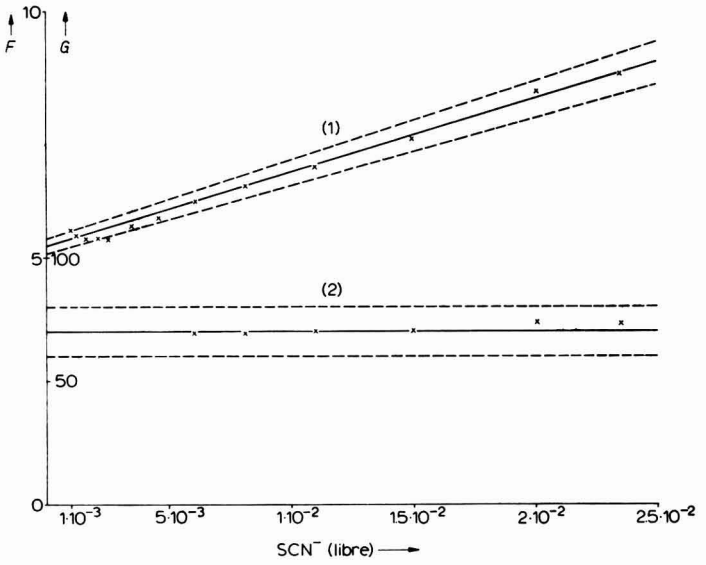

Fig. 7. Fonctions: (1), $F = f(SCN^-)$; (2), $G = f(SCN^-)$.

étant donné la forme des courbes. On doit donc s'attendre à déterminer les constantes supérieures avec une précision moins bonne que celle obtenue dans le cas des mono-

complexes dans le domaine cinétique favorable, ceci indépendamment du fait que les complexes supérieurs existent généralement plus ou moins tous ensemble avec le premier, ce qui diminue encore la précision.

Ces remarques sont valables dans le cas des cations considérés. Il en serait autrement dans le cas de complexes supérieurs plus stables qui seraient déjà formés dans le domaine cinétique[2].

Dans le cas du manganèse, la représentation des fonctions F et G (Fig. 7) nous a donné $\beta_1 = 5.3 \pm 0.1$ et $\beta_2 = 70 \pm 10$ $I\mathrm{NaClO_4} = 1.5$. La valeur de β_1 trouvée coïncide parfaitement avec celle déterminée précédemment dans un autre domaine de concentration des ions SCN^-. Les complexes étant peu stables, la concentration des ions Mn^{2+} diffère au plus de 15% de la concentration totale Mn(II) ce qui permet de calculer un premier jeu de valeurs β_1 et β_2 assez précises sans tenir compte du Mn(II) consommé. La nouvelle valeur de β_1 est ainsi obtenue independamment de celle déterminée dans le domaine cinétique.

Il est normal que l'existence d'un troisième complexe n'influence pas les courbes expérimentales; celui-ci n'est pas assez stable pour exister dans le domaine considéré ($SCN^- \leqslant 5 \cdot 10^{-2}$ M).

La précision est obtenue en faisant varier les courbes expérimentales $i_l = f(SCN^-)$ dans la limite de l'erreur.

Dans le cas des ions Ni^{2+}, Cd^{2+} et Co^{2+}, lorsqu'on tente le même calcul, celui-ci fait apparaître des complexes supérieurs particulièrement stables car il y a une forte disparition de thiocyanate lorsque ce dernier augmente. Nous trouvons en effet pour

$$\text{Ni(II)} : \beta_2 = 80 \pm 15, \quad \beta_3 = (5 \pm 3)10^3, \quad \beta_4 = (3 \pm 3)10^5.$$
$$\text{Cd(II)} : \beta_2 = 100 \pm 50, \quad \beta_3 = (7 \pm 2)10^4.$$
$$\text{Co(II)} : \beta_2 = 100 \pm 20, \quad \beta_3 = (2.5 \pm 1)10^3.$$

Comme le premier complexe existe pratiquement seul dans un domaine notable de SCN^-, le calcul conduit à adopter une grande valeur pour β_3 et une petite pour β_2. Ces résultats sont en contradiction avec les données bibliographiques et nous pensons finalement qu'ils sont aberrants; à la consommation des ions $SCN^- \simeq$ à la formation des complexes supérieurs, il doit s'ajouter soit une disparition supplémentaire d'ions SCN^-, soit une disparition de Ti(IV), cet effet parasite n'apparaissant qu'en présence des cations Ni^{2+}, Cd^{2+} et Co^{2+}. D'après quelques essais, ces cations ne semblent pas catalyser la réduction du thiocyanate dans notre milieu expérimental acide et mercure. Nous chercherons donc par d'autre méthodes si l'hypothèse de l'existence de complexes thiocyanate mixtes Ti(IV) cation M^{2+} peut être ou non retenue.

Sur la Fig. 1, est representée en pointillés la courbe $SCN_l^- = f(SCN^-)_t$ calculée à partir des constantes de FRONAEUS pour le nickel. L'écart entre cette courbe et notre courbe expérimentale est trop grand pour être attribué aux erreurs. Depuis ces essais polarographiques, nous avons repris l'étude des complexes supérieurs de nickel et cadmium, d'une manière toute différente, au moyen des équilibres d'extraction. Les constantes de formation trouvées alors, dans des conditions expérimentales favorables, sont inférieures à celles données ci-dessus[13].

Pour conclure, il faut remarquer la très bonne précision (2–3%) avec laquelle la méthode permet la détermination des constantes dans le cas des monocomplexes

présents dans le domaine cinétique lorsque la réduction du cation étudié ne perturbe pas celle du titane. Cette méthode est d'autre part susceptible d'une certaine généralisation; nous avons observé que d'autres complexes de Ti(IV) donnent des vagues cinétiques dont la hauteur est fonction de la concentration de l'ion complexant. Nous avons commencé l'étude des complexes oxalate, tartrate et citrate.

D'autre part, comme nous l'avons montré dans le cas des complexes chlorure[6], il est possible d'éludier indirectement les associations des cations métalliques considérés avec des anions différents de ceux qui provoquent les vagues cinétiques.

Enfin parmi les ions réductibles lentement à l'électrode à gouttes de mercure, ceux du Ti(IV) ne sont pas les seuls susceptibles de donner des complexes plus électroactifs que les ions simples.

Remarque. Nous n'avons pas tenu compte de la faible proportion d'acide HSCN présente dans les solutions 0.5 N en ions H^+. En fait, toutes les constantes des monocomplexes doivent être multipliées par le facteur $1 + H^+/k_a$, k_a étant la constante de dissociation de l'acide[1].

RÉSUMÉ

La détermination de la hauteur des vagues cinétiques du monocomplexe thiocyanate de Ti(IV) en présence de cations complexant SCN^- nous a permis de déterminer les constantes de formation des complexes monothiocyanate de nickel, cobalt, cadmium et manganèse. Cette nouvelle méthode d'étude des complexes au moyen de vagues cinétiques peut être précise.

Ni(II): $\beta_1 = 16.4 \pm 0.6$ ($I_{NaClO_4} = 0.7$), $\beta_1 = 14.9 \pm 0.5$ ($I = 1.0$), $\beta_1 = 13.2 \pm 0.5$ ($I = 1.5$), $\beta_1 = 13.0 \pm 0.3$ ($I = 2.5$), $\beta_1 = 18.5 \pm 1.5$ ($I = 5.0$).

Co(II): $\beta_1 = 9.6 \pm 0.4$ ($I_{NaClO_4} = 1.5$), $\beta_1 = 9.6 \pm 0.4$ ($I = 2$).

Cd(II): $\beta_1 = 20.4 \pm 1.5$ ($I_{NaClO_4} = 1.0$).

Mn(II): $\beta_1 = 6.3 \pm 0.3$ ($I_{NaClO_4} = 0.7$), $\beta_1 = 5.4 \pm 0.1$ ($I = 1.5$), $\beta_1 = 5.2 \pm 0.1$ ($I = 2.3$)

De l'étude des complexes supérieurs qui a été entreprise ensuite, nous avons retenu seulement celle du Mn(II), $\beta_1 = 5.3 \pm 0.1$, $\beta_2 = 70 \pm 10$ ($I_{NaClO_4} = 1.5$).

Toutes les valeurs ont été obtenues en milieu acide perchlorique, à une température de 25°.

BIBLIOGRAPHIE

1 S. TRIBALAT ET D. DELAFOSSE, *Anal. Chim. Acta*, 19 (1958) 74; D. DELAFOSSE, *Thèse*, Paris, 1956.
2 S. TRIBALAT, D. DELAFOSSE, C. PIOLET ET C. ZELLER, *J. Electronal. Chem.*, 1 (1960) 443.
3 A. KISS ET P. CSOKAN, *Z. Anorg. Allgem. Chem.*, 245 (1941) 355.
4 S. FRONAEUS, *Acta Chem. Scand.*, 7 (1953) 21.
5 J. J. LINGANE ET H. KERLINGER, *Ind. Eng. Chem., Anal. Ed.*, 13 (1941) 77.
6 S. TRIBALAT ET J. M. CALDERO, *C.R.*, 255 (1962) 925.
7 C. ZELLER, *Diplôme d'études supérieures*, Paris, 1959.
S. STRIBALAT ET C. ZELLER, *Bull. Soc. Chim.*, (1962) sous presse.
8 I. A. KORSHUNOV, N. I. MALYVGINA ET O. M. BALANOVA, *Zh. Obshch. Khim.*, 21 (1951) 620.
9 D. N. HUME, D. D. DETFORD ET G. C. B. CAVE, *J. Am. Chem. Soc.*, 73 (1951) 5323.
10 I. A. M. GOLUB ET O. G. BILYK, *Zh. Neorgan. Khim.*, 2 (1957) 2723.
11 K. B. YATSIMIRSKII ET V. D. KORABLEVA, *Zh. Neorgan. Khim.*, 3 (1958) 339.
12 I. LEDEN, *Dissertation*, Lund, 1943.
13 S. TRIBALAT ET J. M. CALDERO, — à paraître.

POLAROGRAPHISCHE UNTERSUCHUNGEN BEI REGULIERUNG DER TROPFZEIT DURCH ABSCHLAGEN DES TROPFENS

I. DIE TROPFZEITABHÄNGIGKEIT POLAROGRAPHISCHER STRÖME

D. WOLF

*Institut für Physikalische Chemie der Universität, Bonn (Deutschland)**

(Eingegangen am 27 August, 1962)

A. EINLEITUNG

Bei dem von der Metrohm AG entwickelten Verfahren der Rapidpolarographie[1] wird der Quecksilbertropfen nach 0.2 bis 1.0 sec von der Kapillare abgeschlagen, bevor er auf Grund seines Gewichtes abreissen kann. Durch die hohe Tropffrequenz können Polarogramme in weniger als 1.5 min aufgenommen werden. Bei Konstanthalten der Niveauhöhe und der Tropfzeit ist der gemessene Grenzstrom proportional der Konzentration des Depolarisators in der Lösung. Er kann also zur vergleichenden, quantitativen Analyse herangezogen werden. Darüberhinaus lässt sich die Tropfzeitabhängigkeit polarographischer Ströme bei Variation der Tropfzeit über einen grösseren Zeitbereich verfolgen. Hierbei wird man aber nur dann einwandfreie Ergebnisse erhalten, wenn der Mechanismus des Elektrodenprozesses durch das Abschlagen des Tropfens nicht verändert wird. In dieser Arbeit wird der Versuch unternommen, die aufgeworfene Frage experimentell durch Messung polarographischer Ströme bekannter Tropfzeitabhängigkeit zu beantworten. Zusätzlich werden Stromstärke–Zeitkurven am Einzeltropfen oszillographisch aufgenommen, um eventuelle Störungen sichtbar zu machen.

B. EXPERIMENTELLES

Zur Ausführung unserer Experimente haben wir den Polarographiestand E 354 der Metrohm AG benutzt. Die Kapillare hatte einen inneren Durchmesser von 0.0052 cm. Ihre Tropfzeit betrug ohne Abschlagen des Tropfens rund 5.0 sec bei einer Niveauhöhe von 70 cm. Die an die Tropfelektrode angelegte Spannung wurde gegen eine Silberchloridelektrode (0.1 *M* NaCl + 0.9 *M* $LiClO_4$/AgCl/AG) gemessen. Nachdem Polarogramme bei Variation der Tropfzeit aufgenommen worden waren, wurde die Elektrolysezelle zur Aufnahme von i–t-Kurven in den Spannungs- und Stromkreis eines Potentiostaten eingeschaltet. Zur Vermeidung des Verarmungseffektes wurde die Spannung erst im Augenblick des Tropfenabfalls angelegt und i–t-Kurven des ersten und zweiten Tropfens aufgenommen. Vor jedem Versuch wurde der Sauerstoff in der Lösung durch Durchleiten von Wasserstoff vertrieben. Während der Versuche lag die Raumtemperatur zwischen 24°–26°. Das Elektrolysegefäss selbst wurde auf 25° ± 0.1° thermostatiert.

* Diese Arbeit ist ein Teil der Dissertation von D. WOLF, Bonn, 1962.

C. DIE TROPFZEITABHÄNGIGKEIT DIFFUSIONSBEGRENZTER STRÖME

I. Der polarographische Grenzstrom der Cd^{2+}-Ionen

In Abb. 1 sind Polarogramme dargestellt, die bei konstanter Niveauhöhe unter Variation der Tropfzeit mit dem Rapidpolarographen aufgenommen wurden. Zu ihrer Auswertung wurde der Grenzstrom gegen den Grundstrom mit einer Genauig-

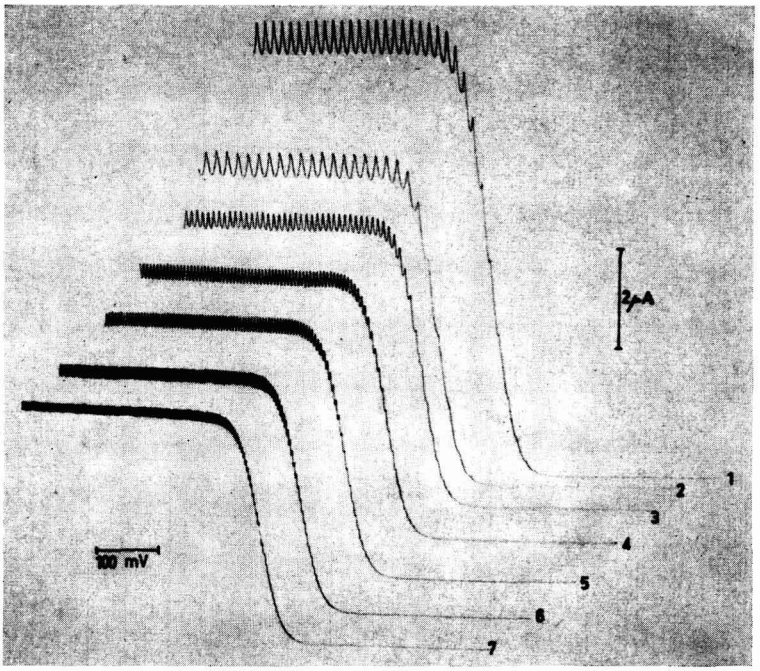

Abb. 1. $1.6 \cdot 10^{-3}$ *M* $CdSO_4$ in 0.99 *M* $LiClO_4$ + 0.01 *M* $HClO_4$ + $2.0 \cdot 10^{-3}$% Triton-x-305 als Maximadämpfer: (1) langsamer Spannungsdurchlauf ohne Abschlagen des Tropfens; (2)–(7) schneller Spannungsdurchlauf bei Abschlagen des Tropfens. Tropfzeit: (1) 3.85 sec; (2) 1.027 sec; (3) 0.530 sec; (4) 0.330 sec; (5) 0.280 sec; (6) 0.213 sec; (7) 0.180 sec.

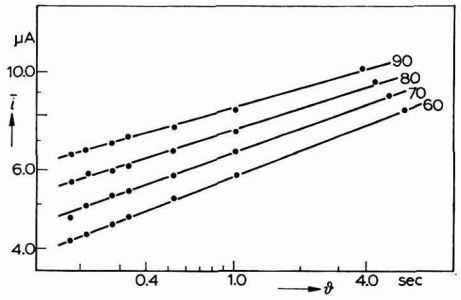

Abb. 2. Grenzstrom der Cd^{2+}-Ionen in Abhängigkeit von der Tropfzeit bei vier verschiedenen Niveauhöhen (90–60 cm Hg). Die Lösung besitzt dieselbe Zusammensetzung wie in Abb. 1, jedoch ohne Maximadämpfer; doppeltlogarithmischer Massstab.

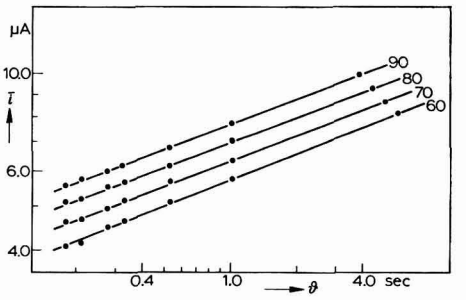

Abb. 3. Grenzstrom der Cd^{2+}-Ionen in Abhängigkeit von der Tropfzeit bei vier verschiedenen Niveauhöhen (9090 cm Hg); doppeltlogarithmischer Massstab; Zusammensetzung der Lösung wie in Abb. 1.

keit von ± 1.0% vermessen. Bei der Bestimmung der kleinen Tropfzeiten wurde die Spannung auf einen Wert im Bereich des Grenzstromes der Cd-Stufe eingestellt und die Zacken während einer Zeit von 1.5 Minuten bei laufendem Papiervorschub aufgezeichnet. Man erhält die Tropfzeit, indem man die Zacken auszählt und ihre Zahl durch die gemessene Zeit dividiert. Die so gewonnenen Tropfzeiten schwanken um ± 0.4%.

Trägt man den Grenzstrom i_d gegen die Tropfzeit ϑ in doppelt logarithmischem Massstab auf, so ergibt sich von der Theorie her bei Zugrundelegung der einfachen Ilkovičgleichung eine Gerade, deren Steigung 1/6 = 0.167 ist. Bei Berücksichtigung der sphärischen Diffusion durch Anwendung der verbesserten Ilkovičgleichung erhöht sich dieser Wert für einen Tropfzeitbereich von 0.2 bis 5.0 sec im Mittel. auf 0.179 ± 0.003.

In Abb. 2 und in Abb. 3 sind die experimentell ermittelten Geraden für vier verschiedene Niveauhöhen eingezeichnet. Die dazugehörigen Steigungen sind in Tabelle I eingetragen.

TABELLE I

Niveauhöhe cm Hg	*Lösung 4 Dämpfer*	*Lösung mit 2.0 · 10⁻³% Triton*	*Spalte ohne*
90	0.147	0.185	0.175
80	0.167	0.185	0.175
70	0.182	0.189	0.179
60	0.193	0.198	0.182

Ohne Zugabe von Maximadämpfer variieren die Neigungen ziemlich stark, was auf die Wirksamkeit des *Spüleffektes* zurückzuführen ist: Das in den Tropfen fliessende Quecksilber verursacht bekanntlich eine Bewegung der Grenzfläche Quecksilber-Elektrolytlösung, so dass eine erhöhte Nachlieferung des Depolarisators durch Konvektion erfolgt. Diese Bewegung ist bei kleinen Tropfen heftiger, da bei konstanter Niveauhöhe der gleiche Impuls auf eine kleinere Masse übertragen wird. Die Stromstärke ist deshalb bei kleinen Tropfzeiten stärker überhöht als bei grossen, so dass die Steigung der Geraden zu klein ausfällt.

Durch Zusatz von genügend Dämpfer lässt sich der Spüleffekt weitgehend ausschalten. Die Steigungen liegen aber nun alle oberhalb der theoretisch zu erwartenden von 0.179. Dieses Ergebnis wird verständlich, wenn man die *Ausfliessgeschwindigkeit* m des Quecksilbers aus der Kapillare ermittelt. Es zeigt sich nämlich, dass der m-Wert umso kleiner ausfällt, je häufiger der Tropfen abgeschlagen wird (s. Abb. 4). Eine qualitative Erklärung für diese Erscheinung ergibt sich bei Berücksichtigung des *Rückdruckes* $p_r = 2\sigma/r$ (σ = Grenzflächenspannung, r = Radius des Tropfens). Zu Beginn des Tropfenwachstums besteht der Tropfen aus einer Halbkugel, deren Radius dem der Kapillare entspricht. In diesem Stadium hat der Rückdruck seinen maximalen Wert[2]*. Er nimmt bei Grösserwerden des Tropfens schnell ab. Je häufiger dieses Stadium durchlaufen wird, umso grösser ist der Einfluss des Rückdrucks auf

* Für die von uns verwendete Kapillare (r = 0.0026 cm) errechnet sich ein Rückdruck im Halbkugelstadium des Tropfens von 23 cm Hg bei einer Grenzflächenspannung von σ = 400 dyn/cm.

die Ausfliessgeschwindigkeit, die proportional zu der Differenz $p_h - p_r$ ist*. Eine quantitative Berechnung des Rückdruckeinflusses ist nicht möglich, da die Grenzflächenspannung während der Lebensdauer des Tropfens durch Adsorption grenzflächenaktiver Stoffe abnimmt. Eine Berechnung dieser zeitlichen Änderung von σ ist nicht möglich, da gerade am Anfang der Tropfzeit der Antransport grenzflächenaktiver Stoffe nicht nur durch Diffusion, sondern auch durch Konvektion erfolgen wird.

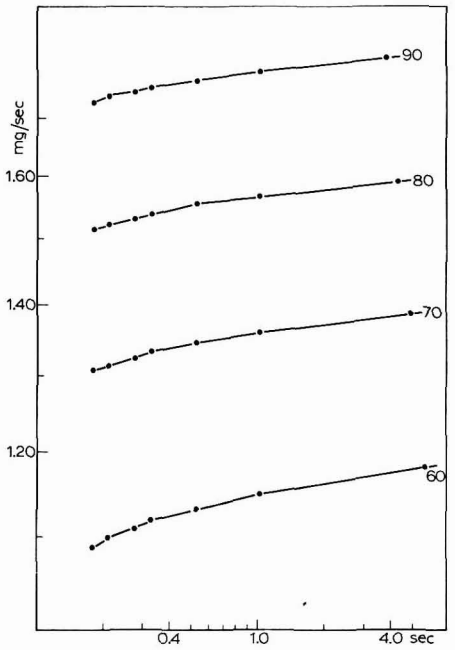

Abb. 4. Ausfliessgeschwindigkeit m des Quecksilbers aus der Kapillare in Abhängigkeit von der Tropfzeit für vier verschiedene Niveauhöhen (90–60 cm Hg); doppeltlogarithmischer Massstab.

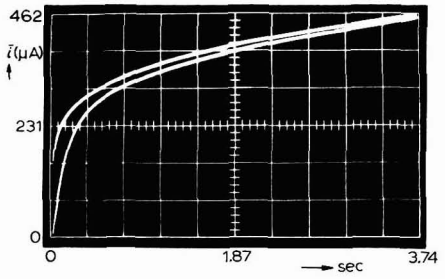

Abb. 5. Oszillographische Aufnahme der i–t-Kurve des 1. und 2. Tropfens ohne Abschlagen bei einer Niveauhöhe von 90 cm (Spannung = −1.0 V gegen N.K.E.); $2 \cdot 10^{-2}$ M $CdSO_4$ in 2.0 M $LiClO_4$ + $2.82 \cdot 10^{-3}$% Triton-x-305.

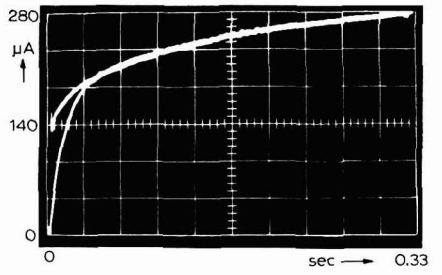

Abb. 6. Oszillographische Aufnahme der i–t-Kurven des 1. und 2. Tropfens bei durch Abschlagen erzeugter kurzer Tropfzeit von 0.33 sec (Zusammensetzung der Lösung wie in Abb. 5), Niveauhöhe 90 cm Spannung = −1.0 V gegen N.K.E.

* p_h = Druck der Quecksilbersäule auf Grund der Höhendifferenz zwischen Niveaugefäss und Kapillare.

Man kann jedoch eine annähernde rechnerische Beseitigung dieser Störung vornehmen, indem man die experimentell ermittelten m-Werte benutzt: Trägt man $\lg(i_d/m^{2/3})$ gegen $\lg \vartheta$ auf, so erhält man Geraden, deren Neigung in Spalte 4 der Tabelle 1 angegeben ist. Die so erzielte Übereinstimmung mit der Theorie ist recht gut, obwohl noch ein Gang in der Steigung zu erkennen ist.

Man kann also schon auf Grund dieser Messungen sagen, dass der Mechanismus des Elektrodenprozesses durch das Abschlagen des Tropfens nicht wesentlich gestört wird. Dieses Ergebnis konnte auch an Hand von i–t-Kurven bestätigt werden.

II. Die Gestalt der i–t-Kurven mit und ohne Abschlagen des Tropfens

Abbildung 5 zeigt zunächst zwei i–t-Kurven am ersten bzw. am zweiten Tropfen ohne Abschlagen des Tropfens, während Abb. 6 dasselbe bei durch Abschlagen erzeugter kurzer Tropfzeit von 0.33 sec wiedergibt.

Vergleicht man beide Bilder, so erkennt man, dass der *Verarmungseffekt* bei der kurzen Tropfzeit etwas geringer ist. Der Tropfen wächst schneller aus der verarmten Lösung heraus*. Besonders wichtig erscheint uns aber ein direkter Vergleich der i–t-Kurven mit und ohne Abschlagen.

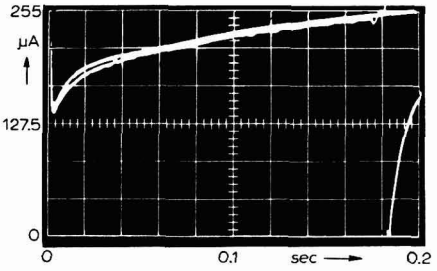

Abb. 7. i–t-Kurven mit und ohne Abschlagen des Tropfens bei einer Niveauhöhe von 90 cm. (Zusammensetzung der Lösung wie in Abb. 5) Spannung = −1.0 V. Erste Tropfen.

In Abb. 7 sind: (1), der Strom ohne Abschlagen während der ersten 0.2 sec, und (2), die gesamte i–t-Kurve bei einer kontrollierten Tropfzeit von 0.18 sec photographiert. Beide Kurven sind am ersten Tropfen gemessen. Sie fallen recht gut zusammen. Bei richtiger Einstellung der Grösse des Abklopfimpulses[1] liefert die Apparatur die gleichen Ströme, wie sie ohne Abklopfen erhalten werden. Das bedeutet, dass die sich ausbildende Diffusionsschicht nicht gestört wird.

D. DIE TROPFZEITABHÄNGIGKEIT REAKTIONSBEDINGER, POLAROGRAPHISCHER STRÖME

I. Kontrolle der Abklopfvorrichtung

Im vorhergehenden Kapitel wurde die Abklopfvorrichtung durch Messung des Diffusionsgrenzstromes untersucht. Eine weitere Kontrolle der Apparatur ist möglich durch Messung von reaktionsbedingten Strömen. In dieser Hinsicht können zwei Wege beschritten werden:

1. Bestimmung der Parameter der Durchtrittsreaktion eines irreversiblen Elektrodenprozesses.

* Die i–t-Kurven am 1. Tropfen beginnen nicht mit der Stromstärke Null, weil die Elektrode schon zu Beginn eine endliche Oberfläche besitzt, die zunächst auf das vorgeschriebene Potential aufgeladen werden muss.

2. Messung der Geschwindigkeit einer vorgelagerten chemischen Reaktion erster Ordnung.

Im Fall 1 wird die Tropfzeitabhängigkeit des Stromes im Stufenanstieg einer irreversiblen Stufe unter Festhalten des Potentials untersucht. Im Fall 2 wertet man den Grenzstrom einer "kinetischen" Stufe aus. KOUTECKÝ[3] hat gezeigt, dass beide Fälle mathematisch durch dieselbe Formel beschrieben werden.

$$\frac{\bar{\imath}}{\bar{\imath}_d} = \frac{k\sqrt{\vartheta}}{1 + k\sqrt{\vartheta}} \tag{1}$$

$\bar{\imath}$ = polarographischer Strom im Stufenanstieg bzw. im Grenzstrom der reaktionsbedingten Stufe

$\bar{\imath}_d$ = Diffusionsgrenzstrom bei unendlich schneller Reaktion

ϑ = Tropfzeit

k = Konstante, die im Falle einer Durchtrittshemmung deren potentialabhängige Geschwindigkeitskonstante, im Falle der kinetischen Hemmung einervorgelagerten Reaktion deren Geschwindigkeits- und Gleichgewichtskonstante enthält.

Nach Gleichung (1) hängt der Logarithmus des Stromes $\bar{\imath}$ nicht linear von lg ϑ ab. Will man die Brauchbarkeit der Abklopfvorrichtung wie in Kapitel C durch Auswertung der lg $\bar{\imath}$ gegen lg ϑ -Kurve kontrollieren, so muss man anstelle des gemessenen Stromes $\bar{\imath}$ den hieraus berechneten rein kinetischen Strom $\bar{\imath}_{kin}$ auftragen, bei dem die in $\bar{\imath}$ nocht enthaltene Diffusionshemmung eliminiert ist und der deshalb proportional zu $\vartheta^{2/3}$ anwächst. Man gewinnt $\bar{\imath}_{kin}$ aus $\bar{\imath}$ nach folgender Gleichung

$$\bar{\imath}_{kin} = \bar{\imath}(1 + k \cdot \sqrt{\vartheta}) \tag{2}$$

Nach Gleichung (2) ist zur Berechnung von $\bar{\imath}_{kin}$ die Kenntnis der Konstanten k erforderlich. Zur Bestimmung von k formt man Gleichung (1) zweckmässig um. Unter Berücksichtigung der hier gegebenen Konstanz der Niveauhöhe, d. h. der Konstanz der Ausfliessgeschwindigkeit m* erhält man durch Multiplikation von(1) mit $(\bar{\imath}_d + \bar{\imath}_d \cdot \sqrt{\vartheta})/k \cdot \vartheta^{2/3})$

$$\frac{\bar{\imath}}{\vartheta^{1/6}} = \text{const} - \frac{1}{k}\left(\frac{\bar{\imath}}{\vartheta^{2/3}}\right) \tag{3}$$

k ergibt sich somit aus der Steigung der Geraden $\bar{\imath}/\vartheta^{1/6} = f(\bar{\imath}/\vartheta^{2/3})$.

Bei unseren Experimenten haben wir einmal den Strom im Stufenanstieg der irreversiblen Ti^{4+}/Ti^{3+} Reduktion gemessen; zum anderen wurde der Grenzstrom der Brenztraubensäurereduktion ausgewertet. Die Auftragung von lg $\bar{\imath}$ gegen lg ϑ (Abb. 8 und Abb. 9) ergibt Kurven, die erwartungsgemäss nicht linear verlaufen.

Zur Bestimmung von k wurden die gemessenen Ströme durch $\vartheta^{1/6}$ bzw. $\vartheta^{2/3}$ dividiert und wieder in ein Koordinatensystem eingetragen. Aus den Steigungen der in den Abb. 10 und Abb. 11 eingezeichneten Geraden wurden die k-Werte berechnet. Sie sind in Tabelle 2 Spalte 4 angegeben.

Mit Hilfe von k wurde nach Gl. (2) nun der rein reaktionsbedingte Strom berechnet

* Die nach Kapitel C durch den Rückdruck veranlasste Inkonstanz von m ist so gering, dass sie innerhalb der Messfehler des Stromes liegt. Voraussetzung hierfür ist, dass mit einem nicht zu kleinen Hg-Druck gearbeitet wird.

und gegen die Tropfzeit in doppeltlogarithmischem Massstab aufgetragen (s. Abb. 12 und Abb. 13). Die eingezeichneten Punkte liegen auf Geraden, deren Steigungen gut mit der von der Theorie geforderten Steigung ($\lg \varphi = {}^2/_3$) übereinstimmen.

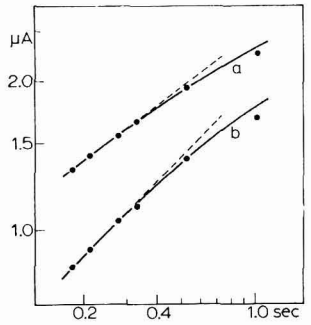

Abb. 8. Strom in Abhängigkeit von der Tropfzeit bei konstantem Potential in doppeltlogarithmischem Massstab. $TiCl_4$, $1.8 \cdot 10^{-3}$ M; HCl, $2.0 \cdot 10^{-2}$ M; NaCl, $8.0 \cdot 10^{-1}$ M; $2.0 \cdot 10^{-3}$% Triton-x305. Niveauhöhe 70 cm; (a), U, -1.090 V; (b), U -1.030 V gegen N.K.E.

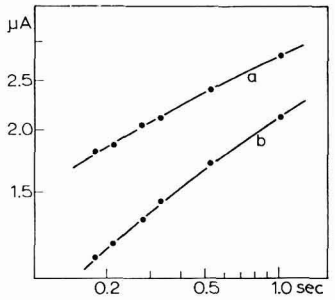

Abb. 9. Grenzstrom in Abhängigkeit von der Tropfzeit in doppeltlogarithmischem Massstab. Brenztraubensäure, $1 \cdot 10^{-3}$ M; Citratpuffer, $2 \cdot 10^{-1}$ M; NaCl, $8 \cdot 10^{-1}$ M; $2.5 \cdot 10^{-3}$% Triton-x-305. Niveauhöhe 70 cm; (a), pH, 5.00; (b), pH, 5.50.

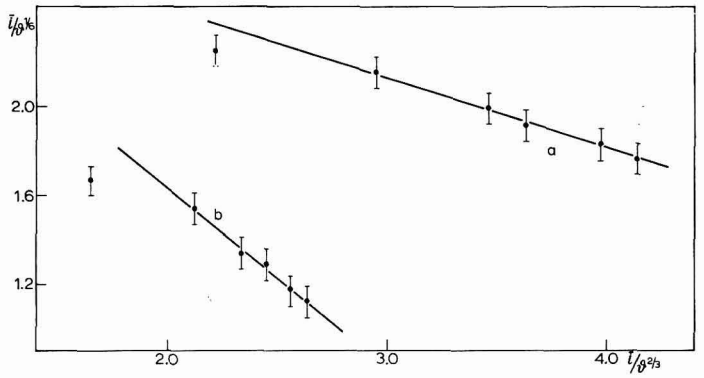

Abb. 10*. Ermittlung der Konstanten k für das System der Ti^{4+} Reduktion. (a), U, -1.090 V; (b), U, -1.030 V.

TABELLE II

	Potential in (V)	*pH*	k	$p_K = -lgK_{HA}$	$lg\ k_f$	$lg\ k_b$	$lg\ k_b$**
$TiCl_4$	-1.030	—	1.24	—	—	—	—
	-1.090	—	3.20	—	—	—	—
Brenztraubensäure	—	5.00	7.00	2.4	7.6	10.0	
	—	5.50	2.06	2.4	7.5	9.9	10.1

* Die beiden in Abb. 10 links eingetragenen Messpunkte ($\vartheta = 1.0$ sec) liegen in grösserer Entfernung von den Geraden. Die Stromstärke ist hier herabgesetzt infolge einer Inhibition des Elektrodenprozesses durch den sich mit der Zeit an der Oberfläche der Elektrode ansammelnden Dämpfer. Bei Tropfzeiten grösser als 2.0 sec zeigen die i–t-Kurven ein Strommaximum und daran anschliessend einen steilen Abfall, der auf die erwähnte Inhibition zurückzuführen ist.
** Angabe von STREHLOW UND BECKER [l mol^{-1} sec^{-1}]

Damit dürfte der Nachweis erbracht worden sein, dass die Abklopfvorrichtung auch bei Messung reaktionsbedingter Ströme einwandfrei arbeitet, wenn einerseits durch Dämpferzusatz eine Störung des Diffusionsvorganges durch den Spüleffekt vermieden wird, andererseits aber auf mögliche Störungen des Reaktionsablaufes durch den Dämpfer geachtet wird.

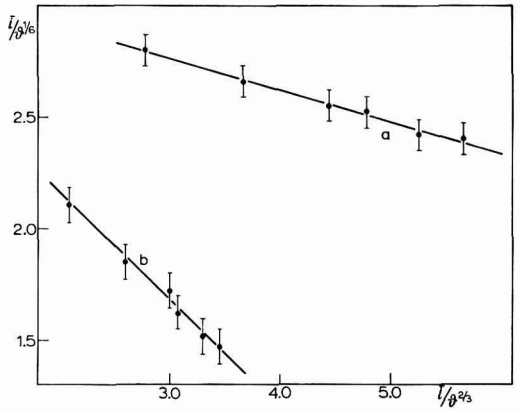

Abb. 11. Ermittlung der Konstanten k für das System der Brenztraubensäurereduktiom.

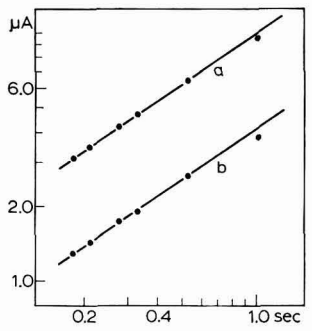

Abb. 12. lg i_{ktn} als Funktion lg ϑ für die Ti^{4+} —Reduktion. (a), U, —1.090 V, lg ψ, 0.67; (b), U, —1.030 V, lg ψ, 0.67.

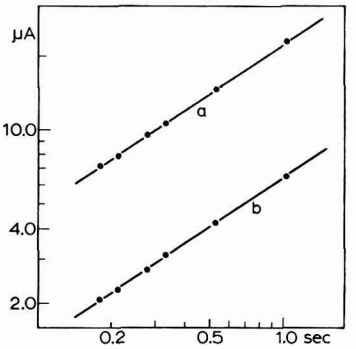

Abb. 13. lg i_{ktn} als Funktion von lg ϑ für die Reduktion der Brenztraubensäure. (a), pH, 5.00, lgψ = 0.68; (b), pH, 5.50, lgψ = 0.68.

II. Berechnung der die Reaktionshemmung charakterisierenden Grössen

Zum Schluss sollen aus den Ergebnissen des Abschnittes DI die den Reaktionsstrom charakterisierenden Grössen berechnet werden. Für die Durchtrittsreaktion der Ti^{4+}/Ti^{3+} Elektrode ergibt sich aus den in Tabelle II angegebenen Konstanten k der Durchtrittsfaktor des kathodischen Teilstromes $(1 - \alpha)$.

$$k = 0.812 \cdot \frac{k_{Ti^{4+}}}{z \cdot F\sqrt{D_{Ti^{4+}}}} \exp\left[-\frac{(1-\alpha)zF}{RT}\varepsilon \right]^{*} \qquad (4)$$

* Für die Ableitung von Gl.(4) s. K. J. VETTER, *Elektrochemische Kinetik*, Springer Verlag, 1961, S. 290.

$k_{Ti^{4+}}$, Geschwindigkeitskonstante des kathodischen Teilstroms,
$D_{Ti^{4+}}$, Diffusionskonstante der Ti^{4+}-Ionen,
z, Zahl der bei der Durchtrittsreaktion umgesetzten Elektronen,
ε, Potential, gemessen gegen die NK-Elektrode.

$$(1 - \alpha) = \frac{1}{\varepsilon_2 - \varepsilon_1} \frac{RT}{zF} \ln \frac{k_1}{k_2} \tag{5}$$

Nach Formel(5) erhält man für die Reaktion $Ti^{4+} + e^- \rightarrow Ti^{3+}$ einen Durchtrittsfaktor $(1 - \alpha) = 0.41 \pm 0.063$. k_1, k_2 sind die Konstanten k bei den Potentialen ε_1, ε_2.

Für die vorgelagerte chemische Reaktion der Bildung von Brenztraubensäure (HA) aus dem Anion (A^-) und Wasserstoffionen (H^+) haben STREHLOW UND BECKER[4] folgende Beziehung zwischen der Konstanten k und der Geschwindigkeitskonstanten der Dissoziation angegeben:

$$k_f = (1 + k_1) \left(\frac{k}{0.812} \frac{k_{HA}}{H^+} \right)^2 \tag{6}$$

$$k_{HA} = \frac{k_f}{k_b}$$

k_f, Geschwindigkeitskonstante der Dissoziation der Saüre HA,
k_b, Geschwindigkeitskonstante der Rekombination von A^- und H^+ zu HA,
k_{HA}, Dissoziations-Gleichgewichtskonstante des Gleichgewichtes $HA \rightleftharpoons H^+ + A^-$,
k_1, Gleichgewichtskonstante für die Hydratisierung der undissoziierten Säure.

Gleichung (6) berücksichtigt für den Fall der Brenztraubensäure das Gleichgewicht zwischen hydratisierter und nicht hüdratisierter Ketogruppe. Es ist nur die nicht hydratisierte Form kathodisch reduzierbar. STREHLOW UND BECKER[4,5] geben für die Gleichgewichtskonstante k_1 einen Wert von 2.38 an.

Die nach Gleichung (6) berechneten Werte von k_f und k_b liegen in derselben Grössenordnung wie die von STREHLOW UND BECKER (s. Tabelle II, Spalte 6,7,8).

ZUSAMMENFASSUNG

Die von der Metrohm AG hergestellte Abklopfvorrichtung zum vorzeitigen Abschlagen des Quecksilbertropfens von der Kapillare liefert Tropfzeiten von 0.18 bis 1.03 sec. Bei Variation der Tropfzeit erhält man sowohl für den Diffusionsgrenzstrom als auch für reaktionsbedingte Ströme die von der Theorie geforderte Tropfzeitabhängigkeit. Störungen, die durch das schnelle Abschlagen auftreten (Rückdruckeffekt), müssen bei Messungen mit hohem Genauigkeitsanspruch berücksichtigt werden.

Mit Hilfe dieser Apparatur wurden die kinetischen Daten der Durchtrittsreaktion $Ti^{4+} + e^- \rightarrow Ti^{3+}$ und die Geschwindigkeitskonstanten der Dissoziation der Brenztraubensäure bestimmt. Die Ergebnisse stimmen gut mit Angaben der Literatur überein.

LITERATUR

1 S. WOLF, *Z. Angew. Chem.*, 72 (1960) 449.
2 M. v. STACKELBERG UND V. TOOME, *Collection Czech. Chem. Commun.*, 25 (1960) 2958.
3 J. KOUTECKÝ, *Collection Czech. Chem. Commun.*, 18 (1953) 597.
4 H. STREHLOW UND M. BECKER, *Z. Elektrochem.*, 64 (1960) 813.
5 H. STREHLOW, *Z. Elektrochem.*, 66 (1962) 392.

ELECTROCHEMICAL OXIDATION OF CYANIDE ION AT PLATINUM ELECTRODES

DONALD T. SAWYER AND ROBERT J. DAY

Department of Chemistry, University of California, Riverside, Calif. (U.S.A.)

(Received July 9th, 1962)

Two recent studies[1,2] have shown that cyanide ion has a pronounced effect on the electrochemical reduction of oxygen at platinum. To understand this phenomenon more fully, as well as the general problem of electrode "poisoning", a detailed investigation of the electrochemical oxidation of cyanide ion at platinum electrodes has been undertaken. This seemed particularly desirable because the mechanisms proposed for the electrochemistry of oxygen and hydrogen at platinum have involved a platinum oxide coating[1,3].

Although cyanide ion has been shown to be oxidized by numerous chemical reactions[4], recent reports of electrochemical oxidations are limited to two studies[5,6]. In these the investigators concluded that cyanide ion is oxidized to cyanogen, which undergoes further reactions to form a brown polymer. SCHMIDT AND MEINERT[6] also concluded that in sufficiently basic solutions the formation of the polymer is inhibited, and cyanate ion is the product of the cyanogen decomposition. They also give references to earlier works in which cyanate ion as well as ammonia and carbon dioxide were found to be the ultimate products of the electrolysis of cyanide solutions.

The present study has been concerned with the effect of solution pH and electrode pre-conditioning upon the kinetics and mechanism for the oxidation of cyanide ion at a platinum surface. The results of such variations have been investigated by voltammetry, chronopotentiometry and the galvanostatic method for electrode kinetics[7].

EXPERIMENTAL

The electrochemical studies were made with a versatile electronic instrument which has been previously described by DEFORD[8]. This instrument, which is based on the use of Philbrick operational amplifiers, permits voltammetric, chronopotentiometric and galvanostatic studies by appropriate interconnection of the operational modules. Potentials were measured to an accuracy of $\pm$ 10 mV and currents to an accuracy of $\pm$ 0.1%. The voltammetric measurements were made in a modified H-cell to prevent attack of the agar salt bridge by alkaline solutions as well as contamination of the calomel electrode[9]. The cell for chronopotentiometric measurements was of conventional design and utilized a platinum foil working electrode and a platinum gauze auxiliary electrode. All potentials were measured relative to a saturated calomel electrode, unless otherwise indicated.

The electrodes for voltammetric measurements were prepared by sealing 18 gauge platinum wire into soft glass tubing; the exposed portion was ground flat to give a planar surface. Chronopotentiometric measurements were made with electrodes prepared from reagent grade platinum foil, 1 cm^2 on each side, welded to 22 gauge platinum wire sealed into soft glass tubing. The effective area of this electrode was determined to be 2.39 cm^2 by using the chronopotentiometric reduction of potassium ferricyanide together with the known diffusion coefficient for ferricyanide ion, $0.77 \cdot 10^{-5}$ cm^2 sec^{-1} (0.004 F $K_3Fe(CN)_6$, 0.5 F KCl)[10], in the Sand equation[11].

pH measurements were made with a Beckman Model G or a line operated Leeds and Northrup pH meter equipped with high range glass electrodes; the meters were standardized using N.B.S. buffers. All measurements were made at 25.0 $\pm$ 0.1° in a thermostatted bath.

The chemicals were reagent grade and were used without further purification. The distilled water used in the experiments was redistilled from an all-glass still containing a basic permanganate solution in distilled water.

The presence of buffering agents eliminated the chronopotentiometric waves for cyanide ion; thus, these measurements were made in the absence of buffers with the pH adjusted by KOH or H_2SO_4. The supporting electrolyte for all electrochemical measurements was 0.1–0.5 F K_2SO_4.

The kinetic parameters for the oxidation of cyanide ion were determined using the galvanostatic method as discussed by DELAHAY[7].

RESULTS AND DISCUSSION

Voltammetry

Cyanide ion gives a well defined anodic wave at the platinum electrode for pH's between 8 and 11 (Fig. 1). Although the diffusion current is proportional to cyanide concentration at a given pH, the diffusion current changes with pH for a given total cyanide concentration. However, if the cyanide ion concentration is computed from the dissociation constant for HCN[12], $pK_{HCN} = 9.21_6$, the curve shown in Fig. 2

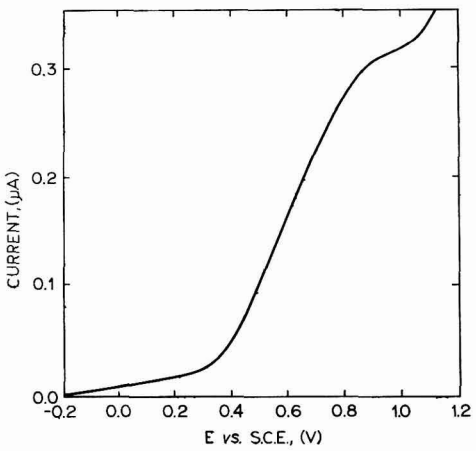

Fig. 1. Voltammetric oxidation of cyanide ion at a platinum electrode. The solution contained $5 \cdot 10^{-3}$ F KCN and 0.1 F K_2SO_4, and was adjusted to pH 10.0. The scan rate was 0.3 V per minute.

results. This behavior indicates that the rate of oxidation is significantly greater than the rate of dissociation for HCN; TANAKA AND MURAYAMA[13] have reported that the rate constant for HCN dissociation is $1 \cdot 10^{-7}$ sec^{-1} at 25°. Thus, these data lead to the conclusion that the electrochemical oxidation of dissolved hydrogen cyanide only occurs for the free cyanide ion and that any kinetic expression should be concerned with the free cyanide ion concentration only.

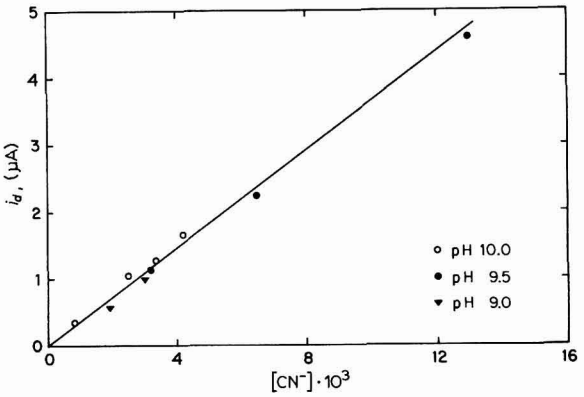

Fig. 2. The voltammetric diffusion current as a function of cyanide ion concentration for three different pH's. The cyanide ion concentration was calculated from the formal concentration of KCN in the solution and the dissociation constant for HCN, which has a pK_a of 9.216 at 25°.

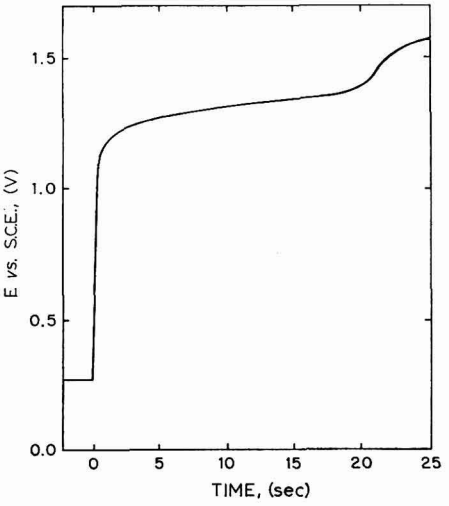

Fig. 3. Chronopotentiometric oxidation of cyanide ion at a platinum foil electrode. The solution contained 0.02 F KCN and 0.5 F K_2SO_4, and was adjusted to pH 10.0. The current was 3.00 mA.

Chronopotentiometry

The chronopotentiometric oxidation wave for cyanide ion is shown in Fig. 3; the high degree of irreversibility is shown by the large overpotential. This particular chronopotentiogram is for an untreated platinum electrode. However, pre-oxidation

of the electrode gives virtually the same curve; a pre-reduced electrode gives a less well-defined wave until it has been oxidized during the course of the anodic pulse. All of the remaining studies have been carried out using an untreated or pre-oxidized electrode.

To establish the current limiting factors for the oxidation of cyanide, a series of chronopotentiometric oxidations at different currents, pH's and cyanide concentrations have been made. For a diffusion controlled process the Sand equation[11]

$$\frac{i\tau^{\frac{1}{2}}}{C} = \frac{\pi^{\frac{1}{2}} n F A D^{\frac{1}{2}}}{2} \tag{1}$$

indicates that $i\tau^{\frac{1}{2}}/C$ is a constant for a given electrode–cell combination at a given temperature. Table I summarizes the values obtained for the cyanide oxidation; cyanide ion concentrations have been calculated from the HCN dissociation constant[12]. The general constancy of the values indicates that the current is diffusion controlled and that adsorption is not a rate-controlling factor.

TABLE I

VALUES OF $i\tau^{\frac{1}{2}}/C$ FOR THE OXIDATION OF CYANIDE ION

	pH	$i\tau^{\frac{1}{2}}$	$i\tau^{\frac{1}{2}}/C$
A. 0.02 *F* KCN, 0.5 *F* K_2SO_4			
	10.5	$1.57 \cdot 10^{-2}$	0.84
	10.0	$1.38 \cdot 10^{-2}$	0.82
	9.7	$1.24 \cdot 10^{-2}$	0.83
	9.5	$1.10 \cdot 10^{-2}$	0.85
	9.3	$0.87 \cdot 10^{-2}$	0.82
	9.0	$0.62 \cdot 10^{-2}$	0.84
B. 0.002 to 0.025 *F* KCN, 0.5 *F* K_2SO_4			
	9.5		0.81 → 0.91

Use of the calculated cyanide ion concentrations in obtaining the constant values further supports the conclusion that only the free cyanide ion is oxidized and that the rate of HCN dissociation is slow relative to the rate of oxidation.

The chronopotentiometric data for cyanide ion can also be used to establish the number of electrons released in the oxidation reaction. By using an average value of 0.83 for $i\tau^{\frac{1}{2}}/C$ and a value of $4.94 \cdot 10^{-3}$ for $D^{\frac{1}{2}}$ (for CN^- in 0.25 *F* NaCl and 0.01 *F* NaOH)[14,15] in eqn. (1), the value of n is calculated to be 0.83. Thus the oxidation reaction can be concluded to be a one electron step and can be written

$$CN^- \rightarrow CN\cdot + e^- \tag{2}$$

with cyanide radicals combining to give cyanogen.

With this preliminary understanding of the system, a series of galvanostatic studies of the rate of cyanide ion oxidation has been made. The potential of the working electrode *vs.* the normal hydrogen electrode for a constant current source has been shown by DELAHAY[7] to be expressed by the relation

$$E = \frac{-RT}{(1-\alpha)\, n_a F} \ln \frac{nFC^0\, k^0_{f,h}}{i_0} - \frac{RT}{(1-\alpha)\, n_a F} \ln \left[\frac{\tau^{\frac{1}{2}} - t^{\frac{1}{2}}}{\tau^{\frac{1}{2}}}\right] \tag{3}$$

where the terms have their usual electrochemical significance. By applying a pulse of known current and following the potential as a function of time with a recorder it is possible, using an extrapolation to time equal to zero, to cause the last term in eqn. (3) to go to zero. With this operation applied at several current densities the anodic transfer coefficient, $(1 - \alpha)$, can be evaluated from the slope of a plot of E *vs.* $\log i_0$. The heterogeneous forward rate constant (relative to the normal hydrogen electrode), $k^0_{f,h}$, can then be evaluated by applying eqn. (3). To evaluate $(1 - \alpha)$, the value of n_a must be known; it is assumed to be one from the arguments given for eqn. (2). Figure 4 shows the extrapolated values of E *vs.* $\log i_0$ for a series of different

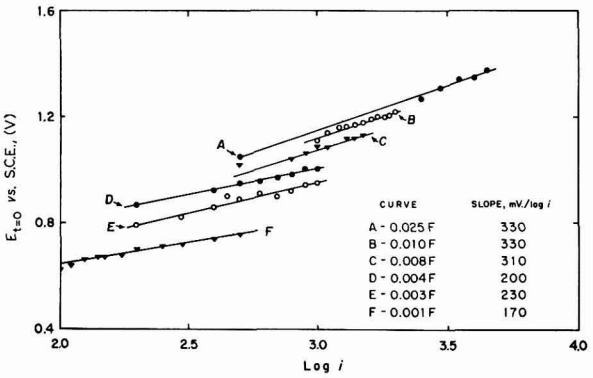

Fig. 4. The extrapolated potentials, $E_{t=0}$ as a function of current for the galvanostatic oxidation of cyanide ion at a platinum foil electrode. The several KCN concentrations studied are indicated as well as the slopes for their respective curves. All of the solutions contained 0.5 F K_2SO_4 and were adjusted to pH 9.5.

concentrations of KCN at pH 9.5. The slopes for the curves, in mV/log i, are given on the figure. Normally the slopes for all of the curves would be expected to be the same; however, for this system there is a trend of increasing slope with increasing KCN concentration. Table II tabulates values of $(1 - \alpha)$ and $k^0_{f,h}$ for various pH's and KCN concentrations. The free cyanide ion concentration calculated from the dissociation constant for HCN, has been used in eqn. (3) to determine the values of $k^0_{f,h}$.

TABLE II

SUMMARY OF KINETIC PARAMETERS EVALUATED FOR THE OXIDATION OF CYANIDE ION AT A PRE-OXIDIZED PLATINUM ELECTRODE

$[KCN]$ (F)	pH	$(1-\alpha)$	$k^0_{f,h}$; $(cm\,sec^{-1})$
0.001	9.5	0.35	$0.4 \cdot 10^{-8}$
0.003	9.5	0.26	$1.6 \cdot 10^{-8}$
0.004	9.5	0.30	$0.1 \cdot 10^{-8}$
0.008	9.5	0.19	$5.0 \cdot 10^{-8}$
0.010	9.5	0.18	$5.0 \cdot 10^{-8}$
0.020	9.5	0.22	$2.0 \cdot 10^{-8}$
0.025	9.5	0.18	$1.6 \cdot 10^{-8}$
0.005	10.5	0.26	$0.8 \cdot 10^{-8}$
0.020	10.5	0.20	$2.0 \cdot 10^{-8}$
		Average	$2.1 \cdot 10^{-8}$

The data in Fig. 4 indicate that the potential required to oxidize cyanide ion becomes more positive as the cyanide ion concentration increases, which is a surprising and unexpected phenomenon. A number of additional experiments have confirmed these observations to the extent that they are believed valid and not due to experimental error. Figure 5 shows a plot of $(1 - \alpha)$ *vs.* $-\log (CN^-)$ which gives an approximately linear curve. The equation for this curve is

$$(1 - \alpha) = -0.06 - 0.123 \log (CN^-) \tag{4}$$

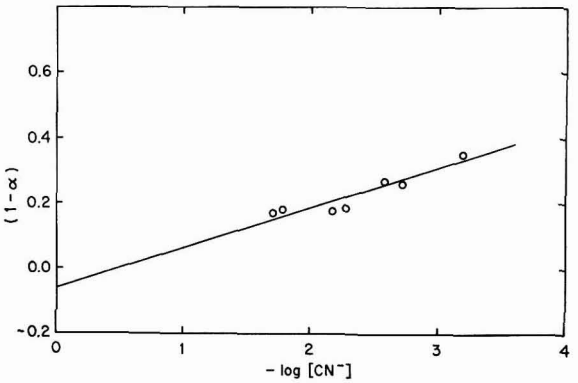

Fig. 5. The anodic transfer coefficient, $(1 - \alpha)$, as a function of cyanide ion concentration. The values of $(1 - \alpha)$ were determined by the galvanostatic method and the cyanide ion concentrations were determined from the formal concentrations of KCN and the dissociation constant for HCN. The slope of the curve is -0.123 and it has an intercept of -0.06.

and indicates that $(1 - \alpha)$ would be negative for a 1 *M* cyanide ion concentration. Equation (4) indicates that the higher the cyanide ion concentration is, the smaller is the fraction of the applied potential that is effective in accelerating the rate of electrochemical oxidation. Such behavior can be thought of as a poisoning of the platinum electrode surface by cyanide ion itself, *e.g.*,

$$Pt(OH)_2 + 2\ CN^- \rightarrow Pt(CN)_2 + 2\ OH^- \tag{5}$$

Thus if $Pt(CN)_2$ (or $Pt(CN)_4^{2-}$) is catalytically much poorer than $Pt(OH)_2$ for the oxidation of cyanide ion, increasing concentrations of cyanide ion would cause the reaction in eqn. (5) to go to the right and bring about a decrease in $(1 - \alpha)$ as indicated by eqn. (4). The observed changes of $(1 - \alpha)$ also might be explained by considerations similar to those presented by TONDEUR, DOMBRET AND GIERST on the effects of changes in the double layer[16]. Thus, increased concentrations of cyanide ion would bring about increased adsorption of CN^- or $Pt(CN)_4^{2-}$ on the electrode and cause attendant changes in the double layer. This would then affect the kinetics of oxidation for cyanide ion in a manner such as has been observed. These phenomena are sufficiently interesting to warrant additional study in the future to establish just what is bringing about the apparent change in $(1 - \alpha)$ with changes of cyanide ion concentration.

Equation (3) indicates that a plot of E *vs.* $\log (\tau^{\frac{1}{2}} - t^{\frac{1}{2}})$ should give a linear curve from which the slope also should permit evaluation of $(1 - \alpha)$. A number of chronopotentiograms similar to Fig. 3 have been plotted and in all cases curves similar to

the one shown in Fig. 6 have resulted. The upper portion of this has a slope approaching 300 mV per log unit, but the lower straight-line portion only has a slope of 73 mV/log $(\tau^{\frac{1}{2}} - t^{\frac{1}{2}})$ unit. This behavior indicates that initially $(1 - \alpha)$ is small, but during the course of the chronopotentiogram its value increases markedly; that is, the electrode becomes more effective catalytically.

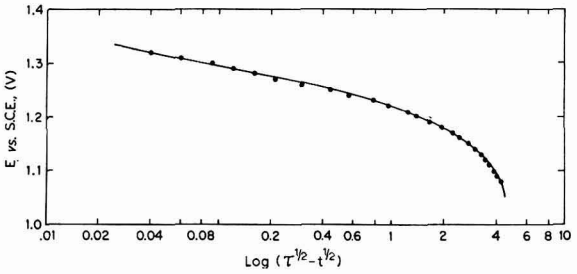

Fig. 6. Voltage–time analysis of the curve for the chronopotentiometric oxidation of cyanide ion at a platinum foil electrode. The upper portion of the curve has a slope approximating 300–400 mV per log unit, while the lower, straight-line portion has a slope of 73 mV per log unit. The solution contained 0.02 F KCN and 0.5 F K_2SO_4 and was adjusted to pH 10.5. The current was 3.00 mA.

CONCLUSIONS

Although $(1 - \alpha)$ changes with cyanide ion concentration, $k^0_{f,h}$ is independent of both pH and cyanide ion concentration. This observation plus the preceding experimental data can be accounted for by the following proposed reaction mechanisms.

$$Pt(OH)_2 + CN^- \rightarrow Pt(OH)_2(CN)^- \qquad \text{fast} \qquad (6)$$

$$Pt(OH)_2(CN)^- \rightarrow Pt(OH)_2 + (CN)\cdot + e^- \qquad \text{slow} \qquad (7)$$

$$2\,(CN)\cdot \rightarrow (CN)_2 \qquad \text{fast} \qquad (8)$$

As the cyanide concentration increases the $Pt(OH)_2$ is metathesized to $Pt(CN)_2$ (or $Pt(CN)_4^{2-}$) as indicated by eqn. (5). The $Pt(CN)_2$ surface is postulated to be ineffective mechanistically and to inhibit the oxidation of cyanide ion.

An alternative mechanism involves the formation of PtO_2

$$Pt(OH)_2 + 2\,OH^- \rightarrow PtO_2 + 2\,H_2O + 2\,e^- \qquad \text{fast} \qquad (9)$$

$$PtO_2 + 2\,CN^- + 2\,H_2O \rightarrow Pt(OH)_2 + 2\,OH^- + 2\,(CN)\cdot \qquad \text{slow} \qquad (10)$$

$$2\,(CN)\cdot \rightarrow (CN)_2 \qquad \text{fast} \qquad (11)$$

Metathesis of $Pt(OH)_2$ by CN^- may lead to a compound, $Pt(CN)_2$, that cannot be oxidized to PtO_2. However, this would tend to decrease the amount of PtO_2 available for the reaction shown by eqn. (10). Because $i\tau^{\frac{1}{2}}/C$ is a constant this seems unlikely; the mechanism expressed by eqns. (6),(7),(8) is thought to be more consistent with the data.

Efforts to isolate oxidation products for the oxidation of cyanide ion have resulted in the detection of ammonia. This product can arise from the basic hydrolysis of cyanogen, first to cyanate and cyanide[17] and then of the cyanate to ammonia and carbon dioxide[18]. Detection of oxidation products by reverse chronopotentiometry has been totally unsuccessful. Electrochemical reduction of dissolved cyanogen gas and of cyanate ion has been unsuccessful also.

The need for a platinum oxide film to catalyze the oxidation of cyanide ion is somewhat similar to the conditions necessary for the reduction of dissolved oxygen[1]. As shown in the latter study, a platinum oxide film is necessary to get a rapid and efficient reduction of dissolved oxygen. Cyanide ion causes a virtual elimination of the oxygen reduction wave, which can be accounted for if there is conversion of the platinum oxide to platinum cyanide. The present study indicates that such a phenomenon probably takes place and leads to an electrode that also is ineffective for the oxidation of cyanide ion. Thus platinum oxide appears to be a highly important catalytic material in electrochemical reactions. This has been seen to be the case for the electrolytic reduction of dissolved oxygen[1,2], the electrolytic oxidation of dissolved hydrogen[3] and now, the electrolytic oxidation of cyanide ion. However, for the last system, the very ion that is being oxidized also is poisoning the electrode for its own oxidation. The decrease of the transfer coefficient with increasing concentrations of the active species, as observed here, is believed to be somewhat unique.

Although the proposed mechanisms are quite tentative, and certainly do not preclude other possibilities, they do account for the observed phenomena and do reasonably explain the rather surprising phenomena of having a higher oxidation potential with increased cyanide concentrations. Without the change in slope of the curves in Fig. 4 and the attendant change in the values for the transfer coefficient, extremely diverse results would have been obtained for the rate constant.

ACKNOWLEDGEMENT

This work was supported by the United States Air Force, Geophysics Research Directorate, Air Force Cambridge Research Laboratories, under Contract No. AF 19(604)-8347.

SUMMARY

Voltammetric, chronopotentiometric and galvanostatic studies have been used to investigate the electrochemical oxidation of cyanide ion at platinum electrodes. The reaction is a diffusion controlled process involving a one-electron oxidation of free cyanide ion to cyanogen. The anodic transfer coefficient, $(1 - \alpha)$, for a pre-oxidized electrode in a pH 9.5 solution varies from 0.35 for 10^{-3} F KCN to 0.18 for 0.25 F KCN. The average value for the forward, heterogeneous rate constant, $k^0_{f,h}$, is $2.1 \cdot 10^{-8}$ cm sec^{-1} (using potentials relative to the normal hydrogen electrode). The proposed mechanism for the oxidation reaction involves a platinum oxide film. Increasing cyanide ion concentrations are postulated to cause metathesis of the oxide to platinum cyanide, which brings about a decrease in $(1 - \alpha)$ and inhibition of the oxidation reaction.

REFERENCES

1 D. T. SAWYER AND L. V. INTERRANTE, *J. Electroanal. Chem.*, 2 (1961) 310.
2 D. T. SAWYER AND E. T. SEO, *ibid.*, 3 (1962) 410.
3 D. T. SAWYER AND E. T. SEO, *ibid.*, 5 (1963) 23.
4 B. RICCA AND F. PERIONE, *Ann. Chim. Applicata*, 18 (1928) 550.
5 J. S. FITSGERALD, *Chem. & Ind.*, (1955) 17.
6 H. SCHMIDT AND H. MEINERT, *Z. Anorg. Allgem. Chem.*, 293 (1957) 214.
7 P. DELAHAY, *New Instrumental Methods in Electrochemistry*, Interscience Publishers, Inc., New York, 1954, p. 186.
8 D. D. DEFORD, Private Communication, presented at the 133rd American Chemical Society Meeting, San Francisco, Calif., April, 1958.

[9] R. L. PECSOK AND R. S. JUVET, JR., *Anal. Chem.*, 27 (1955) 165.
[10] M. VON STACKELBERG, M. PILGRAM, AND V. TOOME, *Z. Elektrochem.*, 57 (1953) 342.
[11] H. J. S. SAND, *Phil. Mag.*, 1 (1901) 45.
[12] K. P. ANG, *J. Chem. Soc.*, (1959) 3822.
[13] N. TANAKA AND T. MURAYAMA, *Z. Physik. Chem. (Frankfurt)*, 15 (1959) 146.
[14] L. MEITES, *Polarographic Techniques*, Interscience Publishers Inc., New York, 1955, p. 256.
[15] W. H. JURA, *Anal. Chem.*, 26 (1954) 1121.
[16] J. J. TONDEUR, A. DOMBRET, AND L. GIERST, *J. Electroanal. Chem.*, 3 (1962) 225.
[17] I. M. KOLTOFF AND J. J. LINGANE, *Polarography*, 2nd ed., Interscience Publishers Inc., New York, 1952, p. 541.
[18] M. W. LISTER, *Can. J. Chem.*, 33 (1955) 426.

THE POLAROGRAPHIC ESTIMATION OF ANIONIC DETERGENTS

G. S. BUCHANAN AND J. C. GRIFFITH*

Department of Physical Chemistry, The University of New South Wales, Kensington, N.S.W.; Division of Textile Physics, C.S.I.R.O., Ryde, N.S.W. (Australia)

(Received July 30th, 1962)

INTRODUCTION

In a review of the various methods available for the analysis of water soluble synthetic soaps[1], mention is made of the application of the polarograph and the work by STACKELBERG and others[2,3]. They used the polarograph to measure the extent to which detergents depress the maxima on current–voltage curves. Another method which may be used is the dyestuff antagonist method which makes use of the power of certain dye cations, for example methylene blue cation, to form complexes with sulphonate and sulphate anions. The present method is based on this property. Methylene blue yields a polarographic step whose height is reduced by the addition of an anionic detergent. This reduction has been measured and results indicate that under suitable conditions, the reduction in height is a linear function of the concentration of the detergent.

APPARATUS

The polarograph was a manually operated type using the galvanometric deflection method for measuring current.

MATERIALS

Methylene Blue B.D.H.

Sodium dodecyl sulphate (SDS) was prepared from dodecanol (boiling point 101.5° at 0.1 mm Hg) by the chlorsulphonic acid method[4].

METHOD

Methylene blue solutions were prepared in a universal buffer of pH 4.5. The buffer consisted of a mixture of acetic, orthophosphoric and boric acids (each $M/20$) adjusted to the required pH by the addition of the requisite amount of sodium hydroxide. The pH was measured with a glass electrode.

A measured volume of methylene blue solution was placed in the polarographic cell, deaerated (with hydrogen) and polarographed. A known quantity of SDS solution was introduced into the methylene blue solution and the cell contents deaerated and repolarographed. Further successive additions of detergent were made and the above procedure repeated.

* Present address: Department of Physical Chemistry, The University of Sydney, Australia.

RESULTS ANS DISCUSSION

Each addition of SDS solution produces a decrease in the step height of the methylene blue reduction step. Some of the methylene blue is therefore removed from the solution and this is due, most likely, to the formation of an insoluble complex with SDS.

If the reduction in step height is plotted against the concentration of detergent in the cell, a straight line is obtained except for the lowest concentration of SDS. The most probable explanation for this departure from linearity is that the small amount of complex formed initially, is soluble in a large excess of dye solution, *i.e.*, the *flocculation zone*[5] has not been reached.

The concentration of methylene blue used initially, will depend on the concentration range of the SDS which it is desired to cover.

For the results shown in Table I and in Fig. 1, 30 ml of $4 \cdot 10^{-3}$ *M* methylene blue

TABLE I

EFFECT OF ADDING 10^{-2} *M* SDS TO 30 ml OF $4 \cdot 10^{-3}$ *M* METHYLENE BLUE SOLUTION

Total number of ml of 10^{-2} *M SDS*	*Concn. of SDS in cell (M)*	i_d° *corrected for dilution (arb. units)*	i_d *after addition of SDS*	*Reduction* $i_d^\circ - i_d$
0.0	0.0	94.0	94.0	0.0
0.5	$1.64 \cdot 10^{-4}$	92.5	92.0	0.5
1.0	$3.24 \cdot 10^{-4}$	91.0	88.0	3.0
2.0	$6.25 \cdot 10^{-4}$	88.0	76.0	12.0
3.0	$9.1 \cdot 10^{-4}$	85.5	60.0	25.5
4.0	$11.8 \cdot 10^{-4}$	83.0	45.0	38.0
5.0	$14.3 \cdot 10^{-4}$	80.5	26.5	54.0
6.0	$16.7 \cdot 10^{-4}$	78.0	12.0	66.0

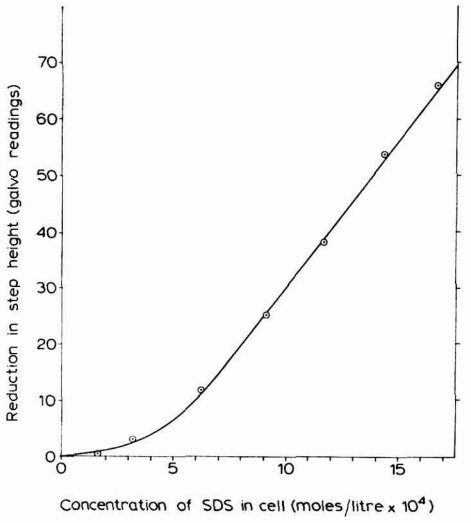

Fig. 1. Reduction in step height of $4 \cdot 10^{-3}$ *M* methylene blue solution (30 ml in cell), as a function of the concentration of SDS in the polarographic cell.

solution were placed in the cell. Seven additions of SDS (10^{-2} *M*) were made to the cell, 0.5 ml for the first addition and 1.0 ml each for the remaining six.

Similar results were obtained in the case of more concentrated solutions of SDS (10^{-1} *M*), by using more concentrated solution of methylene blue ($4 \cdot 10^{-2}$ *M*). The results are shown in Table 2 and Fig. 2.

The effect of dilution on the methylene blue by the addition of detergent solution was taken into account by using the formula $i_d V_1/V_2$, where V_1 is the initial volume and V_2 is the final volume; *i.e.*, the value of i_d is proportional to the concentration of methylene blue over the range of concentrations used.

Similar results were obtained in the case of another anionic detergent, namely sodium tetradecyl sulphate.

Good agreement was obtained between duplicate determinations. The error of the determination was $\pm 3\%$.

Neutral Red was tried in the place of methylene blue but was found to be un-

TABLE II

EFFECT OF ADDING 10^{-1} *M* SDS TO 25 ml OF $4 \cdot 10^{-2}$ *M* METHYLENE BLUE SOLUTION

Total number of ml of 10^{-1} *M SDS*	*Concn. of SDS in cell. (M)*	i_d° *corrected for dilution (arb. units)*	i_d *after addition of SDS*	*Reduction* $i_d^\circ - i_d$
0.0	0.0	99.0	99.0	0.0
0.5	$2.0 \cdot 10^{-3}$	97.0	92.0	5.0
1.0	$4.0 \cdot 10^{-3}$	95.0	78.0	17.0
1.5	$5.7 \cdot 10^{-3}$	93.5	61.0	32.5
2.0	$7.4 \cdot 10^{-3}$	91.5	47.0	44.5
2.5	$9.1 \cdot 10^{-3}$	90.0	32.0	58.0
3.0	$10.7 \cdot 10^{-3}$	88.5	13.5	75.0

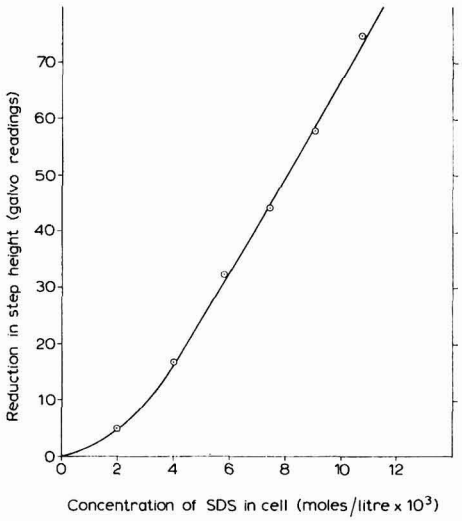

Fig. 2. Reduction in step height of $4 \cdot 10^{-2}$ *M* methylene blue solution (25 ml in cell), as a function of the concentration of SDS in the polarographic cell.

satisfactory. The step height in this case continually diminished over a period of half an hour after each addition of the detergent. Apparently detergents react only slowly with this dye producing a gradual lowering of step height with time.

Although many methods are available for the determination of anionic detergent concentration, this one has the advantage that it can be used at high concentrations above the critical micelle concentration, and for small volumes, *e.g.*, less than 1.0 ml. Since dilutions are made by direct addition to the polarographic cell, errors due to dilution and resampling are eliminated. Once the appropriate calibration curves have been established, solutions of unknown concentration can be rapidly analysed.

It may be possible to use this type of procedure for the analysis of cationic detergents provided that a satisfactory acid dye can be selected.

SUMMARY

A method for the estimation of anionic detergents, based on the dyestuff antagonist method, is described. Methylene blue, which gives a polarographic step, is the dyestuff used. It forms an insoluble complex with anionic detergents causing a reduction in the methylene blue step height. It is possible to calculate the concentration of detergent from this decrease in step height.

REFERENCES

1 N. W. TSCHOEGL, *Rev. Pure Appl. Chem.*, 4, No. 3 (1954) 171–206.
2 K. E. SCHWARZ, H. J. SCHRODER AND M. V. STACKELBERG, *Z. Electrochem.*, 48 (1942) 6.
3 M. V. STACKELBERG AND H. SCHUTZ, *Kolloid-Z.*, 105 (1943) 20.
4 E. E. DREGER, G. I. KEIN, G. D. MILES, L. SHEDLOVSKY AND J. ROSS, *Ind. Eng. Chem.*, 36 (1954) 610.
5 T. KONDO AND K. MEGURO, *Bull. Chem. Soc. Japan*, 32 (1959) 267.

AMPEROMETRIC TITRATION OF LANTHANUM BY FERROCYANIDE

J. N. GAUR AND K. ZUTSHI

Department of Chemistry, University of Rajasthan, Jaipur (India)

(Received May 25th, 1962)

The formation of ferro- and ferricyanides of the rare earths have been studied by PRANDTL AND MOHR[1]. They suggested the formation of the compounds of the type Me(I) Me(III) $Fe(CN)_6.nH_2O$ (in which Me(I) is sodium or potassium and Me(III) is La, Pr, Nd, Sm, Gd, Dy, Er or Y), and basic salts of the type Me(II)OH, Me(III) $Fe(CN)_6.2nH_2O$. The senior author has already estimated lanthanum with ferrocyanide using both electrometric and indicator methods[2]. The work has been further extended by amperometric methods and the results are incorporated in the present communication.

EXPERIMENTAL

A manual polarograph set-up was used for carrying out the titrations. A Vernier Potentiometer (W.G.Pye) was used as a potential divider and the current was measured by a freely suspended reflecting galvanometer (sensitivity at 1 m radius

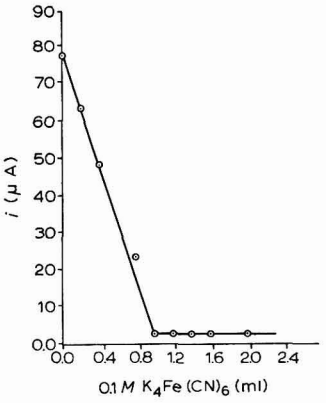

Fig. 1. Titration of lanthanum nitrate against potassium ferrocyanide. 10 ml of 0.001 *M* lanthanum nitrate were used in the cell.

1,500 mm/μA, 48.5 mm/μV, 590 mm/μC with a current constant of $6.7 \cdot 10^{-10}$ A/mm (see W. G. Pye, Catalogue No. 7935). A Sargent capillary with a bore of 0.03 mm and a drop time of 2–3 sec was used for dropping mercury. The polarogram of lantha-

num was registered using potassium nitrate as supporting electrolyte with a 0.005% solution of gelatin as maximum suppressor and it was found that the diffusion current of lanthanum in aqueous solution reaches the limiting value at a potential of -1.8V *vs.* S.C.E.

The titrations were carried out at $E_{d.e.} = -1.58$ V *vs.* S.C.E. Nitrogen was bubbled through the cell after each addition; this ensured a thorough mixing of the reactants and made the mixture oxygen-free. The diffusion current obtained after each addition of the titrant was corrected for the small dilution effect by multiplying the observed value by the factor $(V + v)/V$, where v is the volume of the titrant added up to a given stage, and V is the original volume of the solution to be titrated.

TABLE I

AMPEROMETRIC DETERMINATION OF LANTHANUM BY FERROCYANIDE

No.	*Concentration ratio*	*$La(NO_3)_3$ soln. (ml)*	*$K_4Fe(CN)_6$ soln. required (ml)*	*Ratio at the equivalent point*	*Compound formed*
1	0.02 *M* $La(NO_3)_3$ and 0.1 *M* $K_4Fe(CN)_6$	10	2	1 : 1	$LaKFe(CN)_6$
2	0.01 *M* $La(NO_3)_3$ and 0.1 *M* $K_4Fe(CN)_6$	10	1	1 : 1	$LaKFe(CN)_6$
3	0.004 *M* $La(NO_3)_3$ and 0.04 *M* $K_4Fe(CN)_6$	10	1	1 : 1	$LaKFe(CN)_6$
4	0.002 *M* $La(NO_3)_3$ and 0.04 *M* $K_4Fe(CN)_6$	10	0.5	1 : 1	$LaKFe(CN)_6$
5	0.002 *M* $La(NO_3)_3$ and 0.02 *M* $K_4Fe(CN)_6$	10	1	1 : 1	$LaKFe(CN)_6$
6	0.001 *M* $La(NO_3)_3$ and 0.02 *M* $K_4Fe(CN)_6$	10	0.5	1 : 1	$LaKFe(CN)_6$
7	0.001 *M* $La(NO_3)_3$ and 0.01 *M* $K_4Fe(CN)_6$	10	1	1 : 1	$LaKFe(CN)_6$

Titrations were performed at different concentrations of the two reactants and the results are tabulated in Table I.

From the table it is clear that the formation of the compound $LaKFe(CN)_6$ is indicated at all dilutions, showing that lanthanum nitrate and potassium ferrocyanide react in the equivalent ratio of 1 : 1. This, therefore, affords a sensitive method for the estimation of lanthanum.

SUMMARY

Lanthanum nitrate solutions have been titrated with a standard solution of potassium ferrocyanide at the dropping mercury electrode at a potential of −1.58 V. The two solutions react in the ratio of 1 : 1 with the formation of the compound $LaKFe(CN)_6$.

Amperometric titration of $La(NO_3)_3$ and $K_4Fe(CN)_6$ affords a sensitive method for the estimation of lanthanum.

REFERENCES

1 W. PRANDTL AND S. MOHR, *Z. Anorg. Allgem. Chem.*, 236 (1938) 243.
2 J. N. GAUR, *Z. Anal. Chem.*, [5] 185 (1962) 357.

THE POLAROGRAPHIC STUDY OF THE FORMATION OF HYDROGEN PEROXIDE IN SOLUTIONS OF HYDRAZO-COMPOUNDS IN THE PRESENCE OF OXYGEN

W. KEMULA, E. NAJDEKER AND Z. KUBLIK

Institute of Physical Chemistry, Polish Academy of Sciences, and Department of Inorganic Chemistry, Warsaw University (Poland)

(Received June 14th, 1962)

In our previous paper[1], we stated that hydrogen peroxide was detected during the polarographic investigation of diphenylcarbazone. Hydrogen peroxide was formed in the reaction between the hydrazo-compound and oxygen.

$$R_1NHHNR_2 + O_2 \rightarrow R_1N{=}NR_2 + H_2O_2 \qquad (1)$$

When a solution of ammonia–ammonium chloride buffer containing diphenylcarbazone is investigated under conventional polarographic conditions (*i.e.* deaeration being performed after preliminary preparation of the solutions), considerable amounts of hydrogen peroxide are formed even during a few minutes of deaeration. In earlier papers dealing with the polarographic investigation of hydrazo-compounds[2–5] such an effect was not described. It is therefore possible, that in some cases dissolved oxygen can be reduced by an hydrazo-compound, not to hydrogen peroxide, but to water and that in other cases, reaction (1) does not proceed at all.

The fact that hydrogen peroxide is formed in a solution containing diphenylcarbazone, diphenylcarbazide or dithizone may be of some importance in analytical chemistry, because these compounds are often used as analytical reagents. The investigation of the reaction between the hydrazo-group and oxygen may also be of importance for practical purposes as this reaction has been used for the industrial production of hydrogen peroxide[6].

EXPERIMENTAL PROCEDURE

Polarographic curves were recorded using a Radiometer PO4 polarograph. The characteristics of the dropping mercury electrode were: $m = 2$ mg/sec, $t = 3.5$ sec at $h = 250$ mm. An external saturated calomel electrode, connected with the cell by a suitable salt bridge, was used as reference electrode. Besides the conventional polarographic cell, a special cell which allowed the mixing of deaerated solutions in the absence of air, was used[7]. Solutions were prepared by dissolving purified compounds in 95% ethanol and by dilution of these stock solutions with a suitable buffer. Hydrazobenzene was freshly prepared. Diphenylcarbazone (m.p. 127°) and diphenylcarbazide (m.p. 165°) were purified as described by KRUMHOLTZ[8]. Dithizone was purified according to MARCZENKO[9]. The pH of solutions was kept constant using 0.2 *M* acetate and 0.1 *M* ammonia–ammonium chloride buffers.

Hydrazobenzene

In earlier publications[2,3] it has been stated that one or two waves, depending on the pH occurred in solutions of hydrazobenzene. The first wave, which corresponds to a two-electron oxidation of hydrazobenzene to azobenzene, is found both in acidic and alkaline solutions and is reversible, or almost reversible. The second wave, corresponding to a two-electron reduction of hydrazobenzene to aniline occurs only in acidic solutions, and is irreversible. FOFFANI AND FRAGIACOMO[2] did not observe the hydrogen peroxide wave, since, in their experiments extreme precautions were taken again stair oxidation. From work published by WAWZONEK AND FREDERICKSON[3] it seems that they also did not observe the hydrogen peroxide wave. They did not take into consideration the possibility that such a wave might occur, although under their experimental conditions part of the hydrazobenzene was oxidized to azobenzene.

The formation of hydrogen peroxide from hydrazobenzene and oxygen is easier to investigate in neutral and alkaline solutions, since under these conditions the reduction wave of hydrazobenzene to aniline is not observed, and does not mask the hydrogen peroxide wave. Figure 1 shows the polarographic curves recorded for

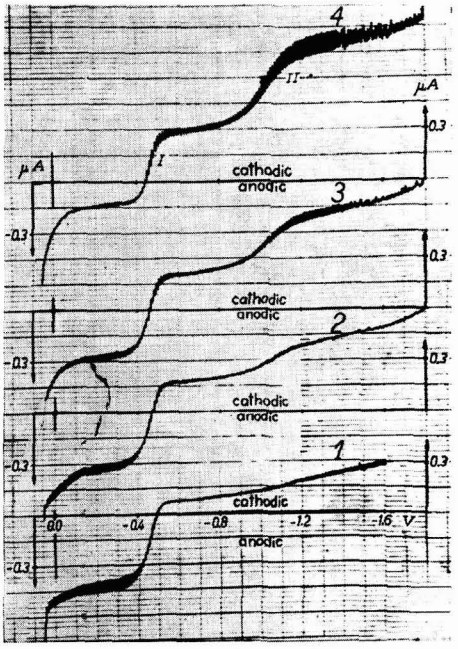

Fig. 1. Polarographic curves for a $1 \cdot 10^{-4}$ *M* solution of hydrazobenzene in 0.1 *M* ammonia–ammonium chloride buffer (pH 10.0), 10% ethanol. (1), recorded after mixing of deaerated solutions; (2–4), recorded after 1.5 6 and 15 min bubbling of oxygen. Potentials *vs.* S.C.E.

$1 \cdot 10^{-4}$ *M* hydrazobenzene in ammonia–ammonium chloride medium. Curve 1 was recorded immediately after mixing deaerated solutions of hydrazobenzene and buffer. Curves 2, 3 and 4 were recorded after prolonged bubbling of oxygen through the solution. In the presence of oxygen the cathodic–anodic wave I gradually changes

from an anodic into a cathodic wave as a result of the disappearance of hydrazobenzene to form azobenzene. The height of wave II, which was very small on curve 1, and which corresponds to the reduction of hydrogen peroxide simultaneously increases (Fig. 1, curves 2–4). Bubbling of air for more than 60 min results in a much higher wave II, but it is probable that other reactions also take place, as wave I simultaneously decreases. When solutions of hydrazobenzene and buffer were mixed without preliminary deaeration, the hydrogen peroxide wave was again observed, and its height was comparable with the height of waves shown in curves 2 and 3 of Fig. 1.

The formation of hydrogen peroxide is as easily investigated in neutral as in alkaline solution, because the reduction wave of hydrazobenzene to aniline does not occur above pH 6.1. At pH *ca.* 7 the hydrogen peroxide wave appears and increases in a similar way in the presence of oxygen, but not as fast as in alkaline solutions. After 60 min of bubbling oxygen the height of this wave attained only 25% of the wave height observed at pH 10. Likewise, on the curves recorded without deaeration of the solution before mixing, the hydrogen peroxide wave occurs also, but its height is lower than that observed at pH 10.

The formation of hydrogen peroxide is more difficult to investigate in acidic solutions, because the reduction waves of hydrogen peroxide and hydrazobenzene occur at about the same potential. Nevertheless, at pH 3.7, besides the upward shift of the cathodic–anodic wave, a considerable rise of wave II was also observed. This rise may be a result of hydrogen peroxide reduction. The oxidation of hydrazobenzene with oxygen from air at pH 3.7 proceeds more slowly than at pH 10. After 45 min of air bubbling only 30% of azobenzene was formed.

Diphenylcarbazide and diphenylcarbazone

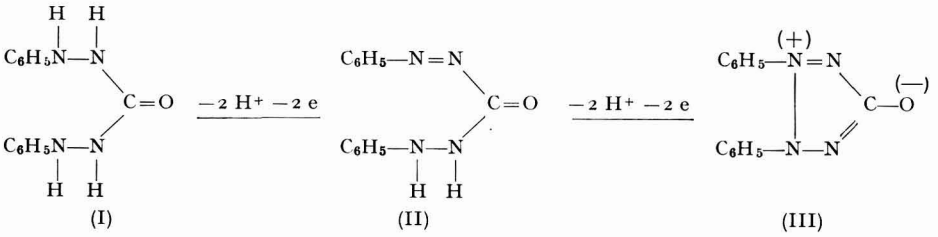

(I) (II) (III)

Oxidation of diphenylcarbazide (I) to diphenylcarbazone (II) and subsequent oxidation of (II) to diphenyloxytetrazolbetaine (III) proceeds easily enough under the influence of different oxidising agents, including oxygen from the air. The products formed as a result of this oxidation can be detected very easily polarographically, because they are reduced at different half-wave potentials[1,4,5]. We have found earlier[1], that only two waves are present when the solutions are deaerated before the mixing of carbazone with ammonia–ammonium chloride buffer. In solutions studied without this special precaution, five waves are observed (Fig. 2, curve 3).

Figure 2 shows the curves recorded for diphenylcarbazone solutions in ammonia–ammonium chloride medium. Curve 1 was recorded immediately after mixing deaerated solutions of carbazone and buffer. Curves 2 and 3 were recorded after bubbling increasing amounts of oxygen. Before recording each curve, unreacted oxygen was removed. Anodic wave I corresponds to the oxidation of carbazone to betaine, and

cathodic wave II to the reduction of carbazone to carbazide. On curve 2, the waves I and II are considerably smaller as a result of diminished carbazone concentration in the solution. Simultaneously, new waves III and IV are recorded. Wave III corresponds to the four-electron reduction of betaine (III) and wave IV to the reduction of hydrogen peroxide. On curve 3 the waves I and II have disappeared almost completely, and the waves III and IV increased considerably. When the amount of hydrogen peroxide becomes considerable a new wave, V, corresponding to the oxidation of hydrogen peroxide to oxygen, can be observed.

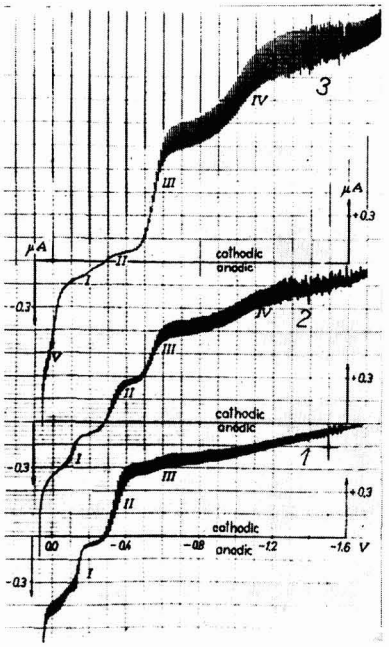

Fig. 2. Polarographic curves for $1 \cdot 10^{-4}$ *M* solution of diphenylcarbazone in 0.1 *M* ammonia–ammonium chloride buffer (pH = 10.0), 10% ethanol. (1), recorded after mixing of deaerated solutions; (2) and (3) recorded after 2 and 6 min bubbling of oxygen. Potentials *vs.* S.C.E.

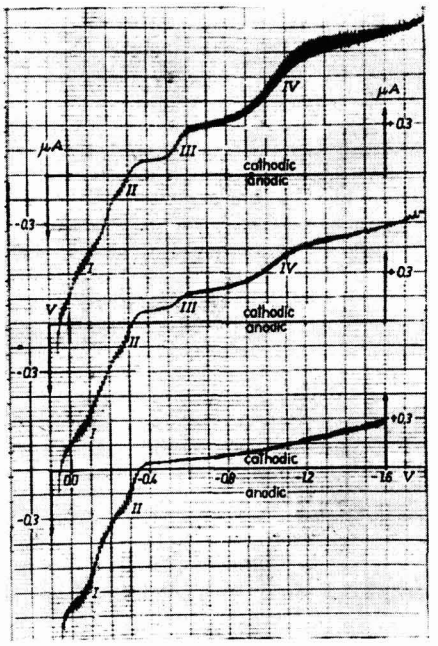

Fig. 3. Polarographic curves for $1 \cdot 10^{-4}$ *M* solution of diphenylcarbazide in 0.1 *M* ammonia–ammonium chloride buffer (pH = 10.0), 10% ethanol. (1) recorded after mixing of deaerated solutions; (2) and (3), recorded after 5 and 15 min bubbling of oxygen. Potentials *vs.* S.C.E.

The formation of hydrogen peroxide in solutions containing carbazone (II) was also studied in neutral and acidic medium. In nearly neutral solutions the hydrogen peroxide wave was observed, although its rise was not as rapid as in alkaline solutions. At pH 3.7 the hydrogen peroxide wave was not observed, even after bubbling oxygen for 20 min.

Similar results have been obtained for solutions of carbazide, for which the hydrogen peroxide wave increased rapidly in alkaline, and slowly in neutral, solutions. In an acidic medium the hydrogen peroxide wave was not observed. The curves obtained in the absence and presence of oxygen for alkaline medium containing carbazide, are shown in Fig. 3. Anodic waves II and I corresponding to the oxidation of carbazide to

carbazone and betaine, respectively, are smaller after reaction with oxygen. At the same time, the cathodic waves III and IV, corresponding to the reduction of betaine and hydrogen peroxide, increase, and so does an anodic wave, V, which corresponds to oxidation of hydrogen peroxide to oxygen.

Dithizone (diphenylthiocarbazone)

It has been stated, that hydrogen peroxide is also formed in solutions of dithizone studied under similar conditions as above, although considerably more slowly than in solutions of hydrazobenzene, diphenylcarbazone and diphenylcarbazide. In alkaline medium, the hydrogen peroxide wave was as high as the dithizone wave only after 120 min of oxygen bubbling.

SUMMARY

It was found that in solutions of all compounds investigated containing the hydrazo group (hydrazobenzene, diphenylcarbazone, diphenylcarbazide and dithizone), hydrogen peroxide is formed in the presence of dissolved oxygen. The rate of the formation of hydrogen peroxide in alkaline solutions decreases in the following order: carbazone, hydrazobenzene, carbazide, dithizone, and increases from acidic to alkaline solutions. In acidic solution the formation of hydrogen peroxide occurs mainly with hydrazobenzene.

REFERENCES

1 W. KEMULA, Z. KUBLIK AND E. NAJDEKER, *Roczniki Chem.*, 36 (1962) 937.
2 A. FOFFANI AND M. FRAGIACCOMO, *Ric. Sci.*, 22 Suppl. A. (1952) 139, 155.
3 S. WAWZONEK AND J. O. FREDERICKSON, *J. Am. Chem. Soc.*, 77 (1954) 3985, 3988.
4 M. FEDORONKO, O. MANOUŠEK AND P. ZUMAN, *Collection Czech. Chem. Commun.*, 21 (1956) 672.
5 N. N. GHOSH AND I. N. RAY, *J. Indian. Chem. Soc.*, 38 (1961) 319.
6 J. H. WALTON AND G. W. FILSON, *J. Am. Chem. Soc.*, 54 (1932) 3228;
G. W. FILSON AND I. H. WALTON, *U. S. Pat.* 2059569 (3.11.1936).
7 S. SIEKIERSKI AND E. K. SIEKIERSKA, *Roczniki Chem.*, 30 (1956) 399.
8 P. KRUMHOLTZ AND E. KRUMHOLTZ, *Monatsh.*, 70 (1937) 431.
9 Z. MARZCENKO, *Odczynniki Organiczne*, Warsaw, P.W.N., 1959.
10 G. IWANTSCHEFF, *Das Ditizon und seine Anwendung*, Verlag Chemie, Weinheim, 1958.

A STUDY OF THE CHRONOPOTENTIOMETRIC REDUCTIONS OF OXYGEN AND HYDROGEN PEROXIDE AT A PALLADIUM ELECTRODE

THOMAS R. BLACKBURN* AND JAMES J. LINGANE

Harvard University, Cambridge, Mass. (U.S.A.)

(Received October 1st., 1962)

Recent studies [1-7] have investigated the effect of oxidized films on noble metal electrodes on electrochemical processes occurring at these electrodes. EL WAKKAD AND SHAMS EL DIN[8] and HICKLING AND VRJOSEK[9] published chronopotentiometric studies of the palladium oxide film in which they found that halts occur in the anodic charging curve whose potentials coincide closely with the estimated standard potentials[10] of the $Pd(OH)_2/Pd$ and $Pd(OH)_4/Pd(OH)_2$ couples, and also with direct measurements of these couples[9]. Both groups of authors concluded that an oxide film containing palladium in the $+2$ and $+4$ oxidation states is formed when a palladium electrode is anodized, but the evidence was indirect. On the other hand, VETTER AND BERNDT[11], in agreement with an earlier study by BUTLER AND DREVER[12], found a linear increase of potential with time during anodization at constant current, and suggested that the anodic potential halts observed by previous authors might have been due to the presence of impurities.

Because the quantity of electricity required to reduce the palladium oxide film was approximately half that produced by its formation, VETTER AND BERNDT concluded that the oxygen in the film was partly reduced to hydrogen peroxide during the cathodic chronopotentiogram. A necessary consequence of this conclusion is that the so-called oxide film must be considered a more or less loosely bound layer of adsorbed oxygen. In the present study, the presence of palladium oxide films has been verified by direct chemical analysis. The occurrence of potential halts in anodic charging curves remains unresolved (none were observed in the present study), but does not appear to be related to any of the more obvious differences in experimental conditions among the various investigators[13].

The chronopotentiometric reduction of oxygen at a mercury cathode has been presented by BERZINS AND DELAHAY[14] as an example of a two-step electrode reaction. The observed ratios of transition times agreed with the theoretical relation adduced for the successive electroreaction of a single substance for which $n_1 = n_2$. LINGANE[5] studied the cathodic chronopotentiometry of oxygen at a platinum electrode in both 1 *M* sulfuric acid and 1 *M* sodium hydroxide, and found that the transition times in both media corresponded to an overall 4-electron reduction to water. The observed currents were corrected for that produced by the simultaneous reduction of a spontaneously formed platinum oxide film (see below). In a similar, though less quantita-

* Present address: Carleton College, Northfield, Minn. (U.S.A.)

tive study, SAWYER AND INTERRANTE[15] found that some hydrogen peroxide was produced by the controlled-potential reduction of oxygen.

The latter authors also compared the behavior of palladium and nickel electrodes to that of platinum, and stated that palladium electrodes behave quite similarly to platinum when used for oxygen reduction. On the basis of the observation that the potentials for the reduction of oxygen and the lower palladium oxide were nearly the same over a wide range of pH, they asserted that the mechanism for the reduction of oxygen at a palladium electrode involved the cyclic oxidation and reduction of the electrode, with intermediate formation of $Pd(OH)_2$ by chemical reaction with the oxygen.

The purpose of the present investigation was to study the effect of palladium oxide films, and of the direct reaction of oxygen with palladium, on the chronopotentiometric reduction of oxygen at a palladium cathode.

EXPERIMENTAL

The chronopotentiometric circuit used was similar to that previously discussed[3,16,17] employing three large, 45 V B batteries in series to power an electrolysis circuit in which nearly all of the resistance was supplied by a 1 watt graphite resistor. The value of the latter determined the magnitude of the current, which was known and constant to $\pm$ 0.1%. Potentials were observed with a Dumont Type 403 oscilloscope, and transition times were measured by means of an electric stopclock (Standard Electric Time Co., Type S-10), running simultaneously with the electrolysis current.

Oxygen was supplied by the Air Reduction Co., and was 99.5% pure, the remainder consisting of nitrogen and argon. Prepurified nitrogen (oxygen content 0.002%) was used to remove oxygen from solutions. Electrodes were constructed of 99.99% pure palladium wire sealed with Tygon paint to expose a known cylindrical area to the solution.

Analysis of palladium oxide films

Figure 1 shows chronopotentiograms for the formation and reduction of an oxide film on a palladium electrode in 1.0 *M* sulfuric acid. Notice that, although the

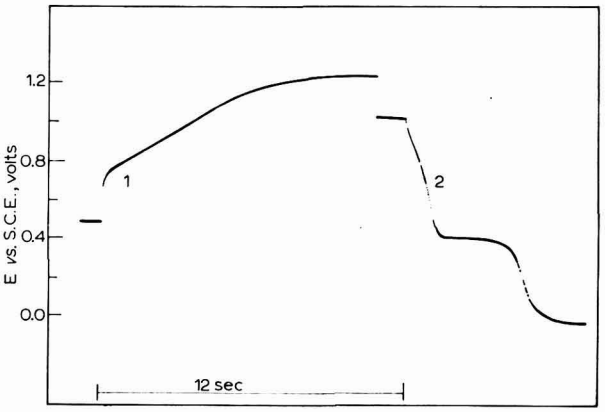

Fig. 1. Chronopotentiograms for oxide film formation (curve 1) and reduction (curve 2) on palladium in oxygen-free 1.0 *M* sulfuric acid. $i/A = 370\ \mu A/cm^2$.

reduction of two species is clearly indicated by the doublet cathodic wave, the anodic chronopotentiogram shows no such division. However, if the anodization is carried out only to a potential of + 1.0 V *vs.* S.C.E., the chronopotentiogram for the reduction of the resulting oxide film shows only a single wave, beginning at + 0.4 V. From evidence cited below, it is clear that only the +2 oxide, and no higher oxide, is formed during anodization to +1.0 V in 1 *M* acid medium, and thus that the cathodic wave beginning at +0.4 V results from the reduction of +2 palladium.

The lower oxide was analyzed, and shown to consist of PdO (or $Pd(OH)_2$) as follows: A large palladium foil immersed in a hydrogen phosphate–dihydrogen phosphate buffer of pH 6.37 was anodized to a potential (+ 0.70 V *vs.* S.C.E.) such that none of the higher oxide was formed, and the quantity of the lower oxide measured by means of cathodic chronopotentiometry. When this quantity was reproducibly established, the foil was anodized for a final time, and the surrounding electrolyte removed from the cell under nitrogen pressure. A known volume of oxygen-free 1 *M* hydrochloric acid was then forced into the cell so as to immerse the oxidized foil. Dissolution of the oxide film was complete within a few seconds at room temperature. The resulting solution of chloropalladite ion was analyzed spectrophotometrically by measurement of the absorbance at 280 mμ in a 10 cm quartz cell.

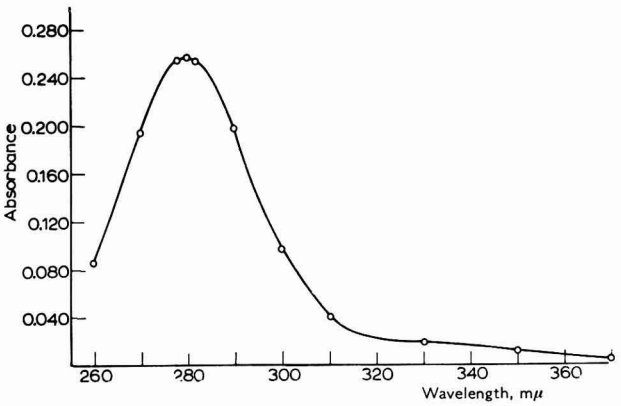

Fig. 2. Spectrum of a typical 1.0 *M* HCl stripping solution after dissolution of an oxide film. The position and absorptivity of the maximum at 280 mμ agree with the spectrum of $PdCl_4^{2-}$ ion published by COHEN AND DAVIDSON[18]. Measurements were made with a Beckman Model DU spectrophotometer, using 10 cm quartz cells. Reference solution is 1.0 *M* HCl.

Spectra of the +2 and +4 palladium chloride complexes have been investigated by COHEN AND DAVIDSON[18]; the spectrum of a typical stripping solution shown in Fig. 2 duplicates the spectrum of the $PdCl_4^{2-}$ ion in 0.998 *M* HCl reported by them. That the predominant palladium species present in 1 *M* hydrochloric acid is indeed $PdCl_4^{2-}$ ion is indicated by a study by DROLL, BLOCK AND FERNELIUS[19] in which they found that the equilibrium constant for the formation of $PdCl_4^{2-}$ from $PdCl_3^-$ is approximately $10^{2.5}$ at 25°. The applicability of Beer's Law to solutions of the composition encountered in this study was investigated using known chloropalladite solutions prepared by dissolving 99.99% pure palladium wire in aqua regia and evaporating to dryness 4 times with hydrochloric acid. The absorption spectrum of

these known solutions also duplicated that presented by COHEN AND DAVIDSON[18]. Figure 3 shows the linear relation of absorbance, measured at 280 mμ, to concentration of chloropalladite in 1 *M* hydrochloric acid. The molar absorptivity calculated from these data is $1.09 \cdot 10^5$ l mol^{-1} cm^{-1}.

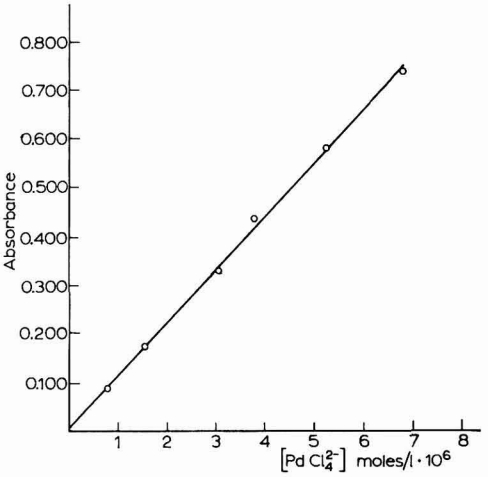

Fig. 3. Absorbance at 280 mμ as a function of concentration of known chloropalladite solutions in 1.0 *M* HCl. 10 cm quartz cells.

TABLE I

DETERMINATION OF THE LOWER OXIDE

First trial is with electrode of 35 cm^2 area, second and third with electrode of 96 cm^2 area. Data in the second column refer to the average of several trials previous to the final anodization; data in columns 3 and 4 taken after the stripping of most of the oxide film by immersion in HCl.

	Oxide film formed (mC)			*Chloropalladite found (mC)*	
	it	it *Residual*	it *Net*	*mmoles* · 10^4	*(as +2)*
Phosphate buffer, pH 6.37	12.5	2.6	9.9	0.45	8.7
	30.8	2.0	28.8	1.57	30.3
1 *M* NaOH	29.1	14.6	14.5	0.71	13.7

The results of three stripping experiments are shown in Table I.

Note that the agreement is generally good between the quantity of palladium found in the stripping solution, expressed as mcoulombs of +2 palladium, and the quantity of electricity which presumably would have been required to reduce the same palladium in the form of an oxide film.

Once this was established, the analysis of the complete oxide film was attempted by the same method, anodizing in this case to oxygen evolution, so that a succeeding cathodic chronopotentiogram measured the total equivalents of both oxidation states. However, the qualitative identification of the oxidation state of palladium in

the higher oxide is prevented in this case by the fact that the higher oxide rapidly and quantitatively reacts with the electrode surface during stripping to produce an equivalent quantity of chloropalladite ion.

The analytical results do indicate unequivocally, however, that the first potential halt in the chronopotentiogram for the reduction of the complete oxide film (curve 2 of Fig. 1) results from the reduction of a genuine palladium oxide, and not of a layer of adsorbed oxygen. The potential of the first cathodic wave is about + 0.9 V *vs.* S.C.E. If the species being reduced were oxygen, the product of this reduction would have to be water, since the reduction of oxygen to hydrogen peroxide requires a potential at least as cathodic as + 0.44 V *vs.* S.C.E. In this case, the quantity of oxidized palladium in the film would be simply the quantity of +2 oxide, or $i\tau_2/2F$ mmoles. On the other hand, if a true higher oxide a palladium were present, then this would produce, during stripping, an additional quantity of chloropalladite ion equivalent to the higher oxide, and the total chloropalladite found should be $i(\tau_1 + \tau_2)/2F$ mmoles, where τ_1 and τ_2 are the separate transition times for the first and second waves. Table II compares these predicted quantities with the quantity of palladium actually found.

TABLE II

ANALYSIS OF FILMS CONTAINING BOTH OXIDES

Oxide films formed on an electrode of 96 cm^2 area, immersed in oxygen-free 1.0 *M* NaOH. Data in columns 1 and 2 are averages of several trials just before each analysis. Units of columns 3 and 4 are mA-sec/faraday, or mmoles.

τ_1(sec)	τ_2(sec)	$i\tau_2/2F$	$i(\tau_1 + \tau_2)/2F$	*Palladium found (mmoles)*
4.5	10.5	$1.80 \cdot 10^{-4}$	$2.34 \cdot 10^{-4}$	$2.38 \cdot 10^{-4}$
5.3	11.6	$1.80 \cdot 10^{-4}$	$2.61 \cdot 10^{-4}$	$2.47 \cdot 10^{-4}$
5.3	11.2	$1.74 \cdot 10^{-4}$	$2.56 \cdot 10^{-4}$	$2.55 \cdot 10^{-4}$
Blank, no oxide formed		0.00	0.00	$0.04 \cdot 10^{-4}$

Comparison of the number of mmoles of palladium found in the stripping solution to column 4 of Table II shows definitely, by the reasoning above, that the species reduced during the first wave of the cathodic reduction of the complete oxide film is a genuine higher palladium oxide, and not a layer of adsorbed oxygen.

While the oxidation state of palladium in the higher oxide is not derivable from the analytical data, the known properties of the higher oxides of palladium[20] suggest that the most likely possibility is +4. However, little reliance can be placed on extrapolations of the bulk properties of substances to what may well be monomolecular films. In addition, all stripping experiments may be criticized on the grounds that they are too indirect; the presence and oxidation state of palladium in the stripping solution does not bear a necessary and unique relationship to the composition of the oxidized film. The possible objection that the film is chemisorbed oxygen which reacts with the electrode surface during the stripping to produce chloropalladite ion is not tenable because the doublet wave for the reduction of the film in 1 *M* sodium hydroxide does not agree with the known course of oxygen reduction in that medium (see below). It will also be shown that the reaction of oxygen with palladium in 1 *M*

hydrochloric acid medium produces chloropalladite ion and hydrogen peroxide in equimolar quantities. This stoichiometry would not produce the quantity of chloropalladite ion actually observed, but about 15% less, in the cases in Table II. However, it is true that a possible +1 palladium oxide which disproportionated during stripping would give results identical to those shown in Tables I and II. The known properties of palladium, specifically the failure of all attempts to prepare compounds in the +1 oxidation state, and the known stability of the +2 oxide, furnish a qualified guide to the interpretation of these experiments.

The reaction of oxygen with palladium

The reaction of palladium metal with dissolved oxygen has a direct bearing on the interpretation both of the stripping experiments discussed above, and of the chronopotentiometry of oxygen reduction at a palladium electrode. The study whose results are presented below was undertaken to establish the products of that reaction.

A large palladium foil was immersed in oxygen-saturated 1.0 *M* sulfuric acid for various times, and the solution was analyzed for palladium by evaporating the solution to dryness and dissolving the residue in 1 *M* hydrochloric acid. The +2 palladium was determined spectrophotometrically. It became clear that after a relatively small quantity of palladium had reacted with oxygen, further exposure to the oxygen-saturated acid caused little further corrosion of the foil. This suggested that the reaction of palladium with oxygen was reaching an equilibrium. This would be the case if the primary reduction product of oxygen were hydrogen peroxide, rather than water, and if the hydrogen peroxide reacted with palladium metal only very slowly. Consequently, in the third experiment in Table III, the sulfuric acid

TABLE III

OXIDATION OF PALLADIUM BY OXYGEN IN ACID SOLUTIONS

Medium	*Exposure (h)*	$[Pd^{2+}] \cdot 10^6$	$[H_2O_2] \cdot 10^6$
1.0 *M* H_2SO_4	8	1.35	—
1.0 *M* H_2SO_4	95	2.24	—
1.0 *M* H_2SO_4	120	1.98	1.5
1.0 *M* HCl	8	42.2	36.1

solution was analyzed by concentrating it to 1/6 its volume by freezing, and forming the yellow titanyl–peroxide complex on addition of an equal volume of 0.400 *M* titanyl sulfate in 1 *M* sulfuric acid. The titanyl–peroxide complex was then determined spectrophotometrically using the titanyl sulfate reagent, appropriately diluted with 1 *M* sulfuric acid, as reference solution. The calculated concentration of hydrogen peroxide in the original solution is approximately equal to that of palladous ion, determined in the usual way in a separate aliquot. From the standard potentials of the oxygen–hydrogen peroxide (+ 0.682 V) and palladous-palladium (+ 0.987 V) couples in a 1 *M* acid medium, one may calculate that the equilibrium concentrations of palladous ion and hydrogen peroxide should be approximately $5 \cdot 10^{-6}$ *M*, in good agreement with the observed values.

The corrosion of palladium in oxygen-saturated 1.0 *M* hydrochloric acid was also

measured in a single experiment involving an exposure of 8 h. In this case as well, hydrogen peroxide was detected in amount nearly equal to the chloropalladite concentration, indicating that the reduction of oxygen by palladium metal in this medium as well as in 1 *M* sulfuric acid stops at hydrogen peroxide. The extent of reaction in 1 *M* HCl is much greater than in sulfuric acid, doubtless because of the formation of the chloride complexes of palladium.

Since palladous hydroxide is very insoluble in alkaline solutions[10,20] the product of the reaction of palladium metal with dissolved oxygen in a sodium hydroxide solution is not free palladous ion, or a basic anion, but a film of palladous oxide on the electrode surface. The extent of this filming in oxygen-saturated 1.0 *M* sodium hydroxide was measured by chronopotentiometric reduction of the film.

The electrode was exposed to the oxygen-saturated sodium hydroxide for the times noted in Table IV, removed and immersed in oxygen-free 1.0 *M* sodium hydroxide,

TABLE IV

CHRONOPOTENTIOMETRIC MEASUREMENT OF SPONTANEOUSLY FORMED FILMS IN OXYGEN-SATURATED 1.0 *M* SODIUM HYDROXIDE

Time of exposure (min)	*Quantity of oxide film (μC)*
0.5	102
1.0	118
2.0	139
30.0	159
210	185

and the latter was stirred with a rapid nitrogen stream to remove from solution oxygen introduced with the electrode. At the end of this time the transition time was measured for the reduction of the oxide film at a low current density. Transition times taken with and without stirring of the electrolyte gave identical results, indicating that it was a film of palladous oxide being reduced, and not dissolved oxygen.

The chronopotentiometric reduction of oxygen

Chronopotentiograms for the reduction of dissolved oxygen in 1.0 *M* sodium hydroxide saturated with oxygen at 750 mm pressure at an originally filmed (curve 1) and unfilmed (curve 2) palladium electrode are shown in Fig. 4. Note that the reduction at a previously reduced electrode (curve 2) proceeds at a potential about 150 mV more oxidizing than does the reduction of palladous oxide in the same medium in the absence of oxygen (curve 3 of Fig. 4). When a full oxide film is present before the reduction of oxygen commences, a characteristic sharp minimum occurs at the onset of oxygen reduction; evidently, a complete oxide film of palladous oxide makes the reduction of oxygen less reversible. However, the minimum does not appear when the electrode initially is only partly filmed.

The concurrent reduction of an oxide film enhances the oxygen reduction transition time. Curve 1 is clearly much longer than curve 2, recorded at the same current density. When successive trials are taken at equal time intervals without re-anodizing the electrode, the transition time for oxygen reduction continues to decrease slowly,

finally reaching a constant value about 20% shorter than the first trial with an unfilmed electrode. In view of the fact that this final transition time is still about 20% longer than the theoretical value (see below), and of our observation of the spontaneous formation of oxide film on the electrode surface during immersion in oxygen-saturated 1 *M* sodium hydroxide, we conclude that it is the reduction of this spontaneously formed oxide film which continues to enhance the transition time, even

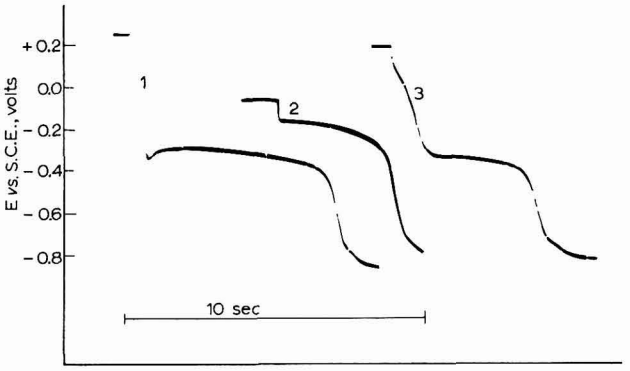

Fig. 4. Chronopotentiograms for the reduction of oxygen in 1.0 *M* NaOH, saturated with oxygen at 750 mm pressure. Oxygen reduction at filmed (curve 1) and unfilmed (curve 2) electrodes, $i/A = 592\ \mu A/cm^2$. Curve 3, reduction of a complete oxide film in oxygen-free 1.0 *M* NaOH, $i/A = 370\ \mu A/cm^2$.

when the original anodic film has been reduced; and that the quantity of spontaneous oxide film formed between trials slowly decreases to a constant value during a period in which the electrode is not anodized.

This behavior is understandable in view of recent evidence[6,7,13] that the reduction of an oxide film results in the deposition of metal on the electrode surface in a finely divided, highly active form, and that these deposits tend to age on standing in contact with electrolytes. Thus, the reduction of an anodic oxide film during trial 1 in Table V resulted in the deposition of a layer finely divided palladium on the electrode surface; between trials 1 and 2, dissolved oxygen reacted with this layer forming a new, less extensive oxide film. During subsequent trials, the aging of the

TABLE V

DECREASE IN TRANSITION TIME FOR OXYGEN REDUCTION AT AN UNFILMED ELECTRODE IN 1 *M* SODIUM HYDROXIDE. SUCCESSIVE TRIALS TAKEN AT TWO-MINUTE INTERVALS. EVERY FOURTH TRIAL IS RECORDED.

Trial	τ *(sec)*	*Trial*	τ *(sec)*
1	4.72	30	2.08
2	2.50	34	2.08
6	2.26	38	2.05
10	2.19	42	2.01
14	2.17	46	2.05
18	2.15	50	2.03
22	2.10	54	2.04
26	2.10		

deposit of finely divided palladium led to the formation of constantly less oxide between trials, until a state was reached in which only that metal deposited during the immediately preceding cathodization was in an active state. The result was a relatively constant quantity of spontaneous film formation between the equally spaced trials, and a consequently constant enhancement of the oxygen reduction transition time.

In order to study quantitatively the chronopotentiometric reduction of oxygen under these conditions, it is necessary to correct for this enhancement of the transition time. As LINGANE[3,5] has shown, a correction may be made to the current efficiency for oxygen reduction if it is assumed that the reductions of oxygen and oxide film each proceed with constant current efficiency during a given trial. If that is true, the current produced by the reduction of the oxide film is equal to Q/τ where Q is the quantity of oxide film expressed in coulombs. The current produced by oxygen reduction is then given simply by

$$i_{O_2} = i_{\text{obs.}} - Q/\tau \tag{1}$$

The use of this simple correction has been discussed in detail in previous publications[3,5].

The value of Q used in this study was that given in Table IV for a time of exposure equal to the interval between successive trials, namely 139 μC cm^{-2} for an exposure of 2 min. Table VI lists transition times as a function of observed and corrected

TABLE VI

CHRONOPOTENTIOMETRIC REDUCTION OF OXYGEN IN OXYGEN-SATURATED 1.0 M SODIUM HYDROXIDE

$i_{corr.} = i_{obs.} - 139/\tau$; $A = 0.906$ cm^2; $r = 0.051$ cm; $D = 1.79 \cdot 10^{-5}$ cm^2 sec^{-1}; $C = 8.45 \cdot 10^{-7}$ mole cm^{-3}.

$i_{obs.}$ (μA)	$i_{corr.}$ (μA)	τ (sec)	$i_{obs.}\tau^{1/2}/AC$	$i_{corr.}\tau^{1/2}AC$	Theor. eqn. (2)
1835	1580	0.49 ± 0.02	1705	1470	1484
1051	960	1.38 ± 0.02	1642	1501	1508
896	828	1.83 ± 0.05	1614	1489	1517
556	530	4.77 ± 0.02	1615	1538	1559
459	441	7.11 ± 0.02	1619	1563	1588
403	390	9.40 ± 0.10	1644	1591	1603
348	338	12.86 ± 0.03	1659	1615	1629
279	273	21.07 ± 0.03	1704	1667	1681

current, with observed and theoretical values of the chronopotentiometric constant, $i\tau^{1/2}/AC$. The theoretical values of $i\tau_1{}^{/2}/AC$ in Table VI were calculated from the equation for chronopotentiometry with cylindrical electrodes derived by PETERS AND LINGANE[4]:

$$\frac{i\tau^{1/2}}{AC} = \frac{\pi^{1/2}nFD^{1/2}}{2\left[1 - \dfrac{\pi^{1/2}D^{1/2}\tau^{1/2}}{4r_0} + \dfrac{D\tau}{4r_0^2} - \dfrac{3\pi^{1/2}D^{3/2}\tau^{3/2}}{32r_0^3} + \ldots\right]} \tag{2}$$

The observed (solid circles) and corrected (open circles) values of $i\tau^{1/2}/AC$ are plotted in Fig. 5 with a graph of the right side of eqn. (2) (solid line). The very close agreement

of the corrected points with the theoretical curve over the entire range of the transition times studied is conclusive evidence that the overall reaction producing the chronopotentiograms in Fig. 4 is the 4-electron reduction of oxygen to water. It should be noted that this conclusion is independent of the validity of the correction

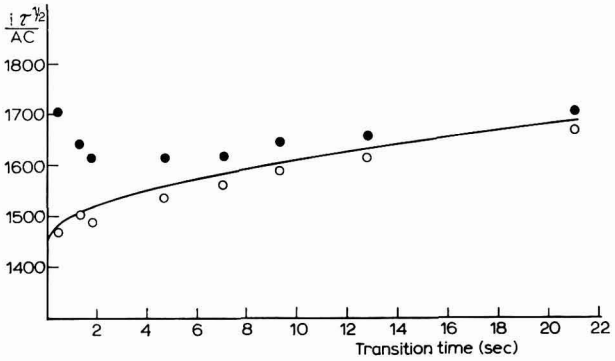

Fig. 5. $i\tau^{1/2}/AC$ (A $sec^{1/2}$ mol^{-1} cm^{-1}) as a function of transition time for oxygen reduction in O_2 saturated 1.0 M NAOH, P_{O_2} = 750 mm. ●, uncorrected data; O, current corrected according to $i_{corr.} = i_{obs.} - 139 \cdot 10^{-6}/\tau$.

for the simultaneous reduction of the spontaneously formed oxide film, since at long transition times, where the ratio of the constant quantity of oxide film to the increasing quantity of oxygen reduced becomes small, the uncorrected points approach within 3% of the theoretical curve.

The chronopotentiometric behavior of oxygen in 1 M sulfuric or perchloric acids is critically dependent on electrode pretreatment. For reasons discussed below, it was found that the pretreatment whose effects were most easily controllable was a cyclic anodization and cathodization of the electrode with formation and reduction of an oxide film just prior to the recording of an oxygen reduction chronopotentiogram. The behavior then observed was found to vary in a relatively simple way with the number of anodic-cathodic cycles used in the pretreatment, and with the time elapsed since the end of the pretreatment.

A new palladium wire, cleaned with acetone and distilled water and sealed with Tygon paint, shows no chronopotentiogram whatsoever for oxygen reduction; however, a single anodization and cathodization produces an ill-defined chronopotentiogram in the next cathodic trial, and a repetition of the cycle increases the reversibility and transition time of the wave (Fig. 6, curves 1–2). If this cyclic pretreatment is repeated many times, an electrode is eventually produced at which the chronopotentiometric waves for oxygen reduction are well-developed and for which the transition times are, under certain circumstances, diffusion-controlled.

Typical chronopotentiograms for such an electrode are shown in Fig. 7. Before the curves in Fig. 7 were recorded, the electrode was subjected to several anodic-cathodic cycles at a current density of 3.3 mA cm^{-2}. When the solution was stirred after the final cathodization of the pretreatment, the first oxygen reduction chronopotentiogram subsequently observed displayed the well-developed doublet wave shown in curves 2 and 8 of Fig. 7. Note that as successive trials were taken, at longer times after the pretreatment, two effects were observed. First, and most obviously, the

potential at which the reduction waves begin is shifted to more and more reducing values until the second wave merges with the reduction of hydrogen ion and eventually loses clear identity, as shown in curves 4–6 for sulfuric acid, and 9–11 for perchloric acid media. On very long standing (3–4 days) with stirring, the first wave also

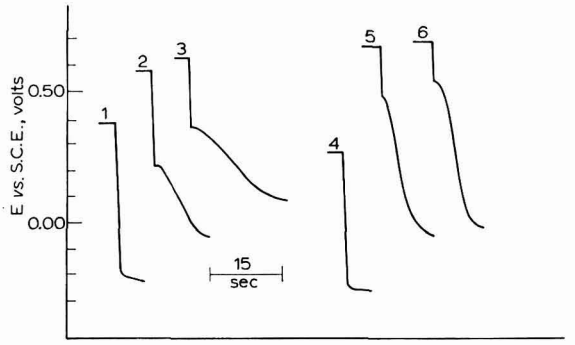

Fig. 6. Effect of finely divided electrode surface on oxygen reduction chronopotentiograms in 1.0 M sulfuric acid, $i/A = 150\ \mu A/cm^2$ throughout. Curves 1 and 4: new electrodes, cleaned with acetone and water; curve 2: after a single anodication and cathodization at $513\ \mu A/cm^2$; curve 3, after a second anodization and cathodization at $513\ \mu A/cm^2$; curve 5, after cathodization for 15 sec at $100\ \mu A/cm^2$ in $7.7 \cdot 10^{-3}$ F $PdCl_4^{2-}$ solution in 1 M HCl; curve 6 after a second such treatment.

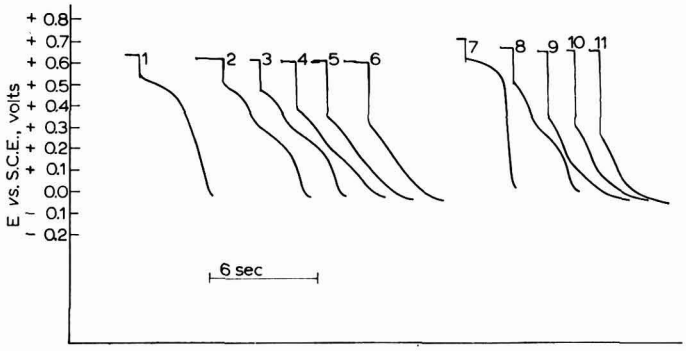

Fig. 7. Oxygen reduction chronopotentiograms in oxygen-saturated acid solutions. Curves 1–6, 1 M sulfuric acid, and Curves 7–11, 1 M perchloric acid; curve 1, 20 sec after electrode activation (see text); curve 2, 2 min; curve 3, 4 min; curve 4, 6 min; curve 5, 20 min; curve 6, 33 min; curve 7, 20 sec after electrode activation; curve 8, 2 min; curve 9, 10 min; curve 10, 15 min; curve 11, 20 min.

merged with hydrogen ion reduction and, depending on the history of the electrode, either disappeared entirely or lingered as an ill-defined 'foot' just preceding the final potential halt. The second trend in the successive chronopotentiograms, concurrent with the increasing overpotential, is a decrease in the transition time of the first wave.

If these two trends are extrapolated to zero time after the final anodic-cathodic pretreatment cycle, one would expect a single wave, beginning at a relatively oxidizing potential, and with a transition time equal to, or slightly greater than, the total for the first well-defined doublet. These hypothetical limiting chronopotentiograms were realized approximately in both sulfuric and perchloric acid solutions by

curves 1 and 7 of Fig. 7. These were obtained by allowing the electrode to stand for only 20 sec after the pretreatment to partly replenish the oxygen concentration at the electrode surface. Since complete replenishment of the oxygen without stirring would have required a longer interval than 20 sec, the transition times for these singlets were about 20% shorter than the total for the succeeding doublets, but the other qualitative expectations are entirely fulfilled. Note that the singlet character is better realized in perchloric than in sulfuric. It should be emphasized that since the last cathodization of the pretreatment cycle reduced any anodically formed film, the singlet waves shown in curves 1 and 7 of Fig. 7 are for the reduction of oxygen alone.

Because of an absence of data in the literature on the solubility of oxygen in perchloric acid solutions, quantitative study of the reduction in acid solution was limited to 1 *M* sulfuric acid, for which the concentration and diffusion coefficient of oxygen in the oxygen-saturated solution have been measured by LINGANE[5].

Both the total transition time for the doublet and the transition time for the first wave pass through reproducible steady values during the decay of the chronopotentiogram illustrated by Fig. 7. In the case of the total doublet, $\tau_1 + \tau_2$ is readily measurable and is constant for the first two or three successive trials after the conclusion of the pretreatment. For any chronopotentiogram for which a well-developed doublet is observed, τ_1 is significantly greater than the theoretical value for a diffusion-controlled, 2-electron reaction calculated from eqn. (2). However, as the decay of the chronopotentiogram proceeds, τ_1 reaches a steady value which corresponds very closely to the theoretical value. This is illustrated by Fig. 8, for a constant current density. The first transition time was measured at intervals as the electrode aged over the course of about 7 h after an anodic-cathodic pretreatment, and eqn. (2) was solved for the apparent n-value of the reaction. For about two hours after the pretreatment, this quantity was somewhat greater than 2, indicating that some additional reaction was accompanying the reduction of oxygen. Experiments discussed later in this paper indicate that this reaction was the disproportionation, catalyzed by the electrode surface, of the hydrogen peroxide formed by the reduction of oxygen.

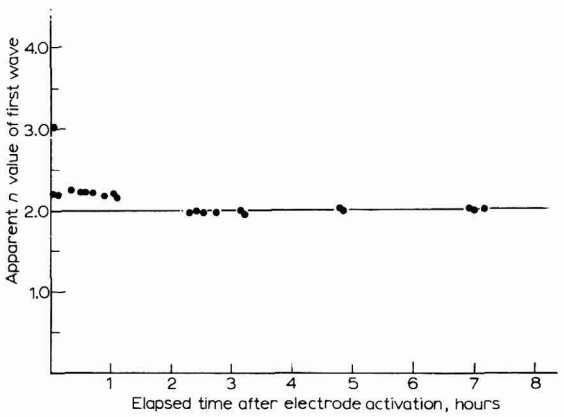

Fig. 8. Apparent n-value of first wave of oxygen reduction in 1.0 *M* sulfuric acid as a function of electrode aging after anodic-cathodic pretreatment.

The chronopotentiometric equation used in the quantitative study of the doublet was derived by PETERS AND LINGANE[21]. The equation derived was a general one for the successive electroreaction of two substances at a cylindrical electrode, and the authors showed that in the case of the two-step reduction or oxidation of a single species, the equation reduces to

$$\frac{i(\tau_1+\tau_2)^{1/2}}{AC} = \frac{\pi^{1/2} n F D^{1/2}}{2\left[1 - \frac{\pi^{1/2} D^{1/2}(\tau_1+\tau_2)^{1/2}}{4V_0} + \frac{D(\tau_1+\tau_2)}{4V_0^2} - \frac{3\pi^{1/2} D^{3/2}(\tau_1+\tau_2)^{3/2}}{32 V_0^3} + \ldots\right]} \quad (3)$$

where the diffusion coefficient and concentration are those of the original unreacted substance, in this case, oxygen.

The total transition time for doublet waves recorded soon after completion of the pretreatment is given for several current densities in Table VII. Before each cathodic trial, the electrode was pretreated with two anodic-cathodic cycles using a current density of 3.3 mA cm^{-2}, and the solution was stirred for 15 sec with a rapid stream of oxygen bubbles. The cathodic trial was taken one minute after the stirring was stopped.

Figure 9 shows the comparison of the experimental points with the theoretical curve for $n_1 = 2$, calculated from eqn. (3).

The transition time of the first wave was studied as a function of current density

TABLE VII

$\tau_1 + \tau_2$ AS A FUNCTION OF CURRENT DENSITY FOR THE OXYGEN REDUCTION DOUBLET IN O_2-SATURATED 1.0 M SULFURIC ACID

Electrode area 0.125 cm^2; r = 0.051 cm.

$i(\mu A)$	$(\tau_1 + \tau_2)$ (sec)	$i(\tau_1 + \tau_2)/AC$	eqn. (3)
219	0.87 ± 0.01	1559	1598
159	1.67 ± 0.01	1563	1607
141	2.13 ± 0.02	1568	1615
114	3.23 ± 0.02	1567	1642
90.9	5.36 ± 0.02	1602	1677
74.2	8.39 ± 0.01	1640	1704
66.4	11.1 ± 0.01	1687	1738

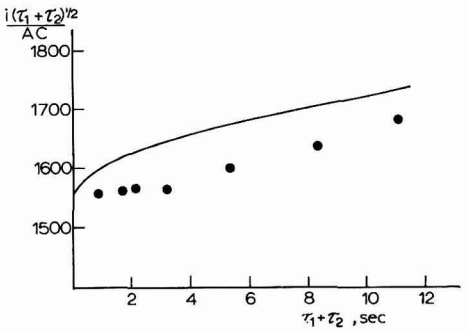

Fig. 9. $i(\tau_1 + \tau_2)^{1/2}/AC$ (A $sec^{1/2}$ mol^{-1} cm^{-1}) as a function of $(\tau_1 + \tau_2)$, oxygen reduction doublet wave in oxygen-saturated 1.0 M sulfuric acid. The solid line is the theoretical curve for $n = 4$.

at an electrode which had aged about 3 h after an anodic-cathodic pretreatment (*cf.* Fig. 8). Good agreement with the theoretical curve for $n = 2$ was observed, confirming hydrogen peroxide as the product of the first step of oxygen reduction in acid medium. The data are presented in Table VIII. The nearness of the wave to the hydrogen ion reduction potential makes the potential inflection indistinct at small current densities, and the longest transition time reliably measurable was 7.4 sec. The experimental values of $i\tau_1^{1/2}/AC$ are plotted in Fig. 10 against the theoretical curve calculated from eqn. (2).

TABLE VIII

TRANSITION TIME *vs.* CURRENT DENSITY FOR THE FIRST STEP OF OXYGEN REDUCTION AT AN AGED ELECTRODE. O_2 SATURATED 1.0 *M* SULFURIC ACID

$i(\mu A)$	$\tau_1(sec)$	$i\tau_1^{1/2}/AC$	*eqn. (2)*
1297	0.30 ± 0.02	801	783
1082	0.44 ± 0.02	812	786
918	0.60 ± 0.02	804	790
569	1.56 ± 0.02	808	803
406	2.45 ± 0.05	834	812
412	3.16 ± 0.03	836	818
284	7.4 ± 0.1	886	846

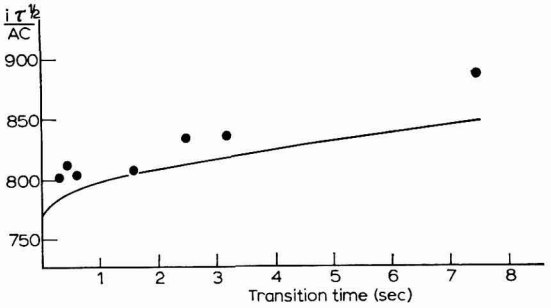

Fig. 10. $i\tau^{1/2}/AC$ (A $sec^{1/2}$ mol^{-1} cm^{-1}) as a function of τ_1, first wave of oxygen reduction at an aged palladium electrode (see Fig. 8), oxygen-saturated 1.0 *M* sulfuric acid. The solid line is the theoretical curve for $n = 2$.

Chronopotentiometric reduction of hydrogen peroxide

In the previous section of this paper we have seen that $i(\tau_1 + \tau_2)^{1/2}/AC$ for the oxygen reduction doublet agrees closely with the theoretical values over a range of current densities; thus it is certain that the sole source of reducible material is the diffusion of oxygen to the electrode surface. Yet the first transition of the doublet wave was significantly longer than that predicted by theory until the electrode had been allowed to age for several hours after an anodic-cathodic treatment. From these observations, it appears that the chronopotentiometric behavior of hydrogen peroxide must play a crucial role in the chronopotentiometry of oxygen reduction.

It was found that hydrogen peroxide yields a well-developed chronopotentiogram, similar in form and potential to the second wave of the oxygen reduction doublet. The values of $i\tau^{1/2}/AC$ calculated from the data indicate a diffusion-controlled, 2-electron reduction. However, it was also found that when an electrode immersed

in a hydrogen peroxide solution was given the same pretreatment as was used in the study of oxygen reduction, the electrode surface became catalytic for hydrogen peroxide disproportionation.

Solutions of hydrogen peroxide were prepared by diluting Merck 'Superoxol' (30% H_2O_2) with sufficient perchloric acid and water to obtain a stock solution approximately 0.1 M in hydrogen peroxide and 1.0 M in perchloric acid. Solutions for chronopotentiometry were prepared by appropriate dilution with 1.0 M perchloric acid immediately after standardization, which was accomplished by titration of an aliquot with a standard ceric sulfate solution, using ferrous orthophenanthroline as indicator.

Curve 1 of Fig. 11 is a typical chronopotentiogram for the reduction of $9 \cdot 10^{-3}$ M hydrogen peroxide in oxygen-free 1.0 M perchloric acid. The electrode was given a single anodic-cathodic pretreatment cycle, following which the solution was stirred

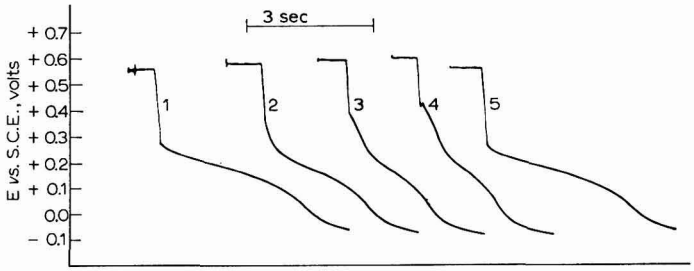

Fig. 11. Chronopotentiograms for the reduction of $9 \cdot 10^{-3}$ M hydrogen peroxide in oxygen-free 1.0 M perchloric acid. Curve 2, 3, and 4 at 10 sec intervals after curve 1; curve 5, 75 sec after curve 4. Solution unstirred between trials. $i/A = 3.39$ mA/cm^2.

TABLE IX

CHRONOPOTENTIOMETRIC REDUCTION OF HYDROGEN PEROXIDE

$[H_2O_2] = 9.36 \cdot 10^{-4}$ M			$[H_2O_2] = 9.55 \cdot 10^{-3}$ M		
$i(\mu A)$	τ(sec)	$i\tau^{1/2}/AC$	$i(\mu A)$	τ(sec)	$i\tau^{1/2}/AC$
141	0.33 ± 0.04	692	1344	0.34*	656
114.4	0.53 ± 0.01	712	1088	0.60 ± 0.01	707
90.7	0.87 ± 0.00	723	609	1.90 ± 0.01	704
74.3	1.30 ± 0.02	724	544	2.33*	696
66.5	1.65 ± 0.01	730	424	4.10 ± 0.01	720
50.6	2.98 ± 0.00	747	339	6.80 ± 0.01	741
46.0	3.61 ± 0.02	747			
37.3	5.86 ± 0.02	771			
28.4	10.2 ± 0.2	794			

* single value

for 2 min with a rapid nitrogen stream. After 1 min of quiescence, curve 1 was recorded at a current density of 3.39 mA cm^{-2}. As long as the working electrode was given only the relatively mild pretreatment of a single anodic-cathodic cycle followed by thorough stirring of the electrolyte before each cathodization, curve 1 was reproduced in subsequent trials. Curves 2–5 of Fig. 11 result under different circum stances, and will be discussed in a later section. Note that there is no evidence for the reduction of hydrogen peroxide at any potential more anodic than +0.25 V *vs.*

S.C.E. It is therefore quite unlikely that the enhancement of the first wave of oxygen reduction could result from the simultaneous reduction of oxygen and hydrogen peroxide at potentials of $+0.3$–$+0.5$ V (*cf.* Fig. 7).

The quantitative study of the transition time as a function of current density for the reduction of hydrogen peroxide was undertaken at concentrations of 10^{-2} and 10^{-3} M. The same pretreatment was used before each trial as was used in recording curve 1 of Fig. 11. The data recorded in Table IX were obtained with a wire electrode having a radius of 0.051 cm and area 0.125 cm^2.

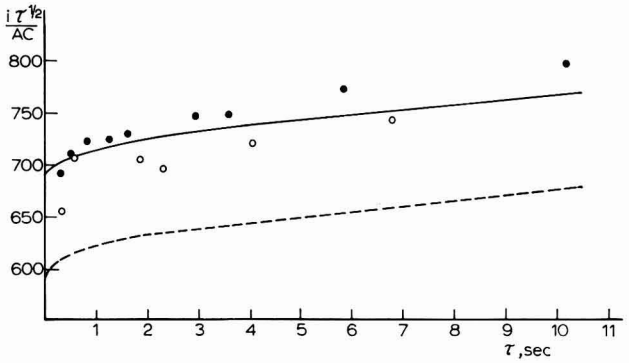

Fig. 12. $i\tau^{1/2}/AC$ (A sec$^{1/2}$ mol^{-1} cm^{-1}) as a function of transition time for reduction of hydrogen peroxide in oxygen-free 1.0 M perchloric acid. ●, $[H_2O_2] = 9.36 \cdot 10^{-4}$ M; ○, $[H_2O_2] = 9.55 \cdot 10^{-3}$ M; ——, theoretical curve for $D_{H2O2} = 1.6 \cdot 10^{-5}$ cm^2/sec; ----, theoretical curve for $D_{H2O2} = 1.2 \cdot 10^{-5}$ cm^2/sec. See text.

The data of Table IX are plotted in Fig. 12. In order to compare the experimental values of $i\tau^{1/2}/AC$ to a theoretical curve, the diffusion coefficient of hydrogen peroxide in 1.0 M perchloric acid must be known. No determination of this constant appears in the literature; however, STERN[22] has reported a value of $1.2 \cdot 10^{-5}$ cm^2 sec^{-1} for 0.1 M aqueous hydrogen peroxide, and KERN[23], from polarographic measurements, calculated $1.7 \cdot 10^{-5}$ cm^2 sec^{-1} for hydrogen peroxide in a buffer of pH 5, but unspecified concentration. KERN, however, used the Ilkovic equation uncorrected for spherical diffusion in calculating D_{H2O2}, and his value may be from 10 to 20% too large. The solid line in Fig. 12 was calculated using a value of D_{H2O2} of $1.6 \cdot 10^{-5}$ cm^2 sec^{-1} selected to give the best fit to the data for both concentrations of hydrogen peroxide. The dotted line is the theoretical curve calculated using STERN's value of $1.2 \cdot 10^{-5}$ cm^2 sec^{-1}.

Catalysis of hydrogen peroxide disproportionation by the electrode surface

It is well known that the uncatalyzed rate of disproportionation of hydrogen peroxide is quite slow. However, when the electrode immersed in a hydrogen peroxide solution was given the same many-cycle anodic-cathodic pretreatment as was used to obtain the well-developed doublet waves for the reduction of oxygen, it was found that oxygen bubbles collected on the electrode surface. When these bubbles were removed by rapid stirring with nitrogen, they returned within a few seconds after

the stirring ceased, and continued to form for several minutes after the original pretreatment. A cathodic chronopotentiogram recorded during this active period (Fig. 13, curve 1) showed an additional wave preceding hydrogen peroxide reduction, at a potential of +0.45 V *vs.* S.C.E., which doubtless results from the reduction of oxygen.

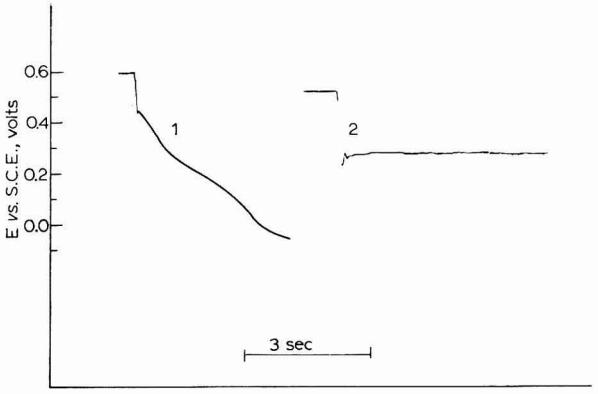

Fig. 13. Curve 1, Appearance of oxygen reduction wave before hydrogen peroxide reduction chronopotentiogram after anodic-cathodic cycling in oxygen-free, 1.0 *M* perchloric acid. $[H_2O_2]$ = 0.01 *M*; curve 2, Same data, but solution stirred during cathodization.

That the oxygen is present only near the electrode and not homogeneously throughout the solution is shown by curve 2 of Fig. 13. This chronopotentiogram resulted when the same pretreatment was used as produced curve 1 of Fig. 13, and the solution was stirred during the electrolysis. The absence of a prewave in this case indicated that the oxygen observed in curve 1 was present only locally near the electrode surface. The presence of oxygen at the electrode surface after an anodic-cathodic pretreatment can only have resulted from the disproportionation of hydrogen peroxide, since any oxygen formed during the anodic phase of the pretreatment was stirred away after its completion.

A second type of catalysis for hydrogen peroxide disproportionation was observed when chronopotentiograms ending at potentials of 0 V *vs.* S.C.E. or lower were recorded successively without stirring between trials. This catalysis, observable by the chronopotentiometric wave for the reduction of the resulting oxygen, is illustrated by curves 2–4 of Fig. 11. In this case, however, the catalysis was of much shorter duration; when the solution was stirred, or when more than 60 sec elapsed between trials, no oxygen reduction wave was observed in a succeeding chronopotentiogram (curve 5 of Fig. 11), indicating that when the oxygen was allowed to stir or diffuse away from the electrode surface, no more was formed.

Since this second type of catalysis was observed only when the potential in the potential in the preceding chronopotentiogram was allowed to fall below 0 V *vs.* S.C.E., it seems plausible that the catalytic agent in this case is the atomic hydrogen which is formed when hydrogen ions are reduced at a palladium cathode. The atomic hydrogen dissolved in palladium, being a fairly stable free radical, could serve to

initiate chain reactions for the decomposition of hydrogen peroxide according to a scheme such as:

$$H^{\cdot} + H_2O_2 \rightarrow H_2O + OH^{\cdot}$$

$$OH^{\cdot} + H_2O_2 \rightarrow HO_2^{\cdot} + H_2O$$

$$HO_2^{\cdot} + H_2O_2 \rightarrow OH^{\cdot} + O_2, \text{ etc.}$$

Since each free radical after H· would be highly unstable in aqueous solution, the chains would quickly be terminated by any of the following reactions:

$$OH^{\cdot} + H^{\cdot} \rightarrow H_2O$$

$$OH^{\cdot} + OH^{\cdot} \rightarrow H_2O_2$$

$$OH^{\cdot} + HO_2^{\cdot} \rightarrow O_2 + H_2O, \text{ etc.}$$

This would account for the great brevity of this type of catalysis, as indicated above. When an attempt was made to magnify the effect by prolonging hydrogen ion reduction at the end of the preceding trial, it was found that, instead, only a very short chronopotentiogram for hydrogen peroxide reduction, preceded by a normal-length oxygen wave, resulted. If H· is indeed the catalytic species, it would appear that in high concentrations on the electrode surface, it simply reduces hydrogen peroxide without causing increased disproportionation.

A scheme similar to that above, beginning with the capture of a hydrogen atom from HO_2^- by palladium, has recently been proposed by POSPELOVA AND KOBOZEV[24] to account for the palladium-catalyzed disproportionation of hydrogen peroxide.

DISCUSSION

The effect of the anodic-cathodic pretreatment cycles used in this study may be traced to observations[6,7,13] that the reduction of an oxide film results in the deposition on the electrode surface of a layer of finely divided metal. ANSON[6] and ANSON AND KING[7] have shown that the presence of such a layer on a platinum electrode greatly increases the reversibility of several reactions occurring at the electrode. At the same time, the study of hydrogen peroxide reduction in the preceding section of this paper makes it clear that a palladium electrode bearing such a layer of finely divided palladium is highly catalytic for the disproportionation of hydrogen peroxide.

According to the studies of BREDIG AND FORTNER[25] and others, the catalysis of hydrogen peroxide disproportionation by finely divided palladium is much greater in 1 *M* sodium hydroxide than in 1 *M* sulfuric acid, and is directly proportional to the true surface area of the metal. The mechanism proposed by POSPELOVA AND KOBOZEV[24] is consonant with these observations.

These two properties of a finely divided surface — the ability to increase the reversibility of reactions at the surface and the catalysis of hydrogen peroxide disproportionation — account very well for the phenomena encountered in the studies of oxygen and hydrogen peroxide reduction. The enhancement of the transition time

of the first wave of oxygen reduction in acid media at a finely divided electrode surface is clearly due to the reduction of additional oxygen supplied by the disproportionation of part of the hydrogen peroxide produced by the reduction of oxygen.

It will be recalled that a new palladium wire, which had never been palladized in this way, showed no chronopotentiometric wave whatsoever for the reduction of oxygen. The effect of anodization and cathodization shown in curves 1–3 of Fig. 6 is nearly duplicated when the layer of finely divided palladium is applied by the reduction of chloropalladite ion from solution. Curve 4 of Fig. 6 is the chronopotentiogram produced by a new palladium wire cathodized in an oxygen-saturated 1.0 *M* sulfuric acid solution. After curve 4 was recorded, the wire was palladized by cathodization for 15 sec at a current density of 100 μA cm^{-2} in a $7.7 \cdot 10^{-3}$ *F* solution of chloropalladite ion in 1.0 *M* HCl. After the wire was removed from the chloropalladite solution, rinsed thoroughly, and restored to the oxygen-saturated acid, curve 5 of Fig. 6 was recorded at the same current density as curves 1–4. Curve 6 shows the effect of a second identical palladizing treatment.

The mechanism of the 'aging' which reverses the effect of palladization of the electrode surface, as shown by the changes in the chronopotentiograms in Fig. 7, is made clear by the experiments on the reaction of oxygen with palladium in acid media. As shown in a previous section of this paper, palladium metal dissolves in oxygen-saturated acid media by reaction with oxygen. It is certainly reasonable to postulate that a finely divided surface will react more rapidly and, indeed, in preference to a smooth surface. The net effect is a smoothing of the electrode surface, and the loss of the two properties characteristic of that surface: increased reversibility for oxygen reduction and catalysis of hydrogen peroxide disproportionation. As a result, as finely divided palladium is removed from the electrode surface, the reduction of oxygen shifts to more reducing potentials, and the enhancement of the first wave decreases. These two processes are illustrated by Figs. 7 and 8.

On the basis of the picture presented above, it is not difficult to understand the reason for the great difference between the relatively constant behavior in alkaline medium, for which the chronopotentiogram is always a singlet, 4-electron wave, and the quite variable behavior in acid medium, with a continuum of chronopotentiograms from a singlet, 4-electron wave through a well-developed doublet to an ill-defined doublet whose second wave merges with the reduction of hydrogen ion. The mechanism for the aging of the electrode surface in acid medium is not available in alkaline solutions, since the product of electrode oxidation is not dissolved palladium, but an oxide film. Furthermore, since the reduction of this oxide film during each trial deposits a fresh layer of finely divided palladium, the activation is continually renewed. The only mechanism for the smoothing of the surface in basic solutions may be by the migration of palladium atoms along the surface from regions of greater to regions of lesser curvature; thus, as we have seen, (Table V), the quantity of spontaneously formed oxide film on the surface appears to decrease after an anodic-cathodic pretreatment to a slightly smaller, steady value.

In addition to the fact that the electrode surface is kept in a constant state of subdivision by spontaneous filming and the reduction of the film, it was observed by BREDIG AND FORTNER[25] that the palladium-catalyzed disproportionation of hydrogen peroxide is much faster in alkaline medium than in acid. Thus, it is quite

possible that the only electrochemical process occurring in alkaline medium is the reduction of oxygen to perhydroxyl ion, and that the disproportionation of the product is so rapid as to proceed at a rate essentially equal to the flux of oxygen to the electrode surface. The result of such a process would be an apparent 4-electron chronopotentiogram.

SUMMARY

The chronopotentiometric reductions of oxygen and hydrogen peroxide at a palladium cathode are profoundly affected by the chemical and physical state of the electrode surface. In alkaline medium, the reduction of oxygen produces a singlet 4-electron wave. In 1 *M* sulfuric or perchloric acid, the chronopotentiogram depends on the state of subdivision of the electrode surface. At an electrode on which a layer of finely divided palladium has been deposited by the reduction of an oxide film, a singlet 4-electron wave, or a well-developed doublet, is observed. As reaction with dissolved oxygen removes the finely divided metal from the electrode surface, the overpotential of the reduction increases, and the first wave of the doublet, originally enhanced by the disproportionation of some of the product hydrogen peroxide, approaches the theoretical transition time.

The direct reaction of dissolved oxygen with palladium has been studied both in acidic and basic media. The dissolution of palladium by reaction with oxygen in acid medium, and the spontaneous formation of an oxide film in oxygen-saturated 1 *M* sodium hydroxide, both affect the electrode surface. A direct analysis of the oxidized film formed during anodization of palladium supplements previous qualitative studies by other authors and indicates the presence of two palladium oxides, the lower of which contains +2 palladium.

REFERENCES

1 J. K. LEE, R. N. ADAMS AND C. E. BRICKER, *Anal. Chim. Acta*, 17 (1957) 321.
2 F. C. ANSON AND J. J. LINGANE, *J. Am. Chem. Soc.*, 79 (1957) 1015, 4901.
3 J. J. LINGANE, *J. Electroanal. Chem.*, 1 (1960) 379.
4 D. G. PETERS AND J. J. LINGANE, *J. Electroanal. Chem.*, 2 (1961) 1.
5 J. J. LINGANE, *J. Electroanal. Chem.*, 2 (1961) 296.
6 F. C. ANSON, *Anal. Chem.*, 33 (1961) 934.
7 F. C. ANSON AND D. M. KING, *Anal. Chem.*, 34 (1962) 362.
8 S. E. S. EL WAKKAD AND A. M. SHAMS EL DIN, *J. Chem. Soc.*, (1954) 3094.
9 A. HICKLING AND G. VRJOSEK, *Trans. Faraday Soc.*, 57 (1961) 123.
10 W. M. LATIMER, *Oxidation Potentials*, 2nd ed., Prentice-Hall, Inc., Englewood Cliffs, N.J., 1952.
11 K. J. VETTER AND D. BERNDT, *Z. Elektrochem.*, 62 (1961) 378.
12 J. A. V. BUTLER AND G. DREVER, *Trans. Faraday Soc.*, 32 (1936) 427.
13 T. R. BLACKBURN, *Ph.D. Thesis*, Harvard University, 1962.
14 T. BERZINS AND P. DELAHAY, *J. Am. Chem. Soc.*, 75 (1953) 4205.
15 D. T. SAWYER AND L. V. INTERRANTE, *J. Electroanal. Chem.*, 2 (1961) 310.
16 J. J. LINGANE, *Electroanalytical Chemistry*, 2nd ed., Interscience Publishing Co., Inc., New York, 1958.
17 J. J. LINGANE, *J. Electroanal. Chem.*, 2 (1961) 46.
18 A. J. COHEN AND N. DAVIDSON, *J. Am. Chem. Soc.*, 73 (1951) 1955.
19 H. A. DROLL, B. P. BLOCK AND W. C. FERNELIUS, *J. Phys. Chem.*, 61 (1957) 1000.
20 N. V. SIDGWICK, *The Chemical Elements and Their Compounds*, Oxford University Press, London, 1950.
21 D. G. PETERS AND J. J. LINGANE, *J. Electroanal. Chem.*, 2 (1961) 249.
22 K. G. STERN, *Ber.*, 66 (1933) 547.
23 D. KERN, *J. Am. Chem. Soc.*, 76 (1954) 4208.
24 T. A. POSPELOVA AND N. I. KOBOZEV, *Russian J. Phys. Chem.*, 35 (1961) 1192.
25 G. BREDIG AND M. FORTNER, *Ber.*, 37 (1904) 798.

MEASUREMENT OF TRANSFER COEFFICIENT AND RATE CONSTANT AT EQUILIBRIUM OF Fe^{2+} (0.002 *M*) Fe^{3+} (0.002 *M*), H_2SO_4 (1 *N*)/Pt ELECTRODE FROM FARADAIC RECTIFICATION

H. P. AGARWAL

Department of Chemistry, Motilal Vigyan Mahavidyalaya, Bhopal (India)

(Received July 14th, 1962)

When an electrode in an aqueous solution containing a reversible redox system is polarised by a sinusoidal alternating current, a small change in mean potential is observed[1]. As the phenomenon is caused by the differential electrode kinetics of the redox system, it was originally named the *redoxokinetic effect*[1]. It has now become more popularly known as faradaic rectification[2,3,4,5].

Earlier the theory was worked out for the particular case of small a.c. fields and for the reactants having equal concentrations and diffusion coefficients[6,7]. BARKER[8] and, independently, VDOVIN[9] generalised this treatment by deriving the shift of the mean potential, assuming that there is control of the alternating current whereas MATSUDA AND DELAHAY[5] state that in most cases there is control of the alternating voltage across the faradaic impedance by the low impedance of the double layer capacity, at the high frequencies at which measurements are made. MATSUDA AND DELAHAY[5] have given an analysis for voltage control and a correction for the double layer structure in solving the boundary value problem. The generalised theory has so far been applied for the measurement of α, the transfer coefficient, and of K_s, the rate constant, at equilibrium using mercury/aqueous solutions[4]. For platinum/-aqueous solutions, however, the values obtained earlier by DOSS AND AGARWAL[6] were reported to be tentative and illustrative of the procedure. NARAYANAN *et al.*[10] made an attempt to measure these quantities after obtaining a reproducible platinum electrode surface, but their observations gave constant values of ψ, the redoxokinetic potential, only between 50 and 250 c/sec. To verify the theory, more constant values of ψ at higher frequencies and the decrease of ψ at low frequencies with the square root of frequency need confirmation, by using improved experimental techniques for measurements in platinum/aqueous solutions.

In the present work, the values of α, and of K_s, have been determined at various temperatures for the platinum/aqueous solution containing equal and low concentrations of oxidant and reductant.

EXPERIMENTAL

The circuit diagram used is given in Fig. 1. A Philips audio oscillator, S (type GM 2315) is an a.c. source, and the current is controlled by the variable resistance R_1. A condenser C_1 is provided in the circuit to cut off any d.c. component that may be

associated with the alternating current. The key K_1 is used for switching the current on and off. The electrolytic cell contains three electrodes E_1, E_2, and R. All of them are polished bright platinum foil, the area of each being 1.6 sq. cm E_1 and E_2 are separated from each other by a sintered glass disc D (porosity 1G4), so that there is a uniform distribution of current density when the alternating current passes

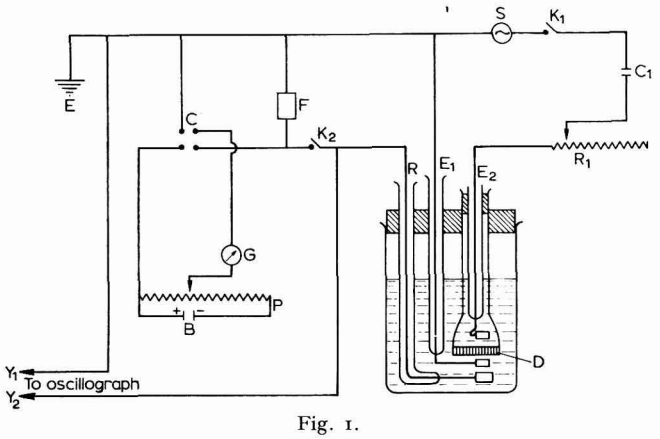

Fig. 1.

through the cell[11]. R is the reference electrode. An iR drop between the reference electrode and the polarised electrode E_1 is avoided by keeping the two within a distance of 0.5 cm[11]. On pressing key K_2, keeping K_1 in the "on" position, the d.c. potential developed between E_1 and R is measured by the potentiometer P, after filtering off a.c. through the low frequency pass filter F. After switching off a.c., the initial d.c. potential, if any, between E_1 and R is again measured. On subtracting this value from the former, ψ, the shift in mean potential *i.e.* the magnitude of rectified d.c. is obtained. The sign of the potential is that of the reference electrode. The potentiometer used could measure correctly potentials of the order of 1 μV using a Pye & Co. moving coil mirror galvanometer G (sensitivity 4.5 mm/μV at a distance of 1.1 m and resistance of 1840 Ω) as a null instrument. B is a dry battery of 1.5 V connected to the potentiometer and C is a commutator used in the potentiometer circuit for reversing the current. When the key K_2 is in the off position, the a.c. potential existing between E_1 and R is measured by connecting them to the Y-axis of a high sensitivity Philips oscillograph type GM 3156, sensitivity 1 mV (r.m.s.)/cm.

The cell, including the partitioned compartment of electrode E_2, contained a solution of ferrous ammonium sulphate (A.R.) and ferric ammonium sulphate (A.R.), the concentration of each cation being 0.002 M. The solutions were prepared in 1 N sulphuric acid (A.R.) which served as a supporting electrolyte. The solution in the cell and also that in the partitioned compartment of electrode E_2 were covered with liquid paraffin (A.R.), to protect them from atmospheric oxidation. All three electrodes were connected to earth and left over-night, to allow the system to attain equilibrium. The cell was immersed in a thermostat maintained at a definite temperature. The results were obtained using an alternating voltage of 4 mV and 8 mV at frequencies varying from 50 to 5000 c/sec. The experiments were carried out at four different

temperatures ranging from 25° to 40°, but the values of ψ were found to be independent of the variation in temperature at any frequency or voltage used. The relationship between ψ and $\sqrt{\omega}$ (ω, is the angular frequency) is given in Fig. 2 at 4 mV a.c. The plot for values of ψ obtained at 8 mV a.c. is not shown as they were exactly four times those obtained at 4 mV a.c. at all frequencies.

RESULTS AND DISCUSSION

The theoretical treatment[7] for a particular case of reactants having equal concentrations (of the order of a few mmoles/l) and equal diffusion coefficients leads to the following final expression,

$$\psi = (0.5 - \alpha)\frac{V^2nE}{2RT}\frac{1}{K}\sqrt{\frac{\omega D}{2}}\,\frac{\frac{1}{K}\sqrt{\frac{\omega D}{2}} + 1}{2 + \frac{1}{K^2}\frac{\omega D}{2} + \frac{2}{K}\sqrt{\frac{\omega D}{2}}}$$

where n is the valency of the ion, F is the Faraday, number, R is the gas constant, T is the absolute temperature, K is the rate of electrode reaction when no external potential is incident (in moles per unit area per sec per unit concentration), D is the diffusion coefficient of the two reactants, V is the amplitude of the sinusoidal component of the interfacial potential, ω is the angular frequency, ψ is the shift in mean potential and α is the transfer coefficient. At sufficiently high frequency, ψ is independent of frequency and the above expression takes the form

$$\psi = \frac{V^2nF}{2RT}(0.5 - \alpha) \qquad (1)$$

From Fig. 2 it can be seen that ψ is constant above a frequency of 500 c/sec. Hence

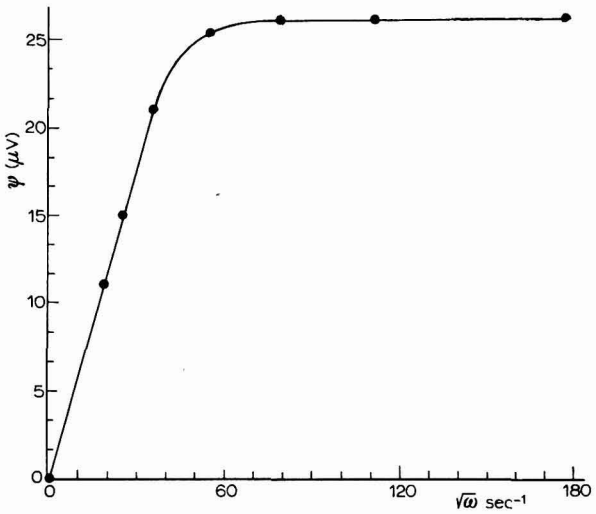

Fig. 2. Relationship between ψ, the shift in mean potential, and $\sqrt{\omega}$, where ω is the angular frequency at 4 mV a.c. at 30°.

on substituting the values of ψ (at frequencies of 1000 c/sec or above, see Fig. 2) in eqn. (1), the value of α can be calculated, as ψ is also proportional to the square of V. At low frequencies, the expression is reduced to the form

$$\psi = (0.5 - \alpha)\frac{V^2nF}{4RT}\frac{1}{K_s}\sqrt{\frac{\omega D}{2}} \qquad (2)$$

Hence at lower frequencies, ψ should be proportional to $\sqrt{\omega}$. The values of ψ at frequencies lower than 500 c/sec are proportional to $\sqrt{\omega}$, as is shown in Fig. 2. Therefore, on substituting the value of α obtained from eqn. (1) and the value of $\sqrt{\omega}/\psi$ (which is equal to $1.7 \cdot 10^6$ sec^{-1}, V^{-1} on measuring the cotangent of the angle made by the linear plot with the abscissa in the frequency range of 0–200 c/sec from Fig. 2. In eqn. (2), the value of K_s can be calculated, provided that the diffusion coefficient of the reactants is known. It is interesting to note that the values of ψ obtained at 25°, 35°, and 40° for the same a.c. potential and frequency were of the same order as those shown in Fig. 2 at 30°. It may be due to the fact that the increase in temperature increased the kinetics of the oxidant as well as the reductant proportionately. Knowing the values of the diffusion coefficient of the reactants at different temperatures, the values of the rate constant can be calculated at varying temperatures using eqn. (2). The diffusion coefficient measurements for the system under study were made using the porous diaphragm cell method whose details are discussed in a separate communication[14]. The values of α and of K_s were calculated at various temperatures. A linear relation was obtained between log K_s and $1/T$, a linear enabling the values of the energy of activation and the frequency factor A to be determined. The values obtained are given in Table I, together with the values of the diffusion coefficient D at the respective temperature.

TABLE I

Temp.	α	$D_2 \cdot 10^6$ *(cm sec^{-1})*	K_s *(cm secM^1)*	H *(Kcals)*	A *(cm sec^{-1})*
25°	0.583	4.7	0.033		
30°	0.585	6.2	0.038		
35°	0.586	8.1	0.044	5.1	1.5
40°	0.587	10.4	0.050		

The faradaic rectification method is not only very useful for the study of rapid electrode processes, but it is also free from errors associated with the resistance of the solution which occur when conventional methods[12] are employed. Further, a correction for low impedance of the double layer capacity at high frequency will not be necessary at the frequency range used[5], and the correction for the double layer structure in the solution of the boundary value problem need not be applied as the reaction under study happens to be moderately fast[13].

SUMMARY

The values of α (transfer coefficient) and of K_s (rate constant) at equilibrium at various temperatures for the Fe^{2+} (0.002 M), Fe^{3+} (0.002) M, H_2SO_4 (1 N)/Pt electrode have been determined by faradaic rectification.

REFERENCES

1 K. S. G. DOSS AND H. P. AGARWAL, *J. Sci. Ind. Res. (India)*, 9B (1950) 280.
2 K. B. OLDHAM, *Trans. Faraday Soc.*, 53 (1957) 80.
3 G. C. BARKER, *Anal. Chim. Acta*, 18 (1958) 118.
4 G. C. BARKER, R. L. FAIRCLOTH AND A. W. GARDENER, *Nature*, 181 (1958) 247.
5 H. MATSUDA AND P. DELAHAY, *J. Am. Chem. Soc.*, 82 (1960) 1547.
6 K. S. G. DOSS AND H. P. AGARWAL, *Proc. Indian Acad. Sci.*, 34 (1951) 263.
7 K. S. G. DOSS AND H. P. AGARWAL, *Proc. Indian Acad. Sci.*, 35 (1952) 45.
8 G. C. BARKER, *Transactions of the Symposium of Electrode Processes*, Philadelphia 1959.
9 VDOVIN, *Dokl. Akad. Nauk SSSR*, 120 (1958) 554.
10 NARAYANAN, SUNDARARAJAN AND NARAYANASWAMI, *Proc. Indian Acad. Sci.*, 48 (1958) 165.
11 P. DELAHAY, *New Instrumental Methods in Electrochemistry*, Interscience Publishers Inc., New York, 1954, p. 358.
12 *ibid.*, pp. 146–168.
13 H. MATSUDA AND P. DELAHAY, *J. Phys. Chem.*, 64 (1960) 332.

Book Reviews

Electrochemical Reactions, by G. CHARLOT, J. BADOZ-LAMBLING AND B. TREMILLON, Elsevier Publ. Co., Amsterdam, 1962, ix + 376 pages, £4.

This is an almost verbatim translation of the book with the same title published by the authors in French in 1959, so that the same comments made in the original review (*J. Electroanal. Chem.*, 1 (1959/60) 343) also apply in this case. The only differences from the preceeding French edition are a few new literature references. The production of this English translation is of the usual high standard common in Elsevier books.

J. Electroanal. Chem., 5 (1963) 241

Chimie et Eléments de Chimie Nucléaire, par D. MONNIER ET J. HOCHSTAETTER, publié par Georg et Cie S.A., Genève, 1961, 312 pages, 28 tableaux synoptiques, 150 exercices et problèmes expliqués, S. Fr. 12.

La cinquième édition, en langue française, de cet ouvrage a été entièrement refondue; en particulier les auteurs ne présentent plus la chimie dans l'ordre chronologique de son développement (matière, molécule etc. . . .) mais aborde cette discipline à partir des particules fondamentales, électron, neutron, proton.

Ce livre est destiné aux élèves des écoles secondaires supérieures et traite également diverses matières figurant au programme des examens d'entrée des grandes écoles. C'est pourquoi la chimie générale sera abordée d'une façon élémentaire dans une première partie (atome, molécule, équations et réactions chimiques), puis complétée par certaines notions plus complexes dans la quatrième partie de l'ouvrage, (mécanisme des réactions chimiques, solutions, produit de solubilité et solubilité, acides et hydroxydes, potentiels d'oxydo-réduction, thermochimie et combustion). La chimie minérale descriptive est présentée sous forme de tableaux résumant clairement les modes de préparation, les applications et les propriétés des principaux éléments. Cette présentation concise permet cependant de placer dans une même région du tableau les phénomènes ayant des liens entre eux. Le lecteur est ainsi à même de faire le rapprochement entre la propriété ,,combustion de l'hydrogène" et l'application ,,chalumeau oxhydrique".

La troisième partie de l'ouvrage concerne la chimie nucléaire et présente les phénomènes de radioactivité naturelle et artificielle en insistant sur les ,,réactions et équations nucléaires". L'énergie nucléaire, la fission, la fusion, la désintégration et l'activation et enfin les isotopes radioactifs font l'objet de paragraphes particuliers.

La chimie organique constitue la cinquième partie de l'ouvrage qui comporte sept chapitres: I, Généralités (tétravalence du carbone et liaisons des atomes de carbone); II, Les hydrocarbures; III, Les fonctions en chimie organique; IV, Dérivés des alcools et des acides; V et VI, Dérivés à fonctions multiples ou diverses; VII, Composés à chaine fermée (série aromatique).

La dernière partie de l'ouvrage s'intitule ,,Chimie industrielle et traite de l'énergie, des combustibles, des carburants, des lubrifiants, des textiles et plastiques, et des produits pharmaceutiques".

Chaque chapitre comporte un certain nombre d'exercices et leur solution.

Cet ouvrage résume d'une façon claire les principales notions fondamentales de la chimie et permet au lecteur d'acquérir de sérieuses connaissances dans cette discipline. Les auteurs ont présenté l'état actuel de cette science, mais ils ont cru devoir faire mention, à titre historique peut être, de notions périmées concernant, par exemple, la définition de l'oxydation ou de l'électrolyse. Cette seule réserve ne diminue en rien la valeur pédagogique incontestable de ce livre qui rendra le plus grand service, non seulement aux étudiants et à leurs maîtres, mais à tous ceux qui désirent compléter leur culture scientifique.

J. BADOZ-LAMBLING, Laboratoire de Chimie Analytique, Paris

Characterisation of Organic Compounds, by F. WILD, Cambridge University Press, London and New York, 1961, vi + 306 pages, $ 2.95.

Several schemes of analysis are available for identifying inorganic compounds. They generally use a separating and a subsequent confirmatory technique. No similar scheme exists for organic analysis, and the usual procedure is to investigate the groups thought to be present independently. Using these results, together with some physico-chemical properties, the compounds can finally be identified. This procedure confers on every book on qualitative organic analysis some characteristics of an inorganic text; individual authors usually overcome this disadvantage. The present book deserves an honourable place among the many other laboratory guides for organic analysis. The various classes of organic compounds are explored and identified on the basis of well-established reactions, but some new reactions are also introduced. Many tables detailing the melting points, and sometimes the boiling points, of many derivatives are particularly useful.

Instrumental Methods for the Analysis of Food Additives, edited by WILLIAM H. BUTZ AND HENRY J. NOEBELS, Interscience Publishers Inc., New York and London, 1961, vii + 288 pages, $11.

On September 6th, 1958, a law was enacted in the United States which allowed the food processor the use of any additive, provided it proved to be safe. The food processors were obliged to submit a petition for approval, containing, among other things, complete pharmacological test data and a detailed specific method of analysis for the additive in question. The law referred not only to intentional food additives, but also to unintentional additives, in other words, those substances which pass into the food after contact with containers or implements used during the various processes for food preparation. This law represented a marked change from the Food, Drug and Cosmetics Act of 1938, in which the burden of providing a safe additive rested with the Food and Drug Administration. The food processors realized the importance of discussing the new law in order to establish tests concerning possible migration of unwanted constituents to the food, and in order to establish analytical methods for food additive research and determination. Therefore, a symposium was held from March 24–26th, 1960, at the Kellog Center for Continuing Education, Michigan State University.

The first three parts of the book deal with the papers, and following discussions, from this symposium. The papers in the first part deal mainly with interpretation of the definitions of the above-mentioned law; the papers in the second part deal with methods for extracting pesticide residues from foods, and tests for possible migration of various container constituents, particularly from plastic containers. The third part, of approximately 100 pages, includes nine papers which emphasize the usefulness of instrumental analysis for solving the analytical problems which interested the symposium. The instrumental analytical methods mentioned are those widely used in all fields of analytical chemistry, *i.e.*, colorimetry, ultra-violet and infra-red spectrophotometry, gas chromatography and isotope dilution.

The last part of the book (approximately 50 pages) is not concerned with the symposium proceedings: it describes laboratory apparatus absolutely indispensable for research in, and determination of, chemical food additives.

This publication is undoubtedly useful for it gives a general picture of the enormous field of chemical additives, which are of interest to all food industries.

R. INTONTI, Istituto Superiore di Sanità, Rome

Bibliografia Polarografia, (1922–1960), Part I, Supplement No. 13, by L. GRIGGIO, Supplement to *Ricerca Scientifica*, 30 (1960) 1961, 94 pages, lire 1000.

A review of Supplement No. 12 in the *Polarographic Bibliography* series has already appeared in the *J. Electroanal. Chem.*, 3 (1962) 83.

Supplement No. 13 deals mainly with 1960, but some additions are also given for 1955–1959.

The Solubility Product Principle, by S. LEWIN, Isaac Pitman & Sons, London, 1960, xvii + 116 pages, £ 1.

Books are seldom written on purely didactic subjects such as solubility product. This principle, perhaps because of its simplicity, has given rise to so many misleading interpretations that we should be grateful to the author for establishing the validity and the limits of the conception with such convincing clarity.

In the introductory passages of the booklet the author distinguishes and characterizes the so-called "reduced product" in terms of anhydrous ions and the comprehensive activity solubility product, and gives the limitations of both.

The second chapter deals with the classical relationship between solubility and solubility product, and the analytical implications.

The third chapter deals with solid solutions and basic salts, but it would have been useful if polymeric basic salts had also been discussed.

The effect of change of medium on dehydration and complex ion formation is dealt with in a classical manner and I found the treatment of the significance of the solubility product in relation to partial ionization and to the formation of ion pairs extremely useful.

The classical equation for the temperature dependence of the equilibrium constants is derived in Chapter VII and the last two chapters deal with the important problem of the meaning of solubility product under conditions where equilibrium has not been established.

Using well chosen examples the author stresses the difference between precipitation under near-equilibrium conditions and rapid precipitation, and follows the transformation of the reactants through different metastable forms to the final crystalline product.

The book has the following useful appendices: thermodynamic derivation of the comprehensive solubility product equation; solid activity; ionic strength; dipole moments; activity and activity coefficients; considerations relating to the applicability of the comprehensive solubility product equation; solubility product values; and the teaching and study of the solubility product principle.

The chapter which summarizes the common errors that people make when dealing with the principle is particularly instructive, not only for students, but also for teachers.

A variety of examples and a complete bibliography are also given.

G. SARTORI, University of Rome

J. Electroanal. Chem., 5 (1963) 243

Selected Papers on New Techniques for Energy Conversion, edited by S. N. LEVINE, Dover Publications Inc., New York, 1961, xxviii + 1151 pages, $2.85.

In the last few years considerable advances have been made in the development of techniques for energy conversion, and relevant general information is scattered in many periodicals. This book, therefore, although containing only a selection of papers, is very welcome. The papers are by outstanding authors in the field of energy conversion and have been reprinted from various leading periodicals. Those on fuels cells, thermoelectricity and electrochemical batteries are particularly useful for electro-chemists. Fusion power, thermionic effect, photo-voltaic effect and solar energy are also dealt with.

J. Electroanal. Chem., 5 (1963) 243

Titrimetric Methods; Proceedings of the Symposium at Cornwall (Ontario), May 8–9th, 1961, edited by D. S. JACKSON, Plenum Press Inc., New York, 185 pages, $ 7.50.

This book contains eleven papers presented at the Symposium. Most of these are of interest to electrochemical analysts.

J. Electroanal. Chem., 5 (1963) 243

Applied Mathematics for Radio and Communication Engineers, by C. E. SMITH, Dover Publications Inc., New York, x + 336 pages, $1.75.

The title of this book leads one to suppose that mathematics has been treated here with a view to the particular needs of radio engineers. A brief survey of the contents, however, gives the impression that it could be very useful to chemists for revising many concepts and procedures also used in chemical calculations. The topics treated are: arithmetic, logarithms, algebra, geometry, trigonometry, vector addition, complex quantities, curves and graphs, simultaneous equations, quadratic equations, hyperbolic trigonometry, differential and integral calculus, and series and wave forms. One cannot, of course, expect rigorous treatment from such a book as this, but with the help of many examples and exercises the manipulation of mathematical formulae and equations is adequately explained.

J. Electroanal. Chem., 5 (1963) 243

Komplexbildung in Lösung, by H. L. SCHLÄFER, Springer Verlag, Heidelberg, 1961, x + 348 pages, D.M. 59.60.

Complexes can only be separated from the solution in which they are formed if their stability constants are high enough and their rates of decomposition low. Many of them , although existing in solution as completely identifiable compounds, do not fulfil these conditions and must therefore be investigated by methods which do not involve a preliminary separation. Physico-chemical methods, depending on the measurement of a particular physical property such as magnetic susceptibility, electro-conductivity, cell potential with suitable electrodes, refractive index, light absorption, etc., are naturally indicated. Descriptions and applications of all these methods concerned with the different problems arising out ot the chemistry of complexes have not previously been collected together in one volume, and from this consideration alone this book fulfils a useful purpose.

Theoretical aspects of chemical complexes are discussed in the first chapter, and each of the other nine chapters is devoted to a particular physico-chemical method. This book can also serve as a practical guide for workers in this field.

J. Electroanal. Chem., 5 (1963) 244

Spektralanalyse von Gasgemischen, by O. P. BOTSCHKOWA AND J. J. SCHNEIDER, translated from the Russian by W. FRIEDL, Akademie Verlag, Berlin, 1960, 160 pages, D.M. 28.

Spectrochemistry is not applied to the analyses of gases as often as to the analyses of solids or liquids. Various reasons can, perhaps, be suggested for this: firstly, the technical equipment for spectrochemical gas analysis is undoubtedly more complicated and requires more skill in operation; secondly, this method would have to compete with mass spectroscopic analyses, which are more sensitive; thirdly, spectrochemical gas analysis is not widely known.

In general, a monograph which gives a clear and simple description of what happens during a gas discharge and of the particular equipment needed for analytical purposes, and which discusses the possibilities and potentialities of this method, is to be welcomed.

This short monograph contains 6 chapters dealing with the following topics: radiation emission of a gas discharge; light sources for spectroanalysis of gases; experimental equipment; qualitative and semiquantitative analysis of gas mixtures; quantitative analysis and analysis by absorption in the i.r. and u.v. A moderately good reproduction of the spectra of some elementary gases (but only in the visible region), and a table of prominent lines and bands complete this monograph.

For a future edition the utilization of the Schumann region should considerably increase the potentialities of this technique, and an extension of the text to include the characteristics of this region would be of value.

J. Electroanal. Chem., 5 (1963) 244

Announcement

14th MEETING OF THE INTERNATIONAL COMMITTEE OF ELECTROCHEMICAL THERMODYNAMICS AND KINETICS (C.I.T.C.E.)

The 14th CITCE meeting will be held in Moscow (USSR), August 19–25, 1963. The general theme of the meeting will be: "Fundamental problems of electrochemical phenomena at interfaces, for instance, elementary acts, structure of double layer, role of adsorption phenomena, electrochemistry of semiconductors". Sessions of the following commissions are scheduled: Commission 2 (Nomenclature and Electrochemical Definitions), Commission 4 (Batteries), Commission 5 (Corrosion) and Commission 6 (Electrochemical Kinetics).

Correspondance regarding attendance or presentation of papers at this meeting should be addressed to N.IBL, Secretary General of CITCE, Department of Industrial and Engineering Chemistry, Swiss Federal Institute of Technology, Universitätstrasse 6, Zurich 6, Switzerland, or to A. N. FRUMKIN, Institute of Electrochemistry of the Academy of Sciences of the USSR, Leninsky Prospect 31, Moscow V-71, USSR.

Summaries of papers should be received before May 1, 1963, the full texts before June 15, 1963,

J. Electroanal. Chem., 5 (1963) 244

CONTENTS

Original papers

ELSEVIER PUBLISHING COMPANY, AMSTERDAM

Printed in The Netherlands by

NEDERLANDSE BOEKDRUK INRICHTING N.V., 'S-HERTOGENBOSCH